UNDERWATER IRRADIANCE ATTENUATION AND PHOTOBLEACHING OF CHROMOPHORIC DISSOLVED ORGANIC MATTER IN SHALLOW ARCTIC LAKES OF THE MACKENZIE DELTA, NWT

by

Jolie A.L. Gareis
B.Sc. (Honours), University of Western Ontario, 2002

THESIS SUBMITTED IN PARTIAL FULFILLMENT OF
THE REQUIREMENTS FOR THE DEGREE OF

MASTER OF SCIENCE

In the
Department of Biological Sciences

SIMON FRASER UNIVERSITY

FALL 2007

APPROVAL

Name: Jolie A.L. Gareis

Degree: Master of Science

Title of Thesis:

Underwater irradiance attenuation and photobleaching of chromophoric dissolved organic matter in shallow Arctic lakes of the Mackenzie Delta, NWT.

Examining Committee:

Chair: Dr. L. Quarmby, Professor

Dr. L. Lesack, Associate Professor, Senior Supervisor
Departments of Biological Sciences and Geography, S.F.U.

Dr. M. Bothwell, Research Scientist
National Water Research Institute, Environment Canada
and Adjunct Professor, Department of Biology, University of Victoria

Dr. O. Hertzman, Senior Lecturer
Department of Geography, S.F.U.

Dr. L. Bendell-Young, Professor
Department of Biological Sciences, S.F.U.
Public Examiner

1 November 2007
Date Approved

ABSTRACT

In situ attenuation of ultraviolet-B (UVB; 310-320 nm subset), ultraviolet-A (UVA) and photosynthetically active radiation (PAR) generally declined over the 2004 open-water season in a set of shallow Mackenzie Delta floodplain lakes. Average 1% photic depths were < 30 cm for UVB and < 50 cm for UVA, indicating that part of the water column remained sunscreened from UV. Average euphotic and lake depths were approximately equal (~2 m), indicating sufficient PAR for photosynthesis at all depths.

In 2005, dissolved organic matter (DOM) quality was examined using optical indices. Both spectral slope (decline in DOM absorbance as wavelength increases) and specific ultraviolet absorbance (average DOM aromaticity) were strongly correlated with sill elevation. UVA dominated *in situ* chromophoric DOM photobleaching, indicating that future increases in UVB fluxes are unlikely to exert as great an influence on *in situ* Mackenzie Delta optical environments as will increased chromophoric DOM from climate change.

Keywords: ultraviolet irradiance; Arctic; dissolved organic-matter; Mackenzie Delta; floodplain lakes

Subject Terms: underwater light; limnology – Northwest Territories – Mackenzie Delta region; lake ecology – Northwest Territories – Mackenzie Delta region; photochemistry; humic acid; ultraviolet radiation – Environmental aspects

ACKNOWLEDGEMENTS

First, my sincere thanks to my supervisor, Dr. Lance Lesack, for his encouragement, support and advice throughout this project, as well as his comments on numerous drafts of this thesis. I must also thank Lance for the incredible opportunity to work in the Mackenzie Delta, doing what I love to do – playing in the field. Not only did I have a lot of fun along the way; I truly feel as though I've learned how to be a better scientist and manager from working with him.

My committee members, Dr. Max Bothwell and Dr. Owen Hertzman, receive my sincere thanks for their valuable comments and priceless help throughout. Max not only loaned me his spectroradiometer, but also helped me wrangle it into a motorboat (no small chore!) and then helped me wade through an ocean of irradiance data. Owen has amazed me with both his genuine interest in this project and his constant, unwavering encouragement. I'd also like to acknowledge Dr. Bill Bailey for his help early in this project – I wish I could have had his input the whole way through. Thanks also go to Dr. Leah Bendell-Young (public examiner) for her helpful comments.

I've been lucky to have such great company in the Lesack Lab along the way – Catherine Febria, Craig Emmerton, Suzanne Tank and Adam Chateauvert. Thank you for your advice, fresh perspectives, help in jury-rigging all kinds of lab equipment, and your crazy sleep-deprived northern antics.

The Aurora Research Institute in Inuvik NT provided field support for this project. Special thanks to Les Kutny, Mike Atkinson and Sharon Katz for their help with field and lab equipment over the years. I'd also like to thank our fabulous field assistants, Shannon Turvey and Adam Chateauvert, for their tireless help and high spirits – even in the face of minor field disasters. Thanks to Benedict, Jared and Robert from Canadian Helicopters for flying us around! I'd also like to acknowledge the financial support received from funding agencies NSERC, PCSP and NSTP.

Chris Osburn and Warwick Vincent have provided valuable advice regarding methods. Donovan Lynch helped immensely with equipment and spectroradiometer quality control – not to mention enforcing regular coffee breaks whenever I'm in Nanaimo. The Bennett Lab at SFU kindly allowed me to use their spectrofluorometer for days at a time.

Thanks to Marlene, Alex, Cheryl and the rest of the BISC staff for their help with everything from pH meters to navigating though graduate school. I'd also like to thank Taskin Shirazi, Kim Blais and Nicole Wright from the Hydrology Lab at SFU for keeping this poor little biologist company in the geography department.

To my family and friends back home in Ontario – thank you for your support, whether it came by phone, email, snail mail, or when you crashed on my couch. Megan, Meredith, Kimmy, Erika, Amanda and Katie – you don't know how often I've smiled when I thought of you! Thanks to my mom for a lifetime of love. Although I don't make it there as often as I like, it's good to know that I can always go home again for a hug, a cup of coffee, and a good laugh.

And finally, thank you to Adam – my chief cook, head cheerleader, tennis partner, and rock in stormy seas. You know what the best part of all this was? You came along for the ride, and we had a lot of fun along the way. I can't wait for our next adventure.

TABLE OF CONTENTS

LIST OF FIGURES

LIST OF TABLES

GLOSSARY

λ	wavelength (nm)
$A\lambda$	raw absorbance at wavelength λ
$a\lambda$	absorption coefficient (m^{-1}) at wavelength λ
asl	above sea level
CDOM	chromophoric dissolved organic matter
Chl-*a*	total chlorophyll *a* pigment
DOC	dissolved organic carbon
DOM	dissolved organic matter
FI	fluorescence index
K_dUVA	diffuse attenuation coefficient, UVA waveband (m^{-1})
K_dUVB	diffuse attenuation coefficient, UVB waveband (m^{-1})
K_dUVB(310-320)	diffuse attenuation coefficient, UVB waveband over wavelength interval of 310-320 nm (m^{-1})
K_dPAR	diffuse attenuation coefficient, PAR waveband (m^{-1})
$K_d\lambda$	diffuse attenuation coefficient at wavelength λ
nm	nanometer (10^{-9} m)
PAR	photosynthetically active radiation (400-700 nm)
TDOC	total dissolved organic carbon
TSS	total suspended solids
ROS	reactive oxygen species

$SUVA_{280}$	specific ultraviolet absorbance at 280 nm
UV	ultraviolet irradiance (200-400 nm)
UVA	ultraviolet-A irradiance (320-400 nm)
UVB	ultraviolet-B irradiance (280-320 nm)
UVC	ultraviolet-C irradiance (200-280 nm)
z	depth (m)
$z_{1\%}$	1% photic depth (m)

1 GENERAL INTRODUCTION

1.1 Thesis Overview

The Mackenzie Delta, on the northwest Canadian coast, is the second largest delta in the circumpolar Arctic. More than 45000 permanent lakes cover half of the Mackenzie floodplain (Emmerton 2006), along with several distributary channels that carry water from the Mackenzie River northwards through the delta. Outflows of Mackenzie Delta discharge ultimately play a substantial role in determining the physical and chemical properties of the Beaufort Sea. During the break-up period each spring, ice jams in delta distributary channels result in elevated water levels and extensive flooding throughout the delta. The annual flood inundates delta lakes with river water carrying high concentrations of sediment and organic matter. These inputs help determine the underwater irradiance field in delta lakes during the open water season, as well as providing photoreactive material in the form of chromophoric dissolved organic matter (CDOM) at a time when the delta is experiencing 24 hour daylengths.

The Arctic environment has been exposed to increased fluxes of ground-level ultraviolet-B irradiance due to atmospheric ozone depletion since at least the late 1980s (e.g. Salawitch et al. 1990, Hofmann et al. 1989). However, few studies have examined the underwater ultraviolet (UV) irradiance environment in Arctic lakes to date. Prior to this study, direct measurements of *in situ* irradiance in Mackenzie Delta lakes had not been attempted. Instead, previous work made inferences of UV attenuation using laboratory-based absorption readings of filtered water samples and extrapolations from integrated underwater photosynthetically active radiation measurements. The objective of Chapter 2 is to investigate the spatial patterns and temporal dynamics of irradiance attenuation in the UV and visible wavebands in representative Mackenzie Delta lakes using *in situ* spectral measurements. In addition, the contributions of total suspended solids, total chlorophyll *a* and CDOM to attenuation of each waveband was calculated in order to examine the influence of the annual flood on the underwater irradiance environment.

Aquatic dissolved organic matter (DOM) may be generated in a variety of ways, but is ultimately derived from one of two sources; either through within-lake processes or through the decomposition of terrestrial organic matter derived from the surrounding catchment and subsequently delivered to water bodies via runoff. DOM from each source

has distinct structural properties, and the proportion of each within a lake's total DOM pool helps determine the *in situ* chemical and optical environments, as well as the bioavailability of nutrients to the microbial food web. The structure and quality of DOM may also be altered through exposure to UV irradiance. Lakes in the Mackenzie Delta floodplain represent a seasonal biogeochemical hotspot due to nearly continuous irradiation during the open water period, which can substantially alter the quality of the DOM pool. The objective of Chapter 3 is to examine the amount and composition of DOM in representative Mackenzie Delta lakes, and to assess the potential responses of DOM-driven chemical and optical properties of delta lakes to increased temperatures and resultant changes in biogeochemical cycles and ice cover durations. Additionally, several parameters used in other freshwater systems to characterize DOM quality and source were applied to delta lakes in order to determine both flood influence and within-lake changes in photoreactive DOM over the course of the open water season.

The potential effects of climate change in Arctic regions have been the focus of many recent studies since many of the predicted changes in biogeochemical cycles will first occur in the circumpolar Arctic (ACIA 2005). The potential repercussions in Arctic environments are substantial since annual mean warming in these regions will likely far exceed annual mean global warming (Christensen et al. 2007, ACIA 2005). In addition, the Mackenzie Delta is characterized by discontinuous permafrost, winter ice cover on water bodies, and widespread spring flooding. Changes in the extent, duration or intensity of these regimes may substantially alter the physical, chemical and optical environment of delta lakes. It is therefore important to establish baseline conditions in the Mackenzie Delta against which future changes may be measured.

1.2 References

Arctic Climate Impact Assessment (ACIA). 2005. Arctic climate impact assessment: scientific report. Cambridge University Press, New York USA. 1042 pp.

Christensen, J.H., B. Hewitson, A. Busuioc, A. Chen, X. Gao, I. Held, R. Jones, R.K. Kolli, W.-T. Kwon, R. Laprise, V. Magaña Rueda, L. Mearns, C.G. Menéndez, J. Räisänen, A. Rinke, A. Sarr and P. Whetton. 2007. Regional climate projections *in* Climate change 2007: The physical science basis. Contribution of Working Group I to the fourth assessment report of the Intergovernmental Panel on Climate Change; Solomon, S., D. Qin, M. Manning, Z. Chen, M. Marquis, K.B. Avery,. M. Tignor and H.L. Miller (eds.). Cambridge University Press, Cambridge UK and New York USA.

Emmerton, C.A. 2006. Downstream nutrient changes through the Mackenzie River Delta and Estuary, western Canadian arctic. M.Sc. Thesis, Simon Fraser University. 181 pp.

Hofmann, D.J., T.L Deshler, P. Aimedieu, W.A. Matthews, P.V. Johnston, Y. Kondo, W.R. Sheldon, G.J. Byrne and J.R. Benbrook. 1989. Stratospheric clouds and ozone depletion in the Arctic during January 1989. Nature 340: 117-121.

Salawitch, R.J., M.B. McElroy, J.H. Yatteau, S.C. Wofsy, M.R. Schoeberl, L.R. Lait, P.A. Newman, K.R. Chan, M. Loewenstein, J.R. Podolske, S.E. Strahan and M.H. Proffitt. 1990. Loss of ozone in the Arctic vortex for the winter of 1989. Geophysical Research Letters 17: 561-564 (supplement).

2 ATTENUATION OF UNDERWATER IRRADIANCE IN MACKENZIE DELTA LAKES

2.1 Introduction

The availability of solar irradiance is an important regulator of production in freshwater ecosystems. Photosynthetically active radiation (PAR, 400-700 nm), the visible portion of the electromagnetic spectrum emitted by the sun, is vital to aquatic life as it provides the energy required for photosynthetic production. Attenuation of PAR irradiance within the water column of freshwater systems can limit the growth of phytoplankton (Crump et al. 1999, Anderson 1993) as well as the extent of the lake bottom that can support benthic and rooted macrophyte life (Häder et al. 1998), and can also limit the efficiency of visually-oriented predators (O'Brien 1987). Conversely, high intensity PAR in the surface layers of aquatic systems may result in photoinhibition of phytoplankton, with maximal photosynthetic rates occurring deeper in the water column (Kirk 1994a). Ultraviolet (UV) irradiance also plays many ecologically significant regulatory roles in freshwater systems that contribute to their overall structure, function and productivity (Obernosterer and Benner 2004, Vant and Davies-Colley 1984).

Only a portion of the UV (200-400 nm) waveband emitted by the sun reaches the surface of the earth. The most highly energetic UV waveband, ultraviolet-C (UVC, 200-280 nm), is completely removed from the incoming irradiance field through strong absorption by ozone and oxygen in the earth's atmosphere. Ultraviolet-A (UVA, 320-400 nm) is the less energetic and less biologically harmful portion of the UV spectrum to reach the earth's surface, while the ultraviolet-B (UVB, 280-320 nm) waveband is considerably more energetic and has many well-documented deleterious effects on biota. Although the most damaging portion of the UVB waveband (below 290 nm) is almost entirely absorbed by the atmosphere, fluxes between 290-320 nm are reaching all latitudes of the earth in increasing quantities due to stratospheric ozone depletion (Zepp et al. 1995).

During the 1980s, an early springtime decline in stratospheric ozone amounts over the Antarctic was discovered (Farman et al. 1985, Madronich 1994). Losses in stratospheric ozone resulted from destructive reactions catalyzed by the chlorinated by-products of industrial chemicals, in combination with sustained and intensely cold temperatures in the Antarctic polar vortex during early spring that further promoted these

reactions. Although springtime conditions in the Arctic are less favourable for the prolonged formation of a polar vortex and the polar stratospheric clouds that are necessary for catalytic ozone destruction, within several years it was discovered that the identical process was occurring there as well (e.g. Salawitch et al. 1990, Hofmann et al. 1989). Since 1979, mean annual total column ozone over the Arctic has declined by about 3% per decade, although there is a high degree of interannual variability in the extent of ozone loss (ACIA 2005). Seasonal Arctic ozone depletion is predicted to increase for the next several decades followed by a gradual recovery as ozone-depleting chemicals, now banned by the Montreal Protocols, are removed from the atmosphere (Baird 1999). However, the period until full recovery of the ozone layer occurs remains uncertain, as climate change effects on temperatures and trace gases may promote additional losses in stratospheric ozone (Wrona et al. 2006, Rex et al. 2004). Therefore, Arctic freshwater ecosystems will be exposed to elevated levels of *in situ* UVB irradiance for at least the next several decades, altering the spectral composition of underwater irradiance upon which many biological and geochemical processes depend (Laurion et al. 1997).

2.1.1 Ultraviolet Irradiance in Freshwater Ecosystems

The intensity of UV irradiance in inland waters influences both *in situ* abiotic and biotic processes. Although much of the incident irradiance received at the earth's surface is converted to thermal energy, a significant portion of the UV range is used to drive biogeochemical cycles (Zepp et al. 1995). Therefore, rates of processes such as nitrogen and phosphorus cycling, and subsequent nutrient levels in lakes, are sensitive to alterations in ground-level irradiance (Steinberg 2003).

Nutrient levels in aquatic systems are determined, in part, by rates of dissolved organic matter (DOM) cycling. DOM is ubiquitous in aquatic systems, and is comprised of a heterogeneous mixture of carbon-based molecules derived from two differing sources; either *in situ* photosynthetic production, or decomposition of terrestrial organic matter originating in the surrounding catchment. Of the two, DOM that is terrestrial in origin (known as chromophoric DOM, or CDOM) is more photolytically active since it contains a higher proportion of aromatic carbon rings that strongly absorb UV irradiance.

The absorption of UV by terrestrially-derived CDOM in aquatic systems results in the photolysis, or breakdown, of CDOM into smaller molecules with different spectral and molecular properties than the parent material (Bertilsson and Tranvik 2000). This process is known as photobleaching, and is well documented in aquatic systems (e.g. Vähätalo et al. 2003, Gibson et al. 2000, Bertilsson and Tranvik 2000, Moran and Zepp 1997, Allard et al. 1994, DeHaan 1993, Valentine and Zepp 1993). While both UVB and UVA irradiance can supply the required energy to fuel CDOM photobleaching, UVB wavelengths are far more energetic and have a greater photobleaching capacity per photon. However, total UVA fluxes are many times higher than UVB fluxes, resulting in UVA driving the majority of *in situ* photobleaching in freshwater ecosystems (Reche et al. 2000).

Complete photolysis results in the production of dissolved inorganic carbon (DIC) compounds such as CO_2, while incomplete photolysis produces a range of lower molecular weight organic compounds that are more UV-transparent than the original CDOM compounds (Moran and Zepp 1997). This reduces the capacity of CDOM to absorb UV irradiance (Lindell et al. 1995), thereby increasing the penetration of UV through the water column over time. Irradiation and photobleaching of CDOM has also been shown to significantly increase the pool of bioavailable carbon substrates, such as carbohydrates and fatty acids (Moran and Zepp 1997), which support increased rates of bacterial growth (Lindell et al. 1995) and as well as increased rates of carbon cycling in aquatic systems (Wetzel et al. 1995). Therefore, CDOM photobleaching can have beneficial effects for aquatic food webs.

The damaging direct effects of UV irradiance on biota are known to increase sharply with decreasing wavelength. For instance, over the range of UV wavelengths reaching the earth's surface (290 to 400 nm), the solar radiation flux drops by three orders of magnitude as wavelength decreases, while the potential for DNA damage increases by three to five orders of magnitude (Laurion et al. 1997). Therefore, it is the UVB waveband that is the most harmful to aquatic biota in spite of the much lower fluxes received at ground level when compared to UVA. Although UVB irradiance is more biologically damaging than are longer wavelengths, it is also more rapidly attenuated in the water column thus mitigating photodamage to aquatic biota (Huovinen et al. 2003).

In spite of this, recent investigations have indicated that many aquatic ecosystems are under considerable UVB stress even at current levels (Häder and Worrest 1997). With climate change scenarios indicating future increases in incident UVB at all latitudes, aquatic ecosystems will certainly experience the effects of elevated UVB (Crump et al. 1999) with even modest increases expected to alter food webs and disrupt the larval stages of many aquatic organisms (Osburn et al. 2001). Elevated underwater UVB irradiance fluxes may be especially harmful in systems of shallow lakes and ponds that are not deep enough to provide a refuge from exposure through water column attenuation, with important implications for non-motile macrophytes and benthic communities (Molot et al. 2004, Häder et al. 1998).

Many aquatic organisms have a low tolerance for UVB exposure and are susceptible to varying amounts of UVB-induced damage at the cellular level. Studies have indicated that UVB irradiance has direct negative effects on freshwater species from bacteria (Medina-Sanchez et al. 2002) and phytoplankton (Hessen et al. 1997) to zooplankton (Molot et al. 2004) and fish (Häder and Worrest 1991). For instance, UVB irradiance may harm zooplankton that remain in surface waters during the day, resulting in increases in less susceptible primary producers that are no longer suppressed by grazing (Williamson et al. 1994). Some UVB-sensitive organisms, such as cladocerans, moderate their exposure to UVB through behavioural avoidance by migrating deeper into the water column during periods of high fluxes (Leech et al. 2005, Leech and Williamson 2001). Other aquatic organisms produce sunscreening pigments to protect against UV exposure. These pigments, such as carotenoids, scytonemin and mycosporine-like amino acids, provide a shield against potential UV-induced damage to the photosynthetic pathway in algal mats (Bonilla et al. 2005), and also shield against DNA damage in some types of zooplankton such as ciliates (Tartarotti et al. 2004) and copepods (Moeller et al. 2005). Additionally, irradiance in the UVA range has been shown to mitigate some forms of UVB-induced photodamage through photorepair processes (Quesada et al. 1995).

CDOM photobleaching may also have indirect harmful effects on aquatic organisms through the production of hydrogen peroxide (H_2O_2) or reactive oxygen species (ROS) such as hydroxyl radical (*OH) or singlet oxygen ($^1O_2$). These toxic by-products of photolysis can lead to cellular damage in organisms (Febria 2005, Cooper et

al. 1989) and may promote other photochemical reactions, such as suppression of enzymatic processing of DOM in the water column (Scully et al. 2003), that may indirectly inhibit organisms such as microbes and bacteria.

2.1.2 Effects of Increased UVB Fluxes on Arctic Freshwater Ecosystems

Arctic lakes experience prolonged periods of irradiance exposure around the summer solstice, when 24 hour daylengths occur during the ice-free open water season. Although irradiance is continuous, low solar elevations at high latitudes result in longer atmospheric paths, and therefore more scattering and higher proportions of diffuse irradiance (Campbell and Aarup 1989), somewhat mitigating deleterious UVB effects on biota. Additionally, instantaneous UVB fluxes in the Arctic have historically been lower than those at lower latitudes (ACIA 2005), although cumulative exposure in the Arctic may not be substantially less due to 24 hour daylengths. If the stratospheric ozone layer continues to thin at high latitudes, instantaneous UVB fluxes during the spring could rise to levels that have not been previously encountered in Arctic freshwater ecosystems, with a variety of direct and indirect harmful effects on biota. Additionally, global circulation models indicate that climate change may result in decreased stratospheric temperatures that will stabilize the Arctic polar vortex each spring (Wrona et al. 2006), increasing rates of catalytic ozone loss in the stratosphere and further increasing ground-level fluxes of UVB irradiance in the Arctic. These increased fluxes are likely to act cumulatively or synergistically with other climate change stressors to alter the physical, chemical and biological characteristics of Arctic freshwater ecosystems (Wrona et al. 2006).

The Mackenzie Delta, located in the western Canadian Arctic, is an extremely lake-rich and productive alluvial ecosystem (Mackenzie River Basin Committee 1981) underlain by permafrost. It is the second largest delta in the circumpolar Arctic (Marsh 1998), and is located in a region that is expected to experience far more extreme climate change than most other areas of the globe. Annual mean temperature in the western Canadian Arctic is expected to increase by between 3-5 °C over the 1981-2000 baseline by 2071-2090, roughly twice the predicted annual mean temperature increase for the entire globe (ACIA 2005). Therefore, indirect consequences of increased temperatures

on the future underwater irradiance environment in Mackenzie Delta lakes are likely to be severe when considered in conjunction with increased regional UVB fluxes.

Increasing air temperatures in the Arctic will reduce the annual period of ice cover on freshwater environments. High latitude aquatic ecosystems are ice covered for the majority of the year, which shields the water column from UVB exposure if it is sufficiently thick. For instance, Perovich (1993) found that 1.3 m of white ice cover would reduce the amount of transmitted irradiance at 300 nm by two orders of magnitude. Each summer, this ice cover melts and allows for increased penetration of all wavelengths of irradiance into the water column. The open water season each summer is a short but intense period when photolytically-driven reactions, such as photosynthesis and photobleaching, can occur continuously in lakes due to 24 hour daylengths. Projected increases in ambient temperatures in the Arctic will likely lead to an earlier break-up and later freeze-up (Prowse et al. 2006), exposing aquatic ecosystems to longer ice-free periods and increased irradiance fluxes. The period when photolytic reactions can occur will lengthen, while simultaneously increasing organism exposure to UVB within the water column (Prowse et al. 2006).

Rising air temperatures will also lead to melting of the permafrost layer (Wrona et al. 2006) and an increase in vegetation at northern latitudes (Pienitz and Vincent 2000). Both will result in increased loads of DOM to Arctic aquatic systems, which will interact with the elevated levels of UVB irradiance that have already been observed at temperate and polar latitudes in the northern hemisphere (Arts et al. 2000; Laurion et al. 1997; Rouse et al. 1997; Williamson et al. 1996; Morris et al. 1995). The underwater irradiance environment will be significantly altered by increased inputs of CDOM derived from decomposing terrestrial vegetation, which acts as a natural sunscreen in freshwater environments by absorbing UV wavelengths and thereby shielding organisms from UVB exposure. The overall effect of CDOM sunscreening will likely outweigh that of increased UVB fluxes, ultimately resulting in lower levels of *in situ* irradiance and a corresponding reduction in UV-induced photodamage and rates of primary production (Obernosterer and Benner 2004). However, an increased pool of CDOM substrate combined with increased UVB fluxes is also likely to increase rates of ROS production during the summer (Febria et al. 2006). This would result in increased indirect harmful

effects on microorganisms, perhaps offsetting some of the benefits of sunscreening by CDOM.

2.1.3 Attenuation of Irradiance within Aquatic Ecosystems

Within natural water columns, incoming solar irradiance may be attenuated through either scattering or absorption of individual photons. Scattering deflects photons and impedes the vertical penetration of irradiance through a water body by increasing the distance photons must travel to reach a certain depth. With the exception of backscatter in the uppermost layers of a water body, which causes some photons to be re-emitted from the surface, scatter does not actually remove irradiance from the water column but instead increases the likelihood that photons will be captured by an absorbing component while passing through the water column (Kirk 1994a, Bowling et al. 1986). Therefore, scatter can play a significant role in determining the rate at which photons are absorbed per unit depth (Kirk 1994b). On the other hand, absorption results in the net removal of photons from the *in situ* irradiance field when they are captured by photoreceptors (Kirk 1994a). Absorbed photons supply the energy needed to drive photolytic reactions, such as photosynthesis, biochemical processes, or geochemical cycling, as well as determining the heat budget within aquatic systems (Belzile et al. 2004). The rate at which irradiance is attenuated is expressed using a diffuse attenuation coefficient (K_d, units of m^{-1}). The construction of *in situ* K_d values assumes the validity of the Beer-Lambert law, which describes the exponential loss in irradiance with increasing depth as particulates and dissolved substances attenuate irradiance within the water column. Values of K_d are more sensitive to changes in the concentration of dissolved and particulate materials, and less to variations in irradiance produced by cloud cover or solar zenith angle (Sommaruga and Psenner 1997).

In addition to small amounts of attenuation in the PAR waveband by water molecules themselves, the majority of irradiance is attenuated within natural water columns by three components. These are CDOM, particulate matter (herein referred to as total suspended solids, or TSS), and photosynthetic chlorophyll *a* pigment (Chl-*a*; Maloney et al. 2005, Belzile et al. 2002, Häder et al. 1998, Jerome and Bukata 1998, Kirk 1994a, Scully and Lean 1994).

Absorption by CDOM alone is usually responsible for the majority of UV attenuation in aquatic systems (Gibson et al. 2000, Laurion et al. 1997, Morris et al. 1995). Additionally, CDOM absorbs small amounts of PAR irradiance in the blue wavelengths (Bowling et al. 1986). TSS scatters incoming irradiance of all wavelengths (Bukaveckas and Robbins-Forbes 2000), while Chl-*a* pigment absorbs some PAR wavelengths to provide the energy needed to fuel photosynthesis as well as contributing to scatter within the water column (Kirk 1994a). While CDOM and TSS often drive attenuation in freshwater systems, the influence of Chl-*a* on total attenuation is normally small, particularly in the UV waveband. For example, in lakes with total Chl-*a* concentrations less than 20 $\mu g\ L^{-1}$, attenuation by Chl-*a* amounted to less than 0.1 m^{-1} (Bukaveckas and Robbins-Forbes 2000).

CDOM and TSS concentrations vary widely among lakes since they are determined by hydrological and climatological characteristics in the surrounding watershed. This leads to a correspondingly wide variation in underwater spectral irradiance among freshwater environments. In high Arctic lakes, attenuation is generally lower than in temperate and subarctic lakes due to lower levels of terrestrial vegetation in the watershed (Vincent and Pienitz 1996). However, attenuation may reach levels comparable to those observed at lower latitudes in lakes within Arctic deltas that are fed by large north-flowing rivers. Arctic deltaic lakes receive inputs from more southerly upstream tributaries that are, comparatively, loaded with allochthonous CDOM derived from the decomposition of terrestrial plants. Following flooded periods during the spring melt, smaller inputs of CDOM are gained from local drainage of floodwaters as they recede over the floodplain. Allochthonous CDOM contains a high proportion of aromatic carbon rings, which strongly absorb UV wavelengths (McKnight et al. 2001). Additionally, deltaic lakes generally contain high concentrations of TSS that are also carried in river water (Welcomme 1979). Once the flatter, broader delta is encountered, flow rates decline as the river spreads out over a greater area, depositing TSS within lakes and further increasing attenuation.

2.1.4 Research Objectives

The objectives of this chapter were: (1) to characterize the underwater spectral irradiance environment in representative Mackenzie Delta lakes and calculate the corresponding diffuse attenuation coefficients (K_dx) and 1% photic depths ($z_{1\%}x$) for the UVB, UVA and PAR wavebands, and (2) to determine the contributions of CDOM, TSS and Chl-*a* to total *in situ* irradiance attenuation within each waveband in lakes with differing hydrological regimes.

In situ measurements of spectral irradiance had not previously been attempted in this system. Prior to this study, inferences of UV attenuation in Mackenzie Delta lakes were made using laboratory-based absorption readings of filtered water samples or extrapolations from integrated underwater PAR measurements (Squires and Lesack 2003, Squires 2002). Therefore, this project represented a first attempt at characterizing *in situ* spectral irradiance environments at biologically relevant wavelengths, as well as linking measured conditions to previous work on CDOM photobleaching (Febria 2005), toxic by-products of photochemical reactions (Febria 2005) and macrophytic production in Mackenzie Delta lakes (Squires 2002). Underwater irradiance can be measured using a variety of commercially available instruments. For this study, an OL 754 Portable High Accuracy UV-Visible Spectroradiometer (Optronics Laboratories, Orlando FL) was used to take measurements of spectral irradiance from 280 to 800 nm at 2 nm intervals. The OL 754 is a very useful instrument for field measurements as the properties of the UV and visible ranges can be separated, and variations in irradiance intensity with wavelength can be determined. It was anticipated that diffuse attenuation coefficients for each waveband would be higher, and the corresponding 1% photic depths shallower, at sites where the influence of a distributary channel was greater during the open water season. Sites more directly connected to distributary channels, and lakes with lower sill elevations, are more likely to receive inputs of channel water which generally contains greater concentrations of TSS and CDOM than does lake water, thereby increasing attenuation. Also, it was expected that attenuation would generally decrease over the open water season as TSS settled out of the water column and CDOM was photobleached, increasing the penetration of all wavelengths.

The second objective of this chapter was to determine the contributions of CDOM, TSS and Chl-*a* to total *in situ* irradiance attenuation within each waveband. A twofold approach was taken to this objective: first, the spatial patterns and temporal variability of waveband attenuation by CDOM, TSS and Chl-*a* , considered individually, were determined in delta lakes. It was hypothesized that the CDOM portion of the total dissolved organic carbon (TDOC) pool would be the dominant attenuator of UV wavebands, while PAR wavelengths would be attenuated by both TSS and Chl-*a*. Therefore, a complex pattern was expected when sites were considered individually, with gradients of limnological parameters predicting which constituents dominated attenuation at a given site. Second, empirical equations that predicted waveband attenuation in delta lakes using measurements of the above limnological parameters were developed. Similar equations have been constructed in other freshwater systems (e.g. Smith et al. 2004, Morris et al. 1995, Scully and Lean 1994) as well as in lakes of the Mackenzie Delta using proxy spectrophotometric measurements as approximations of *in situ* UVB attenuation (Squires 2002). It was hypothesized that, when all sites were considered, reasonably robust equations to predict UVB and UVA attenuation could be constructed from CDOM measurements alone. However, inclusion of TSS was expected to increase the predictive capability of the equations since the annual flood adds high amounts of TSS, which attenuates all wavelengths, to Mackenzie Delta lakes.

2.2 Methods

2.2.1 Study Site and Design

The Mackenzie Delta lies at the northern terminus of the 1700 km long Mackenzie River (Figure 2.1). Much of the delta is underlain by discontinuous permafrost up to 100 m thick, with unfrozen sediment underlying some lakes and river channels. The delta contains approximately 45000 permanent lakes (Emmerton 2006) covering about half of its surface area of 13000 km^2. These lakes are generally small (less than 10 ha), shallow (mean depth less than 2 m), and unstratified (Squires 2002). The abundance of lakes and channels in the delta moderates its climate relative to the surrounding tundra and boreal forest.

The Mackenzie Delta has a complex hydrology resulting from the northward flow of the Mackenzie River. Flooding occurs each spring during the annual melt due to a combination of ice-jamming in distributary channels and inundation by melt water from southerly, upstream tributaries (Mackay 1963). This yearly flooding results in a single large pulse of sediment, nutrients and organic matter entering many delta lakes over a relatively short period of time. During the rest of the open water season, the delta experiences a net loss of water due to evaporation, rapid drops in water levels following flooding, and near-desert levels of annual precipitation (Bigras 1990, Mackay 1963).

A lake will become flooded when water levels in delta distributary channels exceed that of the lake sill, which is the highest topographic point along the route followed by floodwaters as they flow from a distributary channel into a lake (Squires and Lesack 2003). Mackay (1963) proposed three classes of floodplain lakes in the Mackenzie Delta that were later quantified according to sill elevation by Marsh and Hey (1989; Figure 2.2):

No-closure lakes (12% of Mackenzie Delta lakes) are permanently connected to distributary channels and are therefore flooded throughout the entire summer. No-closure lakes have sill elevations less than 1.5 m asl.

Low-closure lakes (55% of Mackenzie Delta lakes) are flooded each spring during the break-up period, but become separated from main distributary channels at some point during the summer due to falling water levels. Low-closure lakes have sill elevations between 1.5 and 4.0 m asl.

High-closure lakes (33% of Mackenzie Delta lakes) have sill elevations in excess of the average annual flood level, and therefore are not flooded during every break-up period. During years that they do receive floodwater, they rapidly become separated from distributary channels due to falling water levels. High-closure lakes have sill elevations greater than 4.0 m asl.

This delta-wide gradient in flooding frequency gives rise to predictable gradients in several limnological parameters that have been observed in past studies (Figure 2.3). Chl-*a* and TSS concentrations are generally higher in no- and low-closure lakes, which receive floodwaters for at least part of the open water season each year. Concentrations of TDOC and its non-chromophoric fraction increase with decreasing flood frequency, while CDOM absorbencies decrease with decreasing flood frequency (Febria 2005). Down-welling irradiance is generally attenuated most rapidly in no-closure lakes, while the lowest attenuation values are found in high-closure lakes (Riedel 2002). In chains of lakes with identical sill elevations that are connected to a distributary channel at a single point, distance from the channel connection determines the water chemistry of individual lakes (Fig 2.4). Those closer to the distributary channel tend to have higher concentrations of TSS and Chl-*a*, as well as higher CDOM absorbencies, while lakes further from the channel connection tend to have higher concentrations of TDOC and non-chromophoric DOM as well as clearer water columns (Squires 2002). However, the severity of the gradient is strongly dependent on the height of the annual flood, and is therefore variable between years.

Two sets of lakes near the town of Inuvik, NT (68°19' N, 133°29' W) were monitored during the summer of 2004 in order to assess the *in situ* attenuation of ultraviolet and visible irradiance. Lake sets were selected based on prior research in the Mackenzie Delta in order to represent a range of water chemistry parameters as determined by either sill elevation or distance from the channel connection.

Sill Set Lakes

All lakes in the sill set are located within 5 km to the southwest of Inuvik (Figure 2.5a). This lake set is comprised of three spatially discrete lakes that span the range of flooding frequencies as determined by sill elevation (Table 2.1a); Lake 129 (a directly connected no-closure lake), Lake 520 (an indirectly connected high-closure lake), and Lake 80 (an indirectly connected no-closure lake). All three lakes were accessible via motorboat or a dock. Vertical profiles of *in situ* downwelling irradiance were taken from 4 to 6 times in the sill set lakes during the open water season of 2004. Lake 80 was scanned least frequently since falling water levels in the delta eventually rendered the lake inaccessible by motorboat. Concentrations of TSS, Chl-*a*, TDOC and CDOM were measured weekly or biweekly in all sill set lakes throughout the 2004 open water season.

Chain Set Lakes

The chain set lakes are a series of three sequentially connected no-closure lakes located approximately 15 km north of Inuvik off the East Channel (Fig 2.5b, Table 2.1b). In this system, all three lakes remain connected to the main distributary channel throughout the open water season with riverine influence controlled by distance from the channel connection. Nine sampling sites spanned the length of the chain set. Vertical profiles of i*n situ* downwelling irradiance were taken at all chain set sites six or seven times during the open water season of 2004. Concentrations of TSS, Chl-*a*, TDOC and CDOM were measured weekly or biweekly throughout the 2004 open water season.

2.2.2 *In Situ* Irradiance Scans

Instrumentation

Spectral downwelling irradiance was measured using a submersible integrating sphere assembly (OL IS-470-WP, Optronics Laboratories, Orlando, FL) attached to a UV-visible scanning spectroradiometer (OL 754-O-PMT, Optronics Laboratories) via a 10 m quartz fibre optic cable. The aperture of the integrating sphere was covered by a UV-grade quartz dome. Field measurements were made possible by routing power from 12 V batteries through a control unit (OL 754-C, Optronics Laboratories) and using a notebook computer as an instrument control terminal and for data storage.

At the beginning of the 2004 field season, the spectroradiometer was calibrated at Pacific Biological Station in Nanaimo, BC, against a NIST traceable 200 W tungsten-halogen lamp (OL 752-10, Optronics Laboratories). A dual calibration and gain check source module (OL 752-150, Optronics Laboratories) was used to confirm the wavelength and gain accuracy of the instrument immediately prior to taking scans each day.

Scanning Procedures

The submersible integrating sphere was extended from the port side of a small aluminium boat on a 3 m parallelogram swing arm equipped with a depth indicator (Figure 2.6). The arm allowed the submersible sphere to be lowered and held at the selected depth while scans were taken. While measurements were taken, the boat was anchored in place with the sun positioned directly off the port side in order to avoid shading of the integrating sphere aperture by the boat. Therefore, only the diffuse component of the global irradiance field was affected by boat shadow.

Vertical profiles consisted of spectral scans of downwelling irradiance (280-800 nm, 2 nm intervals) taken immediately beneath the surface and at several sequential depths in the water column to a maximum depth of 1 m. In most cases, several replicate scans, each lasting 1-2 minutes, were taken at each depth. All scans were taken as close to solar noon (3:00 PM Mountain Daylight Time, MDT) as possible to reduce changes in incident irradiance associated with changing solar elevation.

In situ spectral scans were taken during periods of either clear or evenly overcast sky conditions. Most studies of underwater irradiance only use measurements taken on days with completely clear sky conditions in order to avoid the effects of changing cloud cover on *in situ* measurements. However, summer sky conditions in the western Canadian Arctic are unpredictable and prone to rapid changes in the extent of cloud cover, making scanning during clear sky conditions challenging. Therefore, in order to maximize the frequency of *in situ* irradiance scanning, measurements were taken during periods with constant sky conditions (either clear or overcast) as in Laurion et al. (2000). The direct and diffuse portions of the incident irradiance field at each wavelength were calculated using the Simple Model of the Atmospheric Radiative Transfer of Sunshine (SMARTS2, v.2.9.2) developed by Gueymard (2002). Due to both scattering and absorption of incident irradiance by cloud cover, overcast conditions reduce the

proportion of direct irradiance at all wavelengths (Figure 2.7a), although the reduction is most pronounced at shorter wavelengths (Figure 2.7b). This alters the proportions of total direct UVB, UVA and PAR that are received by the water body when compared to clear sky conditions.

Diffuse light is more likely to be reflected at the surface of the water body, leading to a reduction in total irradiance entering the water column during overcast conditions. However, this study examined the attenuation of light as it passed through the water column, and therefore only the change in irradiance with depth, rather than the total amount present, was important (Kirk et al. 1994). Since all scans used in calculating attenuation coefficients were taken within the water column (i.e. no surface scan was used as a reference), only irradiance that had entered the water column was measured. Therefore, all K_dx values that were calculated for a specific waveband during the summer of 2004 are directly comparable to one another.

Data Processing

Spectral scan data were corrected before diffuse attenuation coefficients ($K_d\lambda$) were calculated. Instrument-specific immersion correction factors were applied to the data in order to correct for differences in the indices of refraction between air (where the instrument was calibrated) and water (where the instrument was operated). These values ranged from 1.6 to 1.8, similar to values obtained for other underwater spectroradiometers (Kuhn et al. 1999). $K_d\lambda$ is considered a quasi-inherent optical property of aquatic systems when the majority of surface irradiance is direct (Kirk 1994); however, this breaks down as solar zenith angles (SZAs) increase as the sun approaches the horizon, resulting in a high proportion of diffuse surface irradiance. For this study, SZAs were calculated for the midpoint time of each scan using the MIDC SOLPOS calculator (National Renewable Energy Laboratory 2005). Since the SZA for all scans of underwater irradiance taken during the summer of 2004 varied from 45 to 75°, there was a high proportion of diffuse light necessitating correction. Therefore, the attenuation coefficients at each wavelength were corrected for the geometric condition of the irradiance field by dividing by Gordon's (1989) wavelength-specific correction factor, $D_0\lambda$:

$$D_0\lambda = \frac{f_\lambda}{\cos v_{0w\lambda}} + 1.197(1 - f_\lambda)$$

where f_λ is the proportion of direct incident irradiance at each wavelength and $v_{0w\lambda}$ is the SZA below the water surface. The factor $v_{0w\lambda}$ was calculated by applying Snell's Law to the SZA above the water surface using the wavelength-specific indices of refraction for water given in Segelstein (1981).

The direct portion of the incident irradiance field at each wavelength was calculated using the SMARTS2 model, version 2.9.2, developed by Gueymard (2002). Model inputs included site latitude, longitude, surface pressure, relative humidity, and altitude as well as the date and time of each scan (further details given in Appendices A and B). Again, the midpoint time of each scan was used as an approximation. Although the resulting $D_0\lambda$ varied with wavelength, uncorrected K_d values at each wavelength always exceeded corrected ones.

Once all data were corrected, diffuse attenuation coefficients normalized to 1 m ($K_d\lambda$, m^{-1}) were calculated for individual wavelengths between all possible pairs of scans taken at a site on the same day (Kirk 1994a):

$$K_d\lambda = \frac{\ln (E_{-0\lambda} / E_{z\lambda})}{\Delta z}$$

where $E_{-0\lambda}$ and $E_{z\lambda}$ represent wavelength-specific irradiance measurements taken at different depths, z (m), in the water column.

At this point, attenuation coefficients were visually inspected for erroneous values. Since by definition attenuation coefficients cannot be negative, any negative values were deleted from the datasets. Attenuation also decreases with increasing wavelength in the UV range, so any UV attenuation coefficients that were lower than those at longer UV wavelengths were deleted. Erroneous values were removed across the entire waveband in order to avoid skewing the resulting average diffuse attenuation coefficients. Attenuation coefficients for wavelengths less than 310 nm were especially prone to error, so all K_d values below this wavelength were removed from all datasets and only the more reliable results from 310 to 320 nm were used to calculate average values for the UVB waveband. At this point, all remaining data were used to calculate average diffuse attenuation coefficients (K_dx) for each site and date; K_dUVB(310-320), covering

the UVB spectrum from 310-320 nm, K_dUVA, covering the UVA spectrum from 320-400 nm, and K_dPAR, covering the PAR spectrum from 400-700 nm.

Since only data from 310 to 320 nm were used to calculate the average diffuse attenuation coefficients for the UVB waveband, these values are underestimates for the true K_dUVB values that would have been found if all data across the waveband were valid. Therefore, an attempt was made to extrapolate the reliable portion of the K_dUVB data back to the waveband boundary of 280 nm. An exponential decline curve was fitted to data from the instance of highest UVB attenuation (S5, 15 June 2004) and lowest UVB attenuation (S8, 6 August 2004) in the chain set lakes. The formula obtained from each decline curve between 310 and 320 nm allowed for $K_d\lambda$ values to be extrapolated back to 280 nm, giving an indication of the range of actual K_dUVB values that are encountered in Mackenzie Delta lakes.

Average 1% depth penetrations ($z_{1\%}x$, m) for all wavebands were calculated for each site and date as follows (Molot et al. 2004):

$$z_{1\%}x = (4.61 / K_dx) * (1 / D_0x)$$

where x denotes a waveband (UVB, UVA or PAR), K_dx denotes the average diffuse attenuation coefficient across that waveband, and D_0x denotes the average Gordon's correction factor across the same waveband.

2.2.3 Laboratory Analyses of Water Samples

Water Sampling

Water samples were taken at the same time as *in situ* irradiance scans in order to assess ambient levels of the three most prevalent attenuators of solar irradiance in freshwater systems: TSS, Chl-*a*, and CDOM. Additionally, the TDOC concentration of each water sample was measured. Both underwater irradiance scans and water samples were taken at standard sites that were marked with a float. All water samples for lab analyses were taken as integrated samples using a 1 m long Tygon tube sampler (6.67 cm inner diameter) and a rubber stopper. Samples of the integrated water column to 1 m depth were taken and transferred to a large bucket until several litres of water were collected. The bucket was then thoroughly mixed before sample bottles were filled.

All samples were collected in polyethylene bottles that were acid washed, copiously rinsed with distilled and deionized (DDI) water, and rinsed three times with sample water before being filled. Sample bottles were stored on ice in dark coolers during transport to the Inuvik Research Centre, Inuvik, NT, where samples were filtered within 10 hours of collection.

Total Suspended Solids

A subsample of known volume was vacuum filtered through a pre-combusted (450°C for 16 h) and pre-weighed GF/C filter with a nominal pore size of 1.2 μm. Filters were then dried at 40°C for 24 hours. TSS filters were stored for up to three months before post-weights were taken, and were placed in a desiccator for several days prior to reweighing in order to remove any accumulated moisture. Filters were weighed on an analytical balance (OHaus Corporation, Pine Brook, NJ) with resolution to 0.0001 g. TSS weight per volume of lake water was calculated as follows:

$$TSS\ (mg\ L^{-1}) = (10^6)\ [(w_2 - w_1) / vol]$$

where w_1 denotes the filter pre-weight (g), w_2 denotes the filter post-weight (g), and vol denotes the known volume of sample water that was passed through the GF/C filter (L).

Total Chlorophyll-a

A known volume of sample water was vacuum filtered through a GF/C filter (nominal pore size of 1.2 μm). Filters were then extracted in a known volume of 90% acetone at a constant temperature of -4°C in dark conditions for 24 to 48 hours. Extracts were gently mixed a few hours prior to measurement in order to ensure that all extracted Chl-*a* pigment was suspended in solution. Chl-*a* was determined fluorometrically in a darkened room using a Turner 111 fluorometer (Turner Designs Inc., Sunnyvale, CA) equipped with a Wratten 47B filter for the excitation light beam (peak wavelength 350 nm) and a Corning 7-60 filter for the emission light beam (peak wavelength 670 nm). The fluorometer was calibrated prior to sample measurement using a lettuce extract in 90% acetone following the methods of Wetzel and Likens (2000). A 90% acetone solution was also used as a blank. Total Chl-*a* concentrations were calculated as follows (Wetzel and Likens 2000):

$$\text{Chl } a \text{ } (\mu g \text{ } L^{-1}) = \frac{F \text{ (fluorometer reading) } (v)}{V}$$

where F is the calibration factor, v denotes the volume of Chl-*a* extract (L), and V denotes the volume of sample water that was passed through the GF/C filter (L).

Total Dissolved Organic Carbon

Sample water was vacuum filtered through pre-combusted (450°C for 6 h) GF/F filters (nominal pore size of 0.7 μm) and stored frozen in leached and rinsed 60 mL polyethylene bottles.

Samples were thawed and warmed to room temperature immediately prior to analysis. TDOC concentrations were measured on a Shimadzu TOC-Vcsh carbon analyzer equipped with an 8 port OCT-1 autosampler (Shimadzu, Kyoto, Japan). TDOC concentrations were measured using high temperature catalytic oxidation and the non-purgeable organic carbon method. Briefly, this method requires acidifying each sample to between pH 2 – 3 by adding 0.5% (vol.) 2M HCl and then sparging for 5 minutes to remove all inorganic carbon. The sample was then combusted at 680°C, converting all organic carbon within the sample to CO_2, which was measured in a non-dispersive infrared gas analyzer. Replicate injections of each sample were run (minimum of 2 injections, maximum of 3) until the coefficient of variation fell below 2%. Calibration curves for TDOC analysis were constructed using standard dilutions of a 20 mg L^{-1} potassium hydrogen phthalate (KHP) solution. A NIST-traceable KHP standard solution (8 mg L^{-1}) was used as a periodic check of instrument accuracy. DDI blanks were run every 12 samples, and all TDOC results were blank corrected following analysis.

TDOC results were generated in units of mg L^{-1}, but were later converted to units of μmol L^{-1} using the following conversion:

$$\text{TDOC } (\mu mol \text{ } L^{-1}) = [\text{TDOC } (mg \text{ } L^{-1}) / 12.011] * 1000$$

Chromophoric Dissolved Organic Matter

Sample water was vacuum filtered through DDI- and sample-rinsed 0.2 μm nitrocellulose Millipore filters and stored in leached and rinsed 60 mL polyethylene bottles at 4°C in the dark until analysis.

CDOM absorbencies were measured spectrophotometrically on either a Spectronic 501 or Spectronic 301 (both instruments manufactured by Milton Roy, Ivyland, PA) using 10 cm optical glass cuvettes. Prefiltered (0.2 μm) DDI was used in the reference cuvette and also to take blank measurements every 10 samples. CDOM absorbance was measured at 330 nm with another reading taken at 740 nm as an index of scatter. All measurements, including blanks, were scatter corrected as follows (Whitehead et al. 2000):

$$A_{330sc} = A_{330} - A_{740}\,(330/740)$$

where A_{330sc} denotes the scatter corrected absorbance at 330 nm and A_{λ} denotes sample absorbance at the designated wavelength. Sample CDOM absorbencies were further corrected by blank subtraction. CDOM absorption coefficients (a_{330}, m^{-1}) are expressed as natural logarithms normalized to one metre, and were calculated according to Kirk (1994a):

$$a_{330} = 2.303 * A_{330sc} / l$$

where l denotes the optical pathlength (m).

2.2.4 Construction of Attenuation Models

Analysis of Significant Attenuators at Individual Sites

Individual sites did not have sufficient data points ($n < 10$) over the open water season of 2004 for robust multiple linear regression analysis. Therefore, JMP 6.0.0 statistical software (SAS Institute, Cary, NC) was used to examine a series of simple linear regressions between attenuator (CDOM, TSS, Chl-*a*) concentrations and average waveband K_dx values for each site. Simple linear regressions between TDOC concentration and K_dx were also examined for each site. The resulting patterns of significant attenuation by individual attenuators were used to examine riverine influence on *in situ* irradiance attenuation within Mackenzie Delta lakes.

Whole Set Models

The chain and sill set lakes were considered separately in the construction of whole system models since hydrological controls on attenuator levels are fundamentally different between the two systems. Total irradiance attenuation for each waveband was partitioned among CDOM, TSS and Chl-*a* using stepwise multiple linear regression analyses (Squires 2002, Vant 1990, Vant and Davies-Colley 1986). All multiple linear regressions were performed using JMP 6.0.0 with a significance level (p) < 0.15 required for an attenuator to be entered into the model. Each model also produced a constant, which is a residual term that represents measurement error as well as attenuation by water and other (non-measured) constituents.

Empirical relationships using only CDOM absorption coefficients to predict attenuation in the UVB and UVA wavebands were also constructed using JMP 6.0.0, again considering the chain and sill sets separately.

2.3 Results

2.3.1 Trends in Dissolved and Particulate Constituent Concentrations over the Open Water Season

In addition to absorption by water molecules themselves, attenuation of *in situ* irradiance in aquatic systems is controlled by the presence of both dissolved and particulate substances within the water column. Concentrations of dissolved and particulate constituents were measured at all sites where *in situ* irradiance scans were taken during the open water season of 2004. Although the same substances were tracked in these lakes during previous open water seasons (e.g. Febria 2005, Riedel 2002, Spears 2002, Squires 2002, Teichreb 1999), they were re-measured during 2004 since the system responds differently to the break-up and flood each year depending on its duration and magnitude (Marsh and Hey 1994). Both determine the extent of the delta that is inundated with floodwater, as well as the amounts of flood-borne constituents that are deposited in lakes.

In the chain set lakes, average open water TSS concentrations decreased rapidly with increasing distance from the channel connection, with sites S4 through S9 displaying similar concentrations (Figure 2.8a). Average Chl-*a* concentrations were varied but similar at all chain set sites, with no obvious decline as distance from the channel connection increased (Figure 2.8b). A previous study in the chain set lakes found that TDOC concentrations increased, and CDOM absorbencies decreased, with increasing distance from the channel connection (Squires 2002). However, these trends were not observed during the summer of 2004; rather, both average open water TDOC and CDOM levels were highest in the middle of the chain set (Figure 2.8c, d). Therefore, spatial patterns of dissolved and particulate concentrations were somewhat different than had been observed during previous years in the chain set lakes.

Average open water TSS and Chl-*a* concentrations, as well as CDOM absorbencies, decreased with increasing sill elevation in the sill set lakes (Figure 2.8a, b, d). Conversely, average TDOC concentrations increased with increasing sill elevation (Figure 2.8c). Trends in the sill set lakes follow those observed during previous studies (Febria 2005, Riedel 2002, Squires 2002), and clearly illustrate the influence of sill

elevation and the annual flood on limnological gradients in discrete Mackenzie Delta lakes.

2.3.2 Attenuation of *In Situ* Irradiance

A time series of *in situ* attenuation at two sites illustrates some general characteristics of irradiance attenuation in freshwaters (Figure 2.9). Two chain set sites were chosen to illustrate differences in attenuation resulting from differing DOM compositions; S5, where CDOM absorption was high throughout the summer, and S9, where CDOM absorption was low. Attenuation decreases as wavelength increases, with UVB wavelengths attenuated most rapidly within the water column at both sites. However, sites with higher CDOM levels as measured by absorption at 330 nm, such as S5, have higher attenuation at all wavelengths in the UV range. Conversely, PAR irradiance is attenuated least rapidly and penetrates most deeply into the water column (Figure 2.10). The ability of the water column to attenuate irradiance of all wavelengths generally decreased over the open water season at monitored Mackenzie Delta sites (Figure 2.9). This is primarily due to two processes that remove light-attenuating constituents from the water column: first, the settling out of TSS carried in floodwaters, thereby reducing scatter of irradiance at all wavelengths, and second, photodegradation of CDOM, which reduces the capacity of the water column to absorb UV and blue irradiance. This loss of absorption capacity is due to the breakdown of chromophoric molecules in the DOM pool that occurs upon photon absorption.

Average K_d values for a portion of the UVB waveband (310-320 nm, Figure 2.11a), the UVA waveband (Figure 2.11b) and the PAR waveband (Figure 2.11c), along with K_d values at each waveband boundary, are shown for all sites in the chain set during the open water season of 2004. A corresponding set of graphs are shown for the sill set lakes (Figure 2.11d). The range of diffuse attenuation coefficients across each waveband were displayed in this manner so that extreme values and averages could be examined simultaneously. Measurements of error were not calculated since the variation in $K_d\lambda$ within each waveband was a result of the rapid decline in attenuation with increasing wavelength, rather than variation in measurements due to instrument error or sampling conditions.

Ultraviolet-B Irradiance

Values of K_dUVB(310-320) are shown in Figures 2.11a and 2.11d. Irradiance measurements at wavelengths < 310 nm were not reliable (i.e. some values of $K_d\lambda$ at wavelengths < 310 nm were either smaller than those at longer UVB wavelengths or were negative numbers). Therefore, all measurements at wavelengths below 310 nm were excluded from analysis in order to maintain a consistent UVB waveband range between all sites, which ensured that all K_dx values calculated for the UVB waveband were comparable.

At most sites, attenuation of UVB wavelengths during the 2004 open water season was highest immediately following the spring flood and declined rapidly thereafter (Figs. 2.11a, 2.11d). In the chain set, the highest initial UVB attenuation was found at S5 in the middle of the chain. Decreases in UVB attenuation over the open water season were largest at sites in the middle of the chain set (S4-S6), followed by sites closest to the channel connection (S1-S3). The decline in UVB attenuation was much less pronounced at sites distant from the channel connection (S7-S9), where the influence of the spring flood was considerably weaker. The higher attenuation of UVB wavelengths in the middle sites of the chain set may be due to the interaction of two factors. First, the influence of the annual flood, when channel levels reach over 4 m above average open water levels (Emmerton et al. 2007), thereby affecting a large lateral extent of the no-closure chain set. Second, dilution throughout the rest of the open water season, when water at sites closest to the channel connection may become diluted by fresh inputs of CDOM-depleted channel water, thereby reducing absorption capacity (see Appendix C for a time series of CDOM absorbency in the East Channel).

In 2004, the highest K_dUVB(310-320) values in the sill set lakes were consistently found in Lake 129, a directly connected no-closure lake (Figure 2.11d). Similar to the three interconnected no-closure lakes comprising the chain set, the K_dUVB(310-320) values for Lakes 129 and 80, both no-closure lakes, were highest immediately following the spring flood and displayed an overall decline for the rest of the open water season. On 8 June, shortly after ice out, Lake 80 had a measured K_dUVB(310-320) value of 32.2 m^{-1} which declined to 15.4 m^{-1} on 28 June, illustrating the very rapid decline in UVB attenuation that occurred at most sites. However, Lake 520, an indirectly connected high-

closure lake, displayed the opposite trend over the open water season. In Lake 520, K_dUVB(310-320) increased from 15.8 m^{-1} on 21 June to 18.9 m^{-1} on 8 August, indicating higher UVB attenuation later in the open water season.

During periods of overcast conditions, $K_d\lambda$ values at the waveband limits 310 and 320 nm were much closer in value to K_dUVB(310-320) measurements than during clear conditions. Some sites (e.g. S2 and S5) had measured $K_d\lambda$ values at the waveband limits that were very close in value on some days. This may be due to a small number of useable measurements during these sampling periods.

All UVB measurements below 310 nm were discarded since they were largely erroneous, and the average diffuse attenuation coefficients for this waveband were therefore calculated over the range of 310-320 nm. An effort was made to estimate the range of true $K_d\lambda$ values for the entire UVB waveband (280-320 nm) over the open water season by considering both an instance of high (S5 on 15 June; K_dUVB(310-320) = 33.4 m^{-1}) and low (S8 on 6 August; K_dUVB(310-320) = 14.9 m^{-1}) attenuation of UVB wavelengths (Figure 2.12). For both instances, the measured $K_d\lambda$ values from 310-320 nm were plotted and an exponential decline curve was fitted to the data. The equations describing these decline curves had reasonably good fit to the measured data (S5 on 15 June, $r^2 = 0.98$; S8 on 6 August, $r^2 = 0.74$). The equations were then used to extrapolate $K_d\lambda$ values back through the UVB waveband to 280 nm. From the extrapolated data, an estimate of true $K_d\lambda$ values at the UVB waveband boundaries could be calculated, as well as estimates of true K_dUVB values. Since the sites that were considered were extreme examples of UVB attenuation, we can conclude that all sites sampled in the summer of 2004 had true K_dUVB values between 17.1 m^{-1} (S8, 6 August) and 57.7 m^{-1} (S5, 15 June). Therefore, K_dUVB(310-320) values calculated at sites with low attenuation, such as S8, were closer to extrapolated true K_dUVB values than were K_dUVB(310-320) values calculated for sites with higher attenuation.

Ultraviolet-A Irradiance

Average diffuse attenuation coefficients for the UVA waveband are shown for both the chain set (Figure 2.11b) and the sill set lakes (Figure 2.11d). Similar to the UVB waveband, K_dUVA values were highest immediately following the flood at most sites, and declined rapidly as floodwaters subsided. The decline in UVA attenuation

coefficients occurred rapidly, with the decline curves flattening out by the middle of the open water season. Again, similar to K_dUVB(310-320) values, K_dUVA values were highest throughout the open water season at sites in the middle of the chain set (S4-S6) where CDOM levels were also highest (Figure 2.8). The lowest K_dUVA values were found at sites S7-S9, where flood influence was considerably weaker than at other sites in the chain set. K_dUVA values remained low at these sites throughout the open water season.

The exception to the observed trend of declining K_dUVA values over the open water season occurred in Lake 520, an indirectly connected high-closure lake. Lake 520 exhibited a very different trend in attenuation when compared to the no-closure lakes that comprised the remainder of the study sites. In Lake 520, K_dUVA values remained fairly constant throughout the open water season of 2004, with values fluctuating between 7.4 m^{-1} and 9.7 m^{-1}.

Photosynthetically Active Radiation

K_dPAR values are shown for the open water season of 2004 for all chain set sites (Figure 2.11c) and sill set lakes (Figure 2.11d). Also shown are the attenuation coefficients for both extremes of the PAR waveband (K_d(400) and K_d(700)). This waveband had the greatest number of measurements incorporated into each K_dx value, and is therefore biased towards attenuation measurements at longer wavelengths due to the very rapid reduction in attenuation as wavelength increases from the UV/PAR boundary at 400 nm. Similar to both the UVB and UVA wavebands, PAR attenuation values were highest immediately following the spring flood, and declined rapidly thereafter. However, the magnitude of the decline in K_dPAR values was much less than for the other wavebands. Observed declines in PAR attenuation were predominantly due to TSS settling out of the water column. Unlike attenuation measurements in the UV wavebands, Lake 520 did not exhibit a K_dPAR trend that was markedly different from the other study sites.

There is evidence at sites closest to the channel connection (S1-S4) and in Lake 129, a directly connected no-closure lake, of a slight but noticeable increase in K_dPAR values at the end of July. This is likely due to a storm surge from the Beaufort Sea that raised channel levels by approximately 0.6 m following several days of sustained high

winds from the north (WSC 2006). This increased the levels of TSS at these sites due to an influx of channel water, thereby increasing PAR attenuation in these lakes for a short period.

2.3.3 1% Photic Depths

Figure 2.13 shows 1% photic depths for all sampling sites where irradiance scans were taken. The 1% photic depth represents the depth to which 1% of the incident irradiance of a waveband penetrates, or conversely, the depth at which 99% of the incident irradiance in that waveband has been attenuated within the water column. Photic depths are related to the average diffuse attenuation coefficient for a waveband, with higher $K_d x$ values indicating more rapid attenuation in the water column (*i.e.* a greater proportion of incident irradiance is attenuated with every metre depth in the water column and therefore, photic depths are shallower).

Ultraviolet-B Irradiance

The 1% photic depths for UVB wavelengths between 310 and 320 nm for the chain set sites are shown in Figure 2.13a, and those for the sill set lakes are shown in Figure 2.13d. In the chain set, $z_{1\%}$UVB(310-320) depths were shallowest at sites in the middle of the chain set, while the deepest photic depths were found at sites furthest from the channel connection. This illustrates that photic depths are influenced by flood-borne constituents, such as CDOM, that are carried in floodwaters and strongly attenuate UVB irradiance in aquatic systems. UVB 1% photic depths increased at most monitored sites over the open water season, from approximately 10-15 cm in mid-June to 20-25 cm in early August. This indicated increasing penetration of UVB irradiance through the water column due to CDOM photodegradation over the course of the open water season. The exception to this trend occurred in Lake 520, where photic depths decreased over the open water period.

Although only a portion of the UVB waveband was directly measured in this study, it can be assumed that virtually all incident UVB was attenuated in the top 30 cm of the water column throughout the 2004 open water season. Since wavelengths between

310 and 320 nm are the least energetic of those comprising the UVB waveband, they penetrate most deeply through the water column.

Ultraviolet-A Irradiance

The 1% photic depths for the UVA waveband are shown in Figure 2.13b (chain set lakes) and Figure 2.13d (sill set lakes). In the chain set lakes, the deepest 1% photic zones for UVA were found at sites S7-S9, furthest from the channel connection and where the spring flood influence was weakest. In contrast to the photic depths found for the UVB waveband, the shallowest 1% photic depths in the chain set were found closest to the channel connection point. At most sites, 1% photic depths for the UVA waveband increased over the course of the open water season from approximately 20-30 cm in mid-June to 35-50 cm in early August. Again, the exception to this trend occurred in Lake 520, where 1% photic depths for UVA decreased over the open water season of 2004.

Since the entire UVA waveband was directly measured, it can be concluded that UVA irradiance was essentially eliminated within the top 50 cm of the water column at all sites.

Photosynthetically Active Radiation

The 1% photic depths for the PAR waveband (also referred to as the photosynthetic compensation depth) are shown in Figure 2.13c (chain set lakes) and Figure 2.13d (sill set lakes). In the chain set lakes, PAR 1% photic depths were greatest at sites distant from the channel connection throughout the open water season. Photic depths for the PAR waveband increased at all sites over the open water season of 2004. Increases in PAR 1% photic depths were greatest at sites that were most distant from channel connections (e.g. S7, S8, S9 and Lake 80), reflecting the decreased lateral influence of distributary channels as water levels dropped post-flood. In the sill set lakes, PAR 1% photic depths increased rapidly in no-closure lakes during the early open water season. In contrast to the UVB and UVA portions of the incoming irradiance field, PAR 1% photic depths also increased in Lake 520 over the open water season. By the end of the open water season Lake 520 displayed the deepest PAR 1% photic depth of all sampling sites.

PAR irradiance penetrates more deeply through any water column than either UVA or UVB. Therefore, PAR 1% photic depths in delta lakes are several times those for the UV wavebands. Since the full PAR waveband was directly measured, it can be concluded that PAR wavelengths were essentially eliminated within the top 2 m of the water column at all Mackenzie Delta sampling sites. Since this is approximately equal to the average depth of delta lakes, most lakes appear to receive sufficient PAR fluxes to support photosynthesis throughout most of their water columns.

Graphs of 1% photic depths for the PAR waveband also show evidence of a storm surge from the Beaufort Sea during late July 2004. Several days of sustained high winds from the north raised channel levels in the mid-delta by approximately 0.6 m (WSC 2006), inundating those sites closest to channel connections with a second, smaller flood of channel water. Although the channel water was depleted in both dissolved and particulate constituents by this point in the open water season, it contained sufficient amounts of TSS to increase PAR attenuation and decrease PAR 1% photic depths. This event is most evident at chain set sites S1-S5, and in Lake 129.

2.3.4 Contributions of Individual Constituents to Attenuation

Patterns of Significant Attenuation by Constituents among Individual Sites

Simple linear regressions were constructed between K_dx values and individual attenuators at each site in order to examine the influence of delta-wide limnological gradients on attenuation. The influence of TDOC concentration on waveband attenuation was also examined. The three wavebands (UVB(310-320), UVA, and PAR) were considered separately.

CDOM absorbencies were significantly correlated with diffuse UV attenuation coefficients at all sites (Table 2.2a, b; $p < 0.05$ in all cases). Generally, r^2 values for CDOM *versus* either $K_dUVB(310\text{-}320)$ or K_dUVA decreased with increasing distance from the channel connection in the chain set lakes. In the sill set, CDOM explained more of the variation in K_dx values in the UV wavebands in Lake 80 (an indirectly connected no-closure lake) and Lake 520 (an indirectly connected high-closure lake) than in Lake 129 (a directly connected no-closure lake), although all were significant relationships. This was contrary to the expected result that Lake 129, being closer to the influence of a

distributary channel, would have much more strongly correlated UV attenuation and CDOM absorbencies than those lakes further from channel connections. TSS was significantly correlated to K_dx values in the UV wavebands at S1, a site directly adjacent to the channel connection, and in Lake 80. TDOC was significantly correlated with UV attenuation only at chain set sites closest to the channel connection, while Chl-*a* was significantly correlated with UV attenuation at only a few sites (S5, S9 and Lake 129).

In contrast to the UV wavebands, CDOM absorbencies were significantly correlated with PAR attenuation only at S1 in the chain set ($r^2 = 0.761$, $p < 0.05$; Table 2.2c), as were TSS concentrations ($r^2 = 0.955$, $p < 0.05$). Chl-*a* concentrations were significantly correlated with K_dPAR values at several sites in the chain set (S3, S5 and S9). In the sill set lakes, only Lake 80 exhibited significant, or near-significant, correlations between attenuator concentrations and K_dPAR values; both CDOM absorption ($r^2 = 0.905$, $p < 0.05$) and TSS ($r^2 = 0.967$, $0.05 < p < 0.06$) were strongly correlated.

Partial Attenuation by Constituents Across Lake Sets

Multiple linear regression analyses were used to determine the contributions of CDOM, TSS and Chl-*a* to overall irradiance attenuation in lakes of the Mackenzie Delta. TDOC was excluded from multiple linear regression analyses since, on a site-by-site basis, it was highly correlated with CDOM, which comprises the chromophoric, irradiance-attenuating subset of the TDOC pool (see Appendix D). As a result, both CDOM and TDOC were strong predictors of attenuation when considered alone. However, when both were introduced to a single model, CDOM was the stronger predictor since it excluded the non-coloured and non-attenuating portion of the TDOC pool. Therefore, TDOC was not considered to remove possible confounding effects from the resulting models.

Since the chain set and sill set lakes have fundamentally different relationships between water transparency and attenuator concentrations, a separate model was used for each system, with all results summarized in Table 2.3. In the chain set lakes, only CDOM and TSS were found to contribute significantly to the overall attenuation of each waveband (Table 2.3a). For all three wavebands, the fit of the model is relatively strong ($r^2 = 0.74$ to 0.81, $p < 0.0001$ in all cases). Both CDOM and TSS are carried in channel

water and predominantly enter delta lakes via floodwater from southern tributaries during the spring melt, with smaller contributions coming from overland flow or leaching from within the surrounding catchment basin. This indicates that, in the chain set lakes, water clarity and irradiance attenuation are strongly influenced by the annual flood. Although the simple linear regression between UVB attenuation and Chl-*a* ($r^2 = 0.228$, $p = 0.0002$; Figure 2.14) is stronger than that between UVB attenuation and TSS ($r^2 = 0.036$, $p = 0.164$), Chl-*a* does not contribute significantly to overall UVB attenuation in the chain set when it is partitioned among multiple attenuators.

Partial attenuation coefficients for the sill set lakes (Table 2.3b) show a very different relationship between irradiance attenuation and attenuator concentrations. The sill set lakes exhibit a good fit of the multiple linear regression models for both UV wavebands (UVB: $r^2 = 0.84$, $p = 0.0002$; UVA: $r^2 = 0.87$, $p < 0.0001$), while the PAR waveband displays a reasonably good fit ($r^2 = 0.68$, $p = 0.0012$). CDOM, TSS and Chl-*a* were all found to contribute significantly to overall attenuation of both UVB and UVA ($p < 0.05$ in all cases). Only TSS was found to be a significant attenuator of the PAR waveband, although inclusion of CDOM and Chl-*a* improved whole-model fit by 10%. Therefore, the equation for the sill set PAR waveband included all three attenuators as well. Although the sill set lakes also display evidence of strong flood influence on water clarity, the presence of Chl-*a* as a significant attenuator in the UVB and UVA wavebands indicates that within-lake processes may also play an important role in irradiance attenuation.

In other systems, empirical power relationships using only TDOC concentrations often provide the best fit for predicting UV attenuation (e.g. Arts et al. 2000, Scully and Lean 1994). However, as the predominant attenuator of irradiance in the UV portion of the solar spectrum, CDOM absorption coefficients alone often give reasonable predictions of *in situ* UV attenuation. Several published studies have attempted to predict UV attenuation in aquatic systems using only CDOM absorbencies (Morris et al. 1995) or other CDOM characteristics such as fluorescence (e.g. Laurion et al. 1997). Both linear relationships using CDOM absorbencies and power relationships using TDOC were constructed for the UVB and UVA wavebands in both lake sets; however, in all instances, linear equations using CDOM proved the better fit. In the chain set lakes, linear

equations using CDOM absorbencies as the sole predictor explained ~69% of the variation in K_dUVB(310-320) values ($p < 0.0001$), and ~58% of the variation in K_dUVA ($p < 0.0001$) (Table 2.4a, b). The fit of the linear predictive relationships in the sill set lakes was weaker, but CDOM absorbencies still accounted for the majority of the variation in UV attenuation. CDOM absorption coefficients alone explained ~53% of the variation in K_dUVB(310-320) values ($p = 0.0047$), and ~56% of the variation in K_dUVA values ($p = 0.0021$) (Table 2.4a, b).

2.4 Discussion

Generally, values of K_dUVB(310-320) and K_dUVA measured in Mackenzie Delta lakes far exceed those measured in other Arctic lakes, and were also higher than values measured in many other subarctic (e.g. northern Quebec; Laurion et al. 1997), temperate (e.g. northeastern United States; Williamson et al. 1996) and alpine (e.g. Austrian Alps; Sommaruga and Psenner 1997) lakes. Records of underwater irradiance in Arctic lakes are predominantly from lakes located in the High Arctic, where *in situ* DOM levels are low due to low amounts of vegetation in the surrounding catchment. By comparison, lakes in the Mackenzie Delta have high TDOC and CDOM levels resulting from riverine inputs, local drainage following flooding, melting permafrost and macrophytic growth (Febria 2005), and have a far greater capacity to attenuate irradiance. Attenuation coefficients calculated over the entire UVB waveband through the extrapolation of measured decline curves from 310-320 nm (Figure 2.12) indicated that true values of K_dUVB in Mackenzie Delta lakes range from 17.1 to 57.7 m^{-1}, corresponding to 1% photic depths for the entire UVB waveband of 6-22 cm. Comparable UVB 1% photic depths have been found in some inland humic lakes in North America (Crump et al. 1999), and comparable 1% photic depths for both the UVB and UVA wavebands were found in humic lakes in central Finland (Huovinen et al. 2003). Therefore, the optical environment of Mackenzie Delta lakes seems to be determined by the presence of humic substances, as expected in a floodplain system.

Unlike all other sites monitored during the open water season of 2004, Lake 520 experienced increased UVB attenuation as the summer progressed while UVA attenuation fluctuated within a fairly narrow range of values (Figure 2.11a, b). Lake 520 is a high-closure lake that is indirectly connected to distributary channels, and as such, experiences either short periods of flooding or no flooding at all in any given year. During the open water season of 2004, Lake 520 had a very clear water column and low levels of TSS. Increases in UVB attenuation over the open water season may be due to the high level of autochthonous DOM that had accumulated over the previous several open water seasons. Observations in other freshwater environments indicate that small autochthonous DOM molecules may aggregate into larger molecules that exhibit properties resembling those of

humic substances (Tranvik 1993). As the only high-closure lake tracked during the summer of 2004, it is difficult to speculate further on why UVB attenuation increased in Lake 520 over the open water season.

Generally, sites that were indirectly connected to distributary channels through a series of lakes and smaller channels (e.g. Lake 520, chain set sites S7-S9) had more stable *in situ* attenuation coefficients over the open water season. Those lakes located near channel connections (e.g. Lake 129, chain set sites S1-S3) received inputs of channel water throughout the open water season. This channel water became depleted in CDOM once the peak flood had receded and melt water from southern areas within the Mackenzie Basin had been flushed through the delta to the Beaufort Sea (see Appendix C for a time series of CDOM absorbency in the East Channel). This lowered both CDOM absorbencies and attenuation at closely connected sites. As a result, these sites displayed more variable attenuation coefficients over the open water season since they were more strongly influenced by channel water.

Measurements of *in situ* irradiance were only taken in one indirectly connected high-closure discrete lake (Lake 520) during 2004. Future measurements of *in situ* irradiance in both of these classes of Mackenzie Delta lakes are necessary in order to better characterize the underwater irradiance environment in this system. Floodplain lakes in the Mackenzie Delta are widely varied in terms of their water chemistry and hydrology, and some lakes within a single class can have very different characteristics than are predicted by the gradients in sill elevation and flooding frequency. For instance, indirectly connected low-closure lakes, if they are far enough removed from the channel connection point, can have levels of dissolved and particulate substances that more closely resemble those of high-closure lakes since the lateral extent of the flood in a given year may not be great enough for flooding to occur. Squires et al. (2002) also demonstrated that macrophyte abundance increased as the distance between a lake and its connection to a distributary channel increased. As well, although high-closure lakes are usually dominated by macrophyte growth, some may be formed through thermokarst processes. Thermokarst lakes likely contain a greater proportion of aged DOM with a more humic character, since DOM may be derived from melting permafrost in the lake bed, or the decomposition of dead vegetation within the lake itself. Both sources

contribute more humic, allochthonous DOM that would give high-closure thermokarst lakes optical properties more typical of lakes with lower sill elevations.

2.4.1 Potential for UVB-Induced Damage to Aquatic Biota

The Mackenzie Delta is located in the western Canadian Arctic (67-70°N, 133-137°W). Due to its high latitude, the delta receives approximately 56 days of 24 hour daylight from around 24 May – 20 July each year. The annual open water season in the Mackenzie Delta, which lasts from June to October, therefore coincides with a prolonged period of continual irradiance when delta lakes are exposed to high cumulative, but fairly low instantaneous, fluxes of UVB irradiance.

The potential for direct UVB-induced biotic damage increases over the open water season due to the interaction of two factors resulting in decreased *in situ* attenuation. First, CDOM is rapidly photobleached by UV wavelengths during the period of continual irradiance immediately following the peak flood, decreasing UVB absorbance within the water column over time. Second, as TSS settles out of the water column, scatter is reduced which also allows UVB to penetrate more deeply.

The calculation of 1% photic depths for UV wavebands revealed that UV irradiance is attenuated rapidly within Mackenzie Delta lakes. At all times during the open water season, the UVB waveband is essentially removed from delta lakes within the first 30 cm of the water column, while UVA is removed within the first 50 cm (Figure 2.13a, b). On average, delta lakes are approximately 2 m deep (Squires 2002), so there appears to be a substantial portion of the water column that remains shielded from the direct effects of UVB irradiance at any time. These refuges at depth may protect fish and zooplankton, which are motile and can avoid UVB if they are able to detect its presence. Some submerged macrophytes and benthic organisms also remain shielded from the direct harmful effects of UVB irradiance in refuges below the maximum depth of UVB penetration. However, delta lakes are well-mixed by wind and do not permanently stratify during the open water season (Squires 2002), so plankton, which are non-motile and lack the ability to determine their position in the water column, are exposed to UVB for variable periods of time since they are passively moved in mixing currents. When wind speeds are low, mixing rates will also be low, and phytoplankton present in the

slow-moving surface layers of delta lakes may receive fluxes of UVB high enough to cause either damage at the cellular level or photosynthetic inhibition (Xenopoulos et al. 2000).

UVA photic depths in Mackenzie Delta lakes are up to 50 cm in depth. Therefore, at shallower depths in the water column sufficient fluxes of UVA irradiance may be present for photorepair processes to occur. However, the delta is located at a high latitude and experiences periods of low water temperatures at the beginning of the open water season due to inputs of melt water and low ambient air temperatures. Therefore, similar to other polar freshwater systems, the Mackenzie Delta experiences low rates of all cellular processes when water temperatures are low. In these situations, it is likely that damage induction via UVB exposure will outpace photorepair via UVA-induced temperature-sensitive enzymatic processes (Wrona et al. 2006). For instance, algal cells exposed to UV in Antarctic waters did not show any recovery in photosynthetic processes for at least 5 hours (Neale et al. 1998).

There are also potential indirect harmful effects of UVB irradiance on aquatic organisms in Mackenzie Delta lakes. Febria et al. (2006) found that photochemical production of H_2O_2, the most stable and long-lived ROS formed in aquatic environments, was highest in low-closure lakes where an optimal trade-off between UV penetration and levels of CDOM substrate for photochemical reactions occurred. Also, past measurements indicate that H_2O_2 may accumulate in the water column over consecutive sunny days during the period of continual solar irradiance following peak flood (Febria et al. 2006). The effects on aquatic biota in the Mackenzie Delta may be significant since H_2O_2 can diffuse throughout the water column, and can therefore harm biota that are located within refuges well below the zone of direct UV exposure.

2.4.2 Photosynthetic Compensation Depths

The photosynthetic compensation depth, or the depth at which oxygen production by photosynthesis is exactly offset by oxygen consumption by respiration, is commonly held to be equal to the 1% photic depth for PAR ($z_{1\%}$PAR) and is located at the lower boundary of the photic zone (Häder et al. 1998). In Mackenzie Delta lakes, values for $z_{1\%}$PAR are generally between 1-4 m, and average photosynthetic compensation depths

are approximately equal to the average lake depth of 2 m by the end of the open water season (Figure 2.13c, d). Therefore, Mackenzie Delta lakes are generally shallow enough, and have clear enough water columns, to support photosynthesis to their bottoms later in the open water season. Delta lakes remain well-mixed throughout the summer, resulting in non-motile plankton being moved within mixing currents. The large relative photosynthetic compensation depth as compared to average depth implies that phytoplankton production is not light limited in most delta lakes within a few weeks following the spring flood. However, abundant macrophyte production in some Mackenzie Delta lakes later in the open water season may inhibit phytoplankton through shading (e.g. Squires 2002).

Attenuation of PAR in delta lakes was generally much higher than in high Arctic lakes where little or no vegetation may be present within the catchment (e.g. Markager and Vincent 2000, Laurion et al. 1997). By comparison, the Mackenzie Delta is a highly flood-driven system receiving large fluxes of terrestrially-derived CDOM and TSS, both of which attenuate in the PAR range.

Photosynthetic compensation depths increased over the open water season at all sites (Figure 2.13c, d), primarily due to TSS settling out of the water column as the flood receded and water levels fell. However, during late July 2004 a storm surge occurred in the lower Mackenzie Delta over a period of several days, with effects felt in the middle delta as well. Recorded water levels in the East Channel near the town of Inuvik rose approximately 0.6 m as a result of sustained high winds from the north (WSC 2006). This pushed channel water back upstream against the flow, and caused a second, smaller flood to enter some delta lakes for a short period. This substantially increased levels of TSS at sites closest to distributary channels over an interval of only a few days. PAR attenuation increased substantially in directly connected, no-closure lakes (see Figure 2.13c). Future climate change is expected to increase the frequency and severity of storm surges due to decreased ice cover in the Beaufort Sea (Manson and Solomon 2007), increasing the variability in open water concentrations of CDOM, and in particular TSS, with short-term implications for *in situ* production. This storm surge occurred during a period of low channel levels during late July of 2004. Previous storm surges in the Mackenzie Delta during low water periods have also exerted large effects on delta water

levels. These effects would have been much smaller, or even gone unnoticed, during periods with higher channel levels (Marsh and Schmidt 1993).

2.4.3 Attenuator Concentrations as Predictors of the Underwater Irradiance Environment in Mackenzie Delta Lakes

Concentrations of TDOC, which includes both chromophoric and non-chromophoric DOM, are often used to construct empirical equations that predict UV attenuation (Bukaveckas and Robbins-Forbes 2000, Vincent et al. 1998, Laurion et al. 1997). For instance, Morris et al. (1995) found that a large fraction (> 85%) of the among-lake variation in K_dUVB values in 65 lakes located throughout Alaska, Colorado, the northeastern US and Argentina could be predicted by power models incorporating only TDOC concentrations. In a study of temperate lakes in Alberta and eastern North America, Scully and Lean (1994) found that 97% of the variation in UVB attenuation was explained by a power model that used TDOC concentration as the sole predictor. This dependence of UV attenuation on TDOC is likely a result of the strong absorbance of UV wavelengths by CDOM, the chromophoric portion of the TDOC pool (Belzile et al. 2002).

These equations have often been used in subsequent studies to calculate UVB attenuation and photic depths using simple measurements of TDOC concentration rather than taking *in situ* measurements of irradiance, which are logistically far more difficult. However, there is some question as to how transferable these equations are among systems. For instance, the predictive power equation constructed by Scully and Lean (1994; K_dUVB(300-320) = $0.42[DOC]^{1.86}$) used pooled data collected from 20 study lakes located in temperate regions of Ontario, Quebec, Pennsylvania and Alberta. In spite of the limited number of lakes that were included in their data set, the Scully and Lean equation has been applied in a variety of other systems. When applied to TDOC data from Mackenzie Delta lakes monitored during the open water season of 2004, the Scully and Lean equation consistently underestimated the actual measured *in situ* K_dUVB(310-320) values (Figure 2.15). The different wavelength ranges used in Scully and Lean (1994; 300-320 nm) and in this study (310-320 nm) did not affect this result. If *in situ* irradiance in Mackenzie Delta lakes could be reliably measured to 300 nm, the resulting

diffuse attenuation coefficients would be greater than those calculated using the current set of measured data, further increasing the magnitude of the underestimate using the Scully and Lean equation. Therefore, the Scully and Lean equation is not applicable in Mackenzie Delta lakes, which have higher attenuation in the UVB waveband than do the set of temperate lakes used to derive the equation.

Additionally, the Scully and Lean equation fails to account for fluctuations in attenuation that are observed over time in most temperate, subarctic and polar lakes due to changing fluxes of solar irradiance, organic matter and sediments. Therefore, the application of equations predicting *in situ* attenuation under circumstances that differ substantially from those in which they were developed should be done with care only after ensuring that their use is valid.

In this study of irradiance attenuation in Mackenzie Delta lakes, CDOM was found to be a much stronger predictor of UV attenuation than TDOC at all sites. CDOM was significantly correlated to both UVB and UVA attenuation at every site that was monitored during 2004, while TDOC was only a significant attenuator of UV wavelengths at those chain set sites that were located closest to the channel connection (Table 2.2). This may indicate that, as the proportion of TDOC composed of CDOM increased along with increased proximity to the channel connection, attenuation by TDOC became significant as well. Conversely, at greater distances from the channel connection where the majority of TDOC was composed of non-chromophoric autochthonous DOM, the allochthonous portion containing chromophores dominated UV attenuation. Therefore, the correlation of TDOC to UV attenuation was far weaker at these sites.

While power relationships using TDOC concentrations to predict UV attenuation generally provide the best fit, linear relationships give better fits when CDOM-specific parameters are used as predictors (e.g. Huovinen et al. 2003, Laurion et al. 1997, Morris et al. 1995, Scully and Lean 1994). In Mackenzie Delta lakes monitored during 2004, the strongest fits were linear relationships using CDOM absorbency at 330 nm to predict UV attenuation (Table 2.4). For both lake sets, over 50% of the variation in attenuation for either waveband could be explained by CDOM absorbencies alone. However, substantial improvements in model predictive ability were found when indices of scatter (i.e. TSS

concentrations) were also included in the empirical equations (Table 2.3). The sizeable contribution of particulate scattering to total attenuation may be due to both the very high concentrations of TSS found in delta lakes at the beginning of the open water season as well as the relatively low concentrations of TDOC found in these lakes when compared to other systems. A previous study in Lake Biwa, a lake that also contains fairly low levels of TDOC, indicated that in lakes with low TDOC concentrations, parameters other than CDOM absorbance must be considered when modeling irradiance attenuation (Belzile et al. 2002).

The inclusion of an index for Chl-*a* in multiple linear regression equations only improved model fit in the sill set lakes (Table 2.3). Chl-*a* was inversely correlated to attenuation across all wavebands, indicating that in sill set lakes with comparable TSS concentrations and CDOM absorbencies, attenuation tended to be higher in lakes with lower Chl-*a* concentrations. Future studies of *in situ* irradiance attenuation in Mackenzie Delta lakes using a spectroradiometer with both upwelling and downwelling sensors would help elucidate the role of Chl-*a* in controlling the underwater light environment; however, further speculation is beyond the scope of this study.

The purpose of constructing multiple linear regressions for waveband attenuation was to develop equations that characterize the underwater irradiance environment in Mackenzie Delta lakes from simple measures of water chemistry. If reasonably robust equations were developed that were valid across broad lake classifications (i.e. no-, low-, and high-closure discrete lakes; directly *versus* indirectly connected chain lakes), then approximations of *in situ* attenuation could be calculated using routine analyses on water samples rather than by taking underwater measurements with a spectroradiometer. This would be preferable since spectroradiometers capable of taking spectral scans are generally large and unwieldy instruments that are impractical in a landscape such as the Mackenzie Delta, where access to lakes is generally via small motorboats. However, robust and reliable equations that accurately predict *in situ* irradiance attenuation for any waveband could not be constructed from one year's worth of data. Although all predictive equations produced through multiple linear regression analysis explained the majority of the observed variation in attenuation (r^2 between 68 and 86%), the likelihood that these equations would be applicable during all open water seasons is low. The

Mackenzie Delta experiences large fluctuations in limnological parameters among years due to variability in the magnitude, duration and extent of the annual flood. Although equations constructed in 2004 were statistically significant ($p < 0.002$ in all cases), broad predictions of UV and PAR attenuation within the thousands of lakes in the middle delta based on a limited set of measurements from only 12 sites would be unadvisable.

Sill set lakes were underrepresented in this study, particularly in the high-closure class, as were discrete lakes that were indirectly connected to distributary channels. Although these lakes represent significant difficulties as far as accessibility via motorboat, further measurement of *in situ* attenuation is required in these lake classes before useful predictive equations can be constructed. Lake connectivity likely plays a large role in determining *in situ* attenuator concentrations, particularly of those constituents carried in flood or channel waters. Directly connected lakes are more frequently flooded, and for longer periods, while indirectly connected lakes may rely more on precipitation and overland flow for inputs of CDOM and TSS. Additionally, when considered as a group, high-closure lakes may have the greatest variability in UV and PAR attenuation due to less than annual inputs of nutrients and DOM from spring flooding.

2.4.4 Effects of Ozone Depletion and Climate Change on the Underwater Irradiance Environment of Mackenzie Delta Lakes

Small but continuing amounts of ozone depletion over the western Canadian Arctic will result in elevated ground-level fluxes of UVB irradiance for at least the next two decades (ACIA 2005, Austin et al. 2000). Although UVB fluxes will increase, fluxes of both UVA and PAR will remain unchanged. Ratios of UVB to PAR within the water column are important predictors of the extent of UVB damage in aquatic systems (Crump et al. 1999), and as amounts of UVB relative to other wavebands increase additional stresses may be placed on some aquatic biota (Sommaruga and Psenner 1997). Arctic aquatic environments are more sensitive than those found at lower latitudes, and an increase in UVB fluxes represents an additional stress for ecosystems that already face high solar fluxes during short ice-free growing seasons. Additionally, lakes in the Mackenzie Delta floodplain average only 2 m deep (Squires 2002). Therefore, any

changes within the water column itself that alter the penetration of *in situ* irradiance could have significant effects on aquatic biota, especially those organisms that lack motility or the ability to detect the presence of UVB.

The Mackenzie Delta's northerly location may make it particularly sensitive to the effects of not only ozone depletion, but also climate change (Lesack et al. 1998). The potential impacts of climate change on the underwater irradiance environment are important factors to consider, especially in regards to UVB exposure. Since CDOM plays a critical role in determining UV penetration through the water column, any change in CDOM absorbencies will also influence *in situ* UV fluxes. Decreases in CDOM, or changes in the larger DOM pool, may therefore have a far greater effect on aquatic ecosystems than will increases in incident UVB resulting from stratospheric ozone depletion (Molot et al. 2004, Schindler et al. 1996). For instance, Vincent et al. (1998) found that a 20% reduction in CDOM levels led to far greater UV inhibition of phytoplankton than did an equal percentage depletion in stratospheric ozone. Similarly, climatic warming at temperate latitudes in the boreal forest resulted in DOC losses that increased UV penetration by up to 30% (Schindler 1997).

Changes in allochthonous CDOM levels and absorbencies in Mackenzie Delta lakes may result from a number of anticipated climate change effects. The predicted increase in annual average temperature in the western Canadian Arctic is far higher than the anticipated global average increase (ACIA 2005). Increased temperatures will allow vegetation and the treeline to move northwards, increasing inputs of terrestrially-derived lignaceous DOM to high latitude aquatic systems (ACIA 2005). Also, the rate of permafrost melting is predicted to increase substantially (ACIA 2005). Permafrost represents a large reservoir of terrestrial DOM that is currently sequestered and unavailable to aquatic systems. When thawed, it releases large amounts of allochthonous DOM to waterways, thereby increasing CDOM absorbencies and shielding the water column from UVB exposure (Wrona et al. 2006). Also, thawed permafrost in the vicinity of delta lakes would increase erosion along their banks, increasing TSS loads to lakes and subsequently increasing *in situ* scatter and attenuation (Prowse et al. 2006). The proportion of the DOM pool composed of CDOM may also change due to increased

precipitation in the southern reaches of the Mackenzie Basin, or increased sea level at the outlet to the Beaufort Sea.

The Mackenzie Delta is currently ice covered from October to June each year (Emmerton et al. 2007). However, future increases in air temperature are predicted to lead to a shorter period of annual ice cover, with a later freeze-up and earlier break-up. This lengthens the period that delta lakes will be exposed to UVB irradiance. The open water season is the period of the highest biological productivity and geochemical activity in the Mackenzie Delta due to the high fluxes of irradiance around the summer solstice. Therefore, the potential for both positive (e.g. increased microbial food supply) and negative (e.g. increased rates of DNA and cellular damage) photochemical effects on aquatic biota are maximal during this time. Decreased periods of ice cover will also increase the amount of wind-driven mixing that occurs in Arctic lakes (Wrona et al. 2006), thereby altering the amount of UV exposure experienced by non-motile aquatic organisms such as phytoplankton.

There is evidence that peak annual water levels in the Mackenzie Delta have declined since 1964 in response to decreased temperature gradients between the northern and southern regions of the basin. Decreased frequencies of ice-jamming and mechanical break-ups from the 1990s onwards also indicate decreased north-south temperature gradients during the spring melt (Lesack and Marsh *in press*). Lower annual flood levels will reduce the volume of water entering delta lakes each spring and decrease the frequency of flooding for high-closure lakes. This would result in lower amounts of both TSS and CDOM entering delta lakes during high water periods, decreasing diffuse attenuation coefficients (Pullin and Cabaniss 1997). The ability of the water column to attenuate incoming irradiance, particularly in the UV range, would decline under this scenario, increasing organism exposure to irradiance. Mackenzie Delta lakes already experience negative water balances in most years due to higher levels of evaporation than precipitation (Marsh 1998), and in years that high-closure lakes are not flooded, this results in an average loss in depth of 0.03 m (Marsh and Lesack 1996). If flood frequency was further reduced in high-closure lakes, it is likely that many would experience declining water levels for several sequential years. Not only would this steadily decrease the portion of the water column that is sunscreened from UVB exposure

by CDOM absorbance, reducing refuges for biota, but reduced levels of TSS and CDOM in delta lakes would allow water columns to become increasingly transparent to UV wavelengths. These effects in combination would leave little to no suitable habitat for UV-sensitive organisms in many high-closure delta lakes.

If predictions of future temperature increases in the western Canadian Arctic and the wider Mackenzie basin are realized, these factors will combine to alter the quantity of irradiance entering Mackenzie Delta lakes, as well as the relative amounts of each waveband present within the water column.

2.5 Conclusions and Recommendations

In situ irradiance measurements taken during the open water season of 2004 revealed several important characteristics of the underwater irradiance environment of Mackenzie Delta lakes. Delta lakes are approximately 2 m deep on average, far more shallow than the depth to which UV wavelengths penetrate in many larger inland aquatic systems. However, measurements of irradiance attenuation reveal that Mackenzie Delta lakes contain sufficient attenuating material to remove virtually all *in situ* UVB irradiance by 30 cm depth, and all *in situ* UVA irradiance by 50 cm depth. This implies that a substantial portion of the water column below these depths remains sunscreened throughout the open water season, thereby protecting biota in these refuges from UV exposure. However, the entire water columns of these shallow delta lakes are well-mixed by wind, so non-motile organisms may ultimately be exposed to large fluxes of UV as they pass through surface layers. Throughout the open water season, PAR irradiance in sufficient quantity to support photosynthesis penetrated to between 1-4 m depth. Therefore, most delta lakes can support photosynthesis throughout most of their water columns.

Measurement of *in situ* irradiance in lakes of the Mackenzie Delta also revealed that, in directly connected no-closure lakes, attenuation of UV irradiance declined rapidly following the spring flood while PAR attenuation remained relatively constant over the open water season. However, in the indirectly connected high-closure lake that was also monitored, increases in UV attenuation over the open water season were observed. The opposing flooding frequencies and DOM compositions between the two lake types are likely responsible for these opposing trends.

Although there are difficulties with using the OL 754 spectroradiometer in isolated Mackenzie Delta lakes that are inaccessible by boat, there is a need to examine *in situ* irradiance conditions in a wider range of lake classes. Delta lakes are differentiated by sill elevation and their connectivity to distributary channels, both of which determine the frequency of spring flooding. In turn, floodwaters carry both CDOM and TSS, the primary controls on *in situ* irradiance attenuation in Mackenzie Delta lakes. Strong relationships were constructed using CDOM absorbencies and TSS concentrations to

predict UV and PAR attenuation in a chain set of no-closure lakes that ranged from directly to indirectly connected to a distributary channel. However, high-closure indirectly connected lake types were represented by only a single lake (Lake 520). Since high-closure indirectly connected lakes are under-represented in this study, further measurements are needed before *in situ* irradiance conditions can be accurately characterized across all lakes of the Mackenzie Delta.

2.6 References

Allard, B., H. Boren, C. Pettersson and G. Zhang. 1994. Degradation of humic substances by UV irradiation. Environment International 20: 97-101.

Anderson, T.R. 1993. A spectrally averaged model of light penetration and photosynthesis. Limnology and Oceanography 38: 1403-1419.

Arctic Climate Impact Assessment (ACIA). 2005. Arctic climate impact assessment: scientific report. Cambridge University Press, New York, USA. 1042 pp.

Arts, M.T., R.D. Robarts, F. Kasai, M.J. Waiser, V.P. Tumber, A.J. Plante, H. Rai and H.J. de Lange. 2000. The attenuation of ultraviolet radiation in high dissolved organic carbon waters of wetlands and lakes on the northern Great Plains. Limnology and Oceanography 45: 292-299.

Austin, J., J. Knight and N. Butchart. 2000. Three-dimensional chemical model simulations of the ozone layer: 1979–2015. Quarterly Journal of the Royal Meteorological Society 126: 1533–1556.

Baird, C. 1999. Environmental chemistry, 2nd ed. W.H. Freeman and Company, New York, USA. 557 pp.

Belzile, C., W.F. Vincent, C. Howard-Williams, I. Hawes, M.R. James, M. Kumagai and C.S. Roesler. 2004. Relationships between spectral optical properties and optically active substances in clear oligotrophic lakes. Water Resources Research 40: W12512, doi:10.1029/2004WR003090.

Belzile, C., W.F. Vincent and M. Kumagai. 2002. Contribution of absorption and scattering to the attenuation of UV and photosynthetically available radiation in Lake Biwa. Limnology and Oceanography 47: 95-107.

Bertilsson, S. and L.J. Tranvik. 2000. Photochemical transformation of dissolved organic matter in lakes. Limnology and Oceanography 45: 753-762.

Bigras, S.C. 1990. Hydrological regime of lakes in the Mackenzie Delta, Northwest Territories, Canada. Arctic Alpine Research 22: 163-174.

Bonilla, S., V. Villeneuve and W.F. Vincent. 2005. Benthic and planktonic algal communities in a high Arctic lake: Pigment structure and contrasting responses to nutrient enrichment. Journal of Phycology 41: 1120-1130.

Bowling, L.C., M.S. Steane and P.A. Tyler. 1986. The spectral distribution and attenuation of underwater irradiance in Tasmanian inland waters. Freshwater Biology 16: 313-335.

Bukaveckas, P.A. and M. Robbins-Forbes. 2000. Role of dissolved organic carbon in the attenuation of photosynthetically active and ultraviolet radiation in Adirondack lakes. Freshwater Biology 43: 339-354.

Campbell, J.W. and T. Aarup. 1989. Photosynthetically available radiation at high latitudes. Limnology and Oceanography 34: 1490-1499.

Cooper, W.J., R.G. Zika, R.G. Petasne and A.M. Fisher. 1989. Sunlight-induced photochemistry of humic substances in natural waters: major reactive species *In* Aquatic humic substances: influence on fate and treatment of pollutants. American Chemical Society, Denver, USA. pp. 333-362.

Crump, D., D. Lean, M. Berrill, D. Coulson and L. Toy. 1999. Spectral irradiance in pond water: influence of water chemistry. Photochemistry and Photobiology 70: 893-901.

Curtis, P.J. 1998. Climatic and hydrologic control of DOM concentration and quality in lakes. *In* Aquatic humic substances. Hessen, D.O. and L.J. Tranvik (eds). Springer-Verlag, Berlin, Germany. pp 93-106.

De Haan, H. 1993. Solar UV-light penetration and photodegradation of humic substances in peaty lake water. Limnology and Oceanography 38: 1072-1076.

Emmerton, C.A. 2006. Downstream nutrient changes through the Mackenzie River Delta and Estuary, western Canadian arctic. M.Sc. Thesis, Simon Fraser University. 181 pp.

Emmerton, C.A., L.F.W. Lesack and P. Marsh. 2007. Lake abundance, potential water storage, and habitat distribution in the Mackenzie River Delta, western Canadian Arctic. Water Resources Research 43: W05419, doi:10.1029/2006WR005139.

Farman, J.C., B.G. Gardiner and J.D. Shanklin. 1985. Large losses of total ozone in Antarctica reveal seasonal ClOx/Nox interaction. Nature 315: 207-210.

Febria, C.M. 2005. Patterns of hydrogen peroxide among lakes of the Mackenzie Delta and potential effects on bacterial production. M.Sc. Thesis, Simon Fraser University. 124 pp.

Febria, C.M., L.F.W. Lesack, J.A.L. Gareis and M.L. Bothwell. 2006. Patterns of hydrogen peroxide among lakes of the Mackenzie Delta, western Canadian Arctic. Canadian Journal of Fisheries and Aquatic Sciences 63: 2107-2118.

Gibson, J.A.E., W.F. Vincent, B. Nieke and R. Pienitz. 2000. Control of biological exposure to UV radiation in the Arctic Ocean: comparison of the roles of ozone and riverine dissolved organic matter. Arctic: 53: 372-382.

Gordon, H.R. 1989. Can the Lambert-Beer law be applied to the diffuse attenuation coefficient of ocean water? Limnology and Oceanography 34: 1389-1409.

Gueymard, C.A. 2002. [Online]. Simple model of the atmospheric radiative transfer of sunshine (SMARTS), version 2.9.2. Available from National Renewable Energy Laboratory: http://rredc.nrel.gov/solar/models/SMARTS/.

Häder, D.-P., H.D. Kumar, R.C. Smith and R.C. Worrest. 1998. Effects on aquatic ecosystems. Journal of Photochemistry and Photobiology B: Biology 46: 53-68.

Häder, D.-P. and R.C. Worrest. 1991. Effects of enhanced solar ultraviolet-radiation on aquatic ecosystems. Photochemistry and Photobiology 53: 717-725.

Hessen, D.O., H.J. De Lange and E. Van Donk. 1997. UV-induced changes in phytoplankton cells and its effect on grazers. Freshwater Biology 38: 513-524.

Hofmann, D.J., T.L Deshler, P. Aimedieu, W.A. Matthews, P.V. Johnston, Y. Kondo, W.R. Sheldon, G.J. Byrne and J.R. Benbrook. 1989. Stratospheric clouds and ozone depletion in the Arctic during January 1989. Nature 340: 117-121.

Huovinen, P.S., H. Penttilä and M.R. Soimasuo. 2003. Spectral attenuation of solar ultraviolet radiation in central Finland. Chemosphere 51: 205-214.

Jerome, J.H. and R.P. Bukata. 1998. Tracking the propagation of solar ultraviolet radiation: dispersal of ultraviolet photons in inland waters. Journal of Great Lakes Research 24: 666-680.

Kirk, J.T.O. 1994a. Light and photosynthesis in aquatic ecosystems, 2nd ed. Cambridge University Press, Cambridge, UK. 509 pp.

Kirk, J.T.O. 1994b. Optics of UVB radiation in natural waters. Archiv für Hydrobiologie 43: 1-16.

Kirk, J.T.O., B.R. Hargreaves, D.P. Morris, R.B. Coffin, B. David, D. Frederickson, D. Karentz, D.R.S. Lean, M.P. Lesser, S. Madronich, J.H. Morrow, N.B. Nelson and N.M. Scully. 1994. Measurements of UV-B radiation in two freshwater lakes: an instrument intercomparison. Archiv für Hydrobiologie 43: 71-99.

Kuhn, P., H. Browman, B. McArthur and J.-F. St-Pierre. 1999. Penetration of ultraviolet radiation in the waters of the estuary and Gulf of St. Lawrence. Limnology and Oceanography 44: 710-716.

Laurion, I., M. Ventura, J. Catalan, R. Psenner and R. Sommaruga. 2000. Attenuation of ultraviolet radiation in mountain lakes: factors controlling the among- and within-lake variability. Limnology and Oceanography 45: 1274-1288.

Laurion, I., W.F. Vincent and D.R.S. Lean. 1997. Underwater ultraviolet radiation: development of spectral models for Northern high latitude lakes. Photochemistry and Photobiology 65: 107-114.

Leech, D.M., C.E. Williamson, R.E. Moeller and B.R. Hargreaves. 2005. Effects of ultraviolet radiation on the seasonal vertical distribution of zooplankton: a database analysis. Archiv für Hydrobiologie 162: 445-464.

Leech, D.M. and C.E. Williamson. 2001. *In situ* exposure to ultraviolet radiation alters the depth distribution of Daphnia. Limnology and Oceanography 46: 416-420.

Lesack, L.F.W., and P. Marsh. *In Press*. Lengthening plus shortening of river-to-lake connection times in the Mackenzie River Delta respectively via two global change mechanisms along the arctic coast. Geophysical Research Letters.

Lesack, L.F.W., P. Marsh and R.E. Hecky. 1998. Spatial and temporal dynamics of major solute chemistry among Mackenzie Delta lakes. Limnology and Oceanography 43: 1530-1543.

Lindell, M.J., W. Granéli and L. Tranvik. 1995. Enhanced bacterial growth in response to photochemical transformation of dissolved organic matter. Limnology and Oceanography 40: 195-199.

Mackay, J.R. 1963. The Mackenzie Delta area, N.W.T., Canada. Canadian Department of Mines and Technical Surveys, Geographical Branch Memoir 8. 202 pp.

Mackenzie River Basin Committee. 1981. Alluvial ecosystems. Mackenzie River Basin Study Report Supplement 2. Report under the 1978-1981 federal-provincial study agreement respecting the water and related resources of the Mackenzie River Basin. Regina, Inland Waters Directorate, Environment Canada. 129 pp.

Madronich, S. 1994. Increases in biologically damaging UV-B radiation due to stratospheric ozone reductions: a brief review. Archiv für Hydrobiologie 43: 17-30.

Maloney, K.O., D.P. Morris, C.O. Moses and C.L. Osburn. 2005. The role of iron and dissolved organic carbon in the absorption of ultraviolet radiation in humic lake water. Biogeochemistry 75: 393-407.

Manson, G.K. and S.M. Solomon. 2007. Past and future forcing of Beaufort sea coastal change. Atmosphere-Ocean 45: 107-122.

Markager, S. and W.F. Vincent. 2000. Spectral light attenuation and the absorption of UV and blue light in natural waters. Limnology and Oceanography 45: 642-650.

Marsh, P. 1998. Lakes and water in the Mackenzie Delta. Scientific Report No. 6, Aurora Research Institute, Inuvik, NT. 13 pp.

Marsh, P. and M. Hey. 1994. Analysis of spring high water events in the Mackenzie Delta and implications for lake and terrestrial flooding. Geografiska Annaler Series A-Physical Geography 76: 221-234.

Marsh, P. and M. Hey. 1989. The flooding hydrology of Mackenzie Delta lakes near Inuvik, N.W.T., Canada. Arctic 42: 41-49.

Marsh, P. and L.F.W. Lesack. 1996. The hydrologic regime of perched lakes in the Mackenzie Delta: potential responses to climate change. Limnology and Oceanography 41: 849-856.

Marsh, P. and T. Schmidt. 1993. Influence of a Beaufort Sea storm surge on channel levels in the Mackenzie Delta. Arctic 46: 35-41.

McElroy, M.B., R.J. Salawitch, S.C. Wofsy and J.A. Logan. 1986. Reductions of Antarctic ozone due to synergistic interactions of chlorine and bromine. Nature 321: 759-762.

McKnight, D.M., E.W. Boyer, P.K. Westerhoff, P.T. Doran, T. Kulbe and D.T. Andersen. 2001. Spectrofluorometric characterization of dissolved organic matter for indication of precursor organic material and aromaticity. Limnology and Oceanography 46: 38-48.

Medina-Sanchez, J.M., M. Villar-Argaiz and P. Carillo. 2002. Modulation of the bacterial response to spectral solar radiation by algae and limiting nutrients. Freshwater Biology 47: 2191-2204.

Moeller, R.E., S. Gilroy, C.E. Williamson, G. Grad and R. Sommaruga. 2005. Dietary acquisition of photoprotective compounds (mycosporine-like amino acids, carotenoids) and acclimation to ultraviolet radiation in a freshwater copepod. Limnology and Oceanography 50: 427-439.

Molot, L.A., W. Keller, P.R. Leavitt, R.D. Robarts, M.J. Waiser, M.T. Arts, T.A. Clair, R. Pienitz, N.D. Yan, D.K. McNicol, Y.T. Prairie, P.J. Dillon, M. Macrae, R. Bello, R.N. Nordin, P.J. Curtis, J.P. Smol and M.S.V. Douglas. 2004. Risk analysis of dissolved organic matter-mediated ultraviolet B exposure in Canadian inland waters. Canadian Journal of Fisheries and Aquatic Science 61: 2511-2521.

Moran, M.A. and R.G. Zepp. 1997. Role of photoreactions in the formation of biologically labile compounds from dissolved organic matter. Limnology and Oceanography 42: 1307-1316.

Morris, D.P., H. Zagarese, C.E. Williamson, E.G. Balseiro, B.R. Hargreaves, B. Modenutti, R. Moeller and C. Queimalinos. 1995. The attenuation of solar UV radiation in lakes and the role of dissolved organic carbon. Limnology and Oceanography 40: 1381-1391.

National Renewable Energy Laboratory (NREL). 2005. [Online]. Available: http://www.nrel.gov/midc/srrl_bms/.

Neale, P.J., R.F. Davis and J.J. Cullen. 1998. Interactive effects of ozone depletion and vertical mixing on photosynthesis of Antarctic phytoplankton. Nature 392: 585-589.

Obernosterer, I. and R. Benner. 2004. Competition between biological and photochemical processes in the mineralization of dissolved organic carbon. Limnology and Oceanography 49: 117-124.

O'Brien, W.J. 1987. Planktivory by freshwater fish: thrust and parry in the Pelagia. *In* Predation: Direct and indirect impacts on aquatic communities. Kerfoot, W.C. and A. Sih (eds.). University Press of New England, Hanover, USA. pp. 3-16.

Osburn, C.L., H.E. Zagarese, D.P. Morris, B.R. Hargreaves and W.E. Cravero. 2001. Calculation of spectral weighting functions for the solar photobleaching of chromophoric dissolved organic matter in temperate lakes. Limnology and Oceanography 46: 1455-1467.

Perovich, D.K., 1993. A theoretical model of ultraviolet light transmission through Antarctic sea ice. Journal of Geophysical Research 98: 22579–22587.

Pienitz, R. and W.F. Vincent. 2000. Effect of climate change relative to ozone depletion in subarctic lakes. Nature 404: 484-487.

Prowse, T.D., F.J. Wrona, J.D. Reist, J.J. Gibson, J.E. Hobbie, L.M.J. Lévesque and W.F. Vincent. 2006. Climate change effects on hydroecology of Arctic freshwater ecosystems. Ambio 35: 347-358.

Pullin, M.J. and S.E. Cabaniss. 1997. Physicochemical variations in DOM-synchronous fluorescence: implications for mixing studies. Limnology and Oceanography 42: 1766-1773.

Quesada, A., J.-L. Mouget and W.F. Vincent. 1995. Growth of Antarctic cyanobacteria under ultraviolet radiation: UVA counteracts UVB inhibition. Journal of Phycology 31: 242-248.

Reche, I., M.L. Pace and J.J. Cole. 2000. Modeled effects of dissolved organic carbon and solar spectra on photobleaching in lake ecosystems. Ecosystems 3: 419-432.

Rex, M., R.J. Salawitch, P. von der Gathen, N.R.P. Harris, M.P. Chipperfield and B. Naujokat. 2004. Arctic ozone loss and climate change. Geophysical Research Letters 31:L04116, doi:10.1029/2003GL018844.

Riedel, A.J. 2002 Zooplankton composition and control of heterotrophic flagellates among lakes of the Mackenzie Delta. M.Sc. Thesis, Simon Fraser University. 99 pp.

Rouse, W.R., M.S.V. Douglas, R.E. Hecky, A.E. Hershey, G.W. Kling, L. Lesack, P. Marsh, M. McDonald, B.J. Nicholson, N.T. Roulet and J.P. Smol. 1997. Effects of climate change on the freshwaters of arctic and subarctic North America. Hydrological Processes 11: 873-902.

Salawitch, R.J., M.B. McElroy, J.H. Yatteau, S.C. Wofsy, M.R. Schoeberl, L.R. Lait, P.A. Newman, K.R. Chan, M. Loewenstein, J.R. Podolske, S.E. Strahan and M.H. Proffitt. 1990. Loss of ozone in the arctic vortex for the winter of 1989. Geophysical Research Letters 17: 561-564 Suppl. S.

Schindler, D.W. 1997. Widespread effects of climatic warming on freshwater ecosystems in North America. Hydrological Processes 11: 1043-1067.

Schindler, D.W., P.J. Curtis, B.R. Parker and M.P. Stainton. 1996. Consequences of climatic warming and lake acidification for UV-B penetration in North American boreal lakes. Nature 379: 705-708.

Scully, N.M. and D.R.S. Lean. 1994. The attenuation of ultraviolet radiation in temperate lakes. Archiv für Hydrobiologie 43: 135-144.

Scully, N.M., L.J. Tranvik and W.J. Cooper. 2003. Photochemical effects on the interaction of enzymes and dissolved organic matter in natural waters. Limnology and Oceanography 48: 1818-1824.

Segelstein, D.J. 1981. The complex refractive index of water. M.Sc. Thesis, University of Missouri-Kansas City. 167 pp.

Smith, R.E.H., C.D. Allen and M.N. Charlton. 2004. Dissolved organic matter and ultraviolet radiation penetration in the Laurentian Great Lakes and tributary waters. International Association of Great Lakes Research 30: 367-380.

Sommaruga, R. and R. Psenner. 1997. Ultraviolet radiation in a high mountain lake of the Austrian Alps: air and underwater measurements. Photochemistry and Photobiology 65: 957-963.

Spears, B.M. 2002. Effects of nutrient limitation on heterotrophic bacterial productivity and edible phytoplankton biomass among lakes of the Mackenzie Delta, Western Canadian arctic. M.Sc. Thesis, Simon Fraser University. 159 pp.

Squires, M.M. 2002. The distribution and abundance of autotrophs among lakes of the Mackenzie Delta, western Canadian Arctic. Ph.D. Thesis, Simon Fraser University. 195 pp.

Squires, M.M., L.F.W. Lesack and D. Huebert. 2002. The influence of water transparency on the distribution and abundance of macrophytes among lakes of the Mackenzie Delta, Western Canadian Arctic. Freshwater Biology 47: 2123-2135.

Squires, M.M. and L.F.W. Lesack. 2003. Spatial and temporal patterns of light attenuation among lakes of the Mackenzie Delta. Freshwater Biology 48: 1-20.

Steinberg, C.E.W. 2003. Ecology of humic substances in freshwaters. Springer-Verlag, Heidelberg, Germany. 440 pp.

Stolarski, R.S., A.J. Krueger, M.R. Schoeberl, R.D. McPeters, P.A. Newman and J.C. Alpert. 1986. Nimbus 7 satellite measurements of the springtime Antarctic ozone decrease. Nature 322: 808-811.

Tartarotti, B., G. Baffico, P. Temporetti and H.E. Zagarese. 2004. Mycosporine-like amino acids in planktonic organisms living under different UV exposure conditions in Patagonian lakes. Journal of Plankton Research 26: 753-762.

Teichreb, C.J. 1999. Effects of dissolved organic carbon as a bacterial growth substrate and as an ultraviolet-B radiation sunscreen for aquatic microbial foodwebs in Mackenzie Delta lakes, Northwest Territories. M.Sc. Thesis, Simon Fraser University. 196 pp.

Tranvik, L.J. 1993. Microbial transformation of labile dissolved organic-matter into humic-like matter in seawater. FEMS Microbial Ecology 12: 177-183.

Vähätalo, A.V., K. Salonen, U. Münster, M. Järvinen and R.G. Wetzel. 2003. Photochemical transformation of allochthonous organic matter provides bioavailable nutrients in a humic lake. Archiv für Hydrobiologie 156: 287-314.

Valentine, R.L. and R.G. Zepp. 1993. Formation of carbon monoxide from the photodegradation of terrestrial dissolved organic carbon in natural waters. Environmental Science and Technology 27: 409-412.

Vant, W.N. 1990. Causes of light attenuation in nine New Zealand estuaries. Estuarine, Coastal and Shelf Science 31: 125-137.

Vant, W.N. and R.J. Davies-Colley. 1986. Relative importance of clarity determinants in Lakes Okaro and Rotorua. New Zealand Journal of Marine and Freshwater Research 20: 355-363.

Vant, W.N. and R.J. Davies-Colley. 1984. Factors affecting clarity of New Zealand lakes. New Zealand Journal of Marine and Freshwater Research 18: 367-377.

Vincent, W.F., I. Laurion and R. Pienitz. 1998. Arctic and Antarctic lakes as optical indicators of global change. Annals of Glaciology 27: 691-696.

Vincent, W.F., and R. Pienitz. 1996. Sensitivity of high-latitude freshwater ecosystems to global change: temperature and solar ultraviolet radiation. Geoscience Canada 23: 231-236.

Water Survey of Canada (WSC). 2006. [Online]. Data products and services. Available: http://scitech.pyr.ec.gc.ca/waterweb/formnav.asp?lang=0.

Welcomme, R.L. 1979. Fisheries ecology of floodplain rivers. Longman, New York, USA. 317 pp.

Wetzel, R.G., P.G. Hatcher and T.S. Bianchi. 1995. Natural photolysis by ultraviolet irradiance of recalcitrant dissolved organic matter to simple substrates for rapid bacterial metabolism. Limnology and Oceanography 40: 1369-1380.

Wetzel, R.G. and G.E. Likens. 2000. Limnological Analyses, 3rd ed. Springer-Verlag, New York, USA. 429 pp.

Whitehead, R.F., S. de Mora, S. Demers, M. Gosselin, P. Monfort and B. Mostajir. 2000. Interactions of ultraviolet-B radiation, mixing, and biological activity on photobleaching of natural chromophoric dissolved organic matter: a mesocosm study. Limnology and Oceanography 45: 278-291.

Williamson, C.E., H.E. Zagarese, P.C. Schulze, B.R. Hargreaves and J. Seva. 1994. The impact of short-term exposure to UV-B radiation on zooplankton communities in north temperate lakes. Journal of Plankton Research 16: 205-218.

Worrest, R.C. and D.-P. Häder. 1997. Overview of the effects of increased solar UV on aquatic microorganisms. Photochemistry and Photobiology 65: 257-259.

Wrona, F.J., T.D. Prowse, J.D. Reist, J.E. Hobbie, L.M.J. Lévesque, R.W. Macdonald and W.F. Vincent. 2006. Effects of ultraviolet radiation and contaminant-related stressors on Arctic freshwater ecosystems. Ambio 35: 388-401.

Xenopoulos, M.A., Y.T. Prairie and D.F. Bird. 2000. Influence of ultraviolet-B radiation, stratospheric ozone variability, and thermal stratification on the phytoplankton biomass dynamics in a mesohumic lake. Canadian Journal of Fisheries and Aquatic Sciences 57: 600-609.

Zepp, R.G., T.V. Callaghan and D.J. Erickson. 1995. Effects of increased solar ultraviolet radiation on biogeochemical cycles. Ambio 24: 181-187.

2.7 Tables

Table 2.1 Physical data pertaining to all sites sampled in a) the sill set lakes and b) the chain set lakes during the open water season of 2004.

a) Sill Set Lakes

Lake	Spring Sill (m asl)	Connection	Coordinates		Lake Area (ha)
			North	West	
129	2.363	direct	68 18.330'	133 50.566'	37.8
80	2.631	indirect	68 19.399'	133 52.324'	19.3
520	5.169	indirect	68 18.816'	133 42.854'	0.2

b) Chain Set Lakes

Lake Site	Spring Sill (m asl)	Connection	Coordinates	
			North	West
S1	1.500	direct	68 28.494'	133 49.814'
S2	1.500	direct	68 28.422'	133 49.178'
S3	1.500	direct	68 28.110'	133 49.060'
S4	1.500	indirect	68 27.803'	133 48.740'
S5	1.500	indirect	68 27.805'	133 48.303'
S6	1.500	indirect	68 27.722'	133 47.765'
S7	1.500	indirect	68 27.586'	133 48.003'
S8	1.500	indirect	68 27.294'	133 48.023'
S9	1.500	indirect	68 27.192'	133 48.419'

Table 2.2 Correlations (r^2) between diffuse attenuation coefficients and individual attenuators CDOM (a330, m^{-1}), TSS, Chl-*a*, and TDOC, at each site studied during the open water season of 2004. Correlations are examined by waveband; a) K_dUVB(310-320), b) K_dUVA, and c) K_dPAR. All displayed correlations are simple linear regressions and are significant at $p \leq 0.05$ (with the exception of correlations in bold type, which indicate near-significant results: $0.05 < p < 0.06$).

a) K_dUVB(310-320)

	Chain Set Lakes									**Sill Set Lakes**		
	S1	S2	S3	S4	S5	S6	S7	S8	S9	L129	L80	L520
a330	0.956	0.956	0.685	0.942	0.825	0.740	0.655	0.689	0.685	0.764	0.995	0.914
TSS	0.854										0.994	
Chl-*a*					0.947				0.991	0.779		
TDOC	0.843	0.840	0.750	0.907								

b) K_dUVA

	Chain Set Lakes									**Sill Set Lakes**		
	S1	S2	S3	S4	S5	S6	S7	S8	S9	L129	L80	L520
a330	0.868	0.894	0.696	0.915	0.831	0.709	0.701	0.757	0.757	0.847	0.970	0.870
TSS	0.932										0.931	
Chl-*a*					0.903				0.978	0.850		
TDOC	0.789	0.692	0.696	0.852								

c) K_dPAR

	Chain Set Lakes									**Sill Set Lakes**		
	S1	S2	S3	S4	S5	S6	S7	S8	S9	L129	L80	L520
a330	0.761										0.905	
TSS	0.955										**0.967**	
Chl-*a*			**0.595**		**0.568**				0.941			
TDOC												

Table 2.3 Partial attenuation coefficients for attenuators of UVB(310-320 nm), UVA and PAR irradiance in a) the chain set, and b) the sill set lakes during the open water season of 2004.

a) Chain Set Lakes

waveband	constant	CDOM	TSS	r^2	model p
UVB(310-320)	9.42	0.73	0.24	0.80	<0.0001
p-value	<0.0001	<0.0001	<0.0001		
UVA	3.93	0.44	0.21	0.81	<0.0001
p-value	<0.0001	<0.0001	<0.0001		
PAR	0.49	0.05	0.11	0.74	<0.0001
p-value	0.0091	<0.0001	<0.0001		

b) Sill Set Lakes (Lakes 129, 80 and 520)

waveband	constant	CDOM	TSS	Chl-*a*	r^2	model p
UVB(310-320)	2.87	1.31	0.54	-1.26	0.84	0.0002
p-value	0.3853	0.002	0.0045	0.01		
UVA	0.75	0.64	0.37	-0.46	0.86	<0.0001
p-value	0.6523	0.0023	0.0006	0.0454		
PAR	-0.21	0.14	0.12	-0.19	0.68	0.0012
p-value	0.7707	0.0623	0.0035	0.055		

Table 2.4 Empirical relationships using CDOM absorption coefficients (a330, m^{-1}) as a predictor of diffuse UV attenuation coefficients in both the chain set and the sill set lakes during the open water season of 2004. The (a) UVB(310-320 nm) and (b) UVA wavebands are considered separately.

a) UVB(310-320 nm)

System	Relationship	r^2	p
Chain Set Lakes	K_dUVB(310-320) = 11.929 + 0.678 a330	0.692	<0.0001
Sill Set Lakes	K_dUVB(310-320) = 1.171 + 1.436 a330	0.531	0.0047

b) UVA

System	Relationship	r^2	p
Chain Set Lakes	K_dUVA = 6.211 + 0.390 a330	0.584	<0.0001
Sill Set Lakes	K_dUVA = -0.858 + 0.855 a330	0.560	0.0021

2.8 Figures

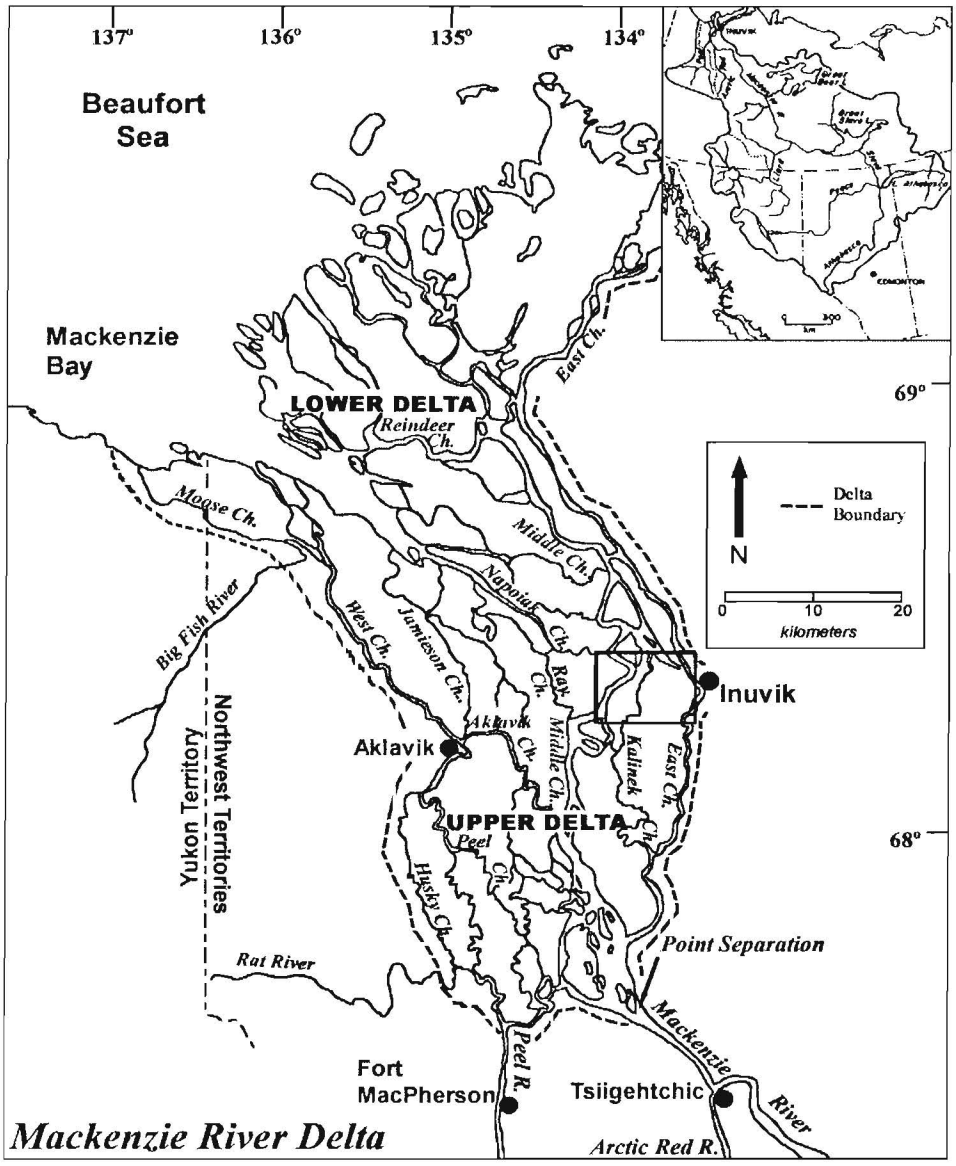

Figure 2.1 The Mackenzie Delta, western Canadian Arctic. All lake sampling sites are located within 15 km of the town of Inuvik off the East Channel of the Mackenzie River (within the square).

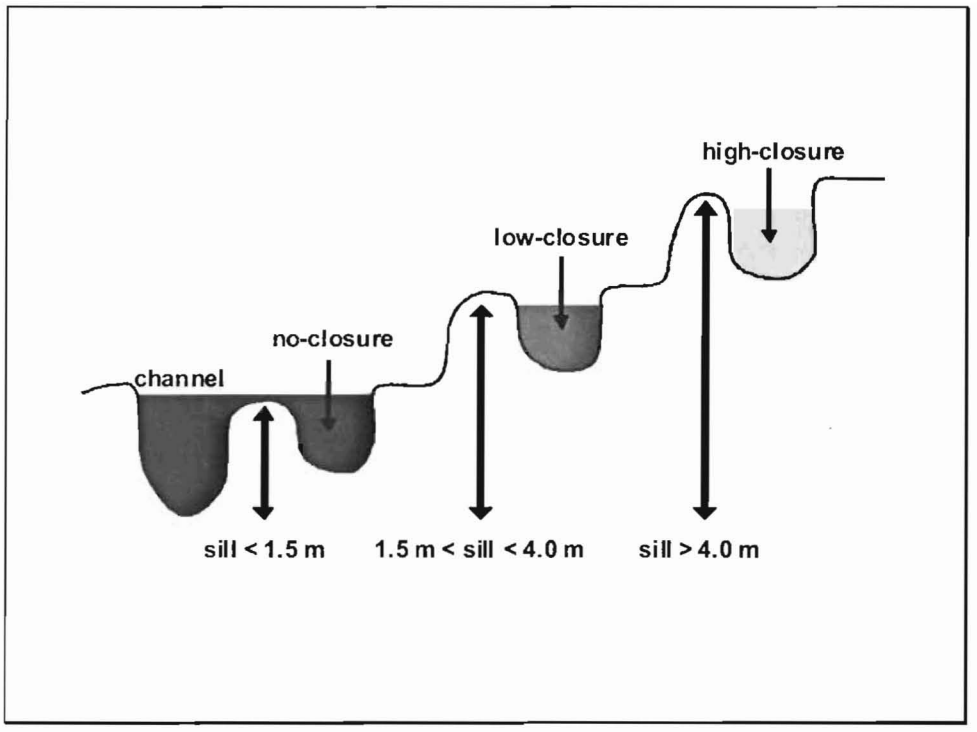

Figure 2.2 Lakes in the Mackenzie Delta are classified as no-, low-, or high-closure based on their sill elevation.

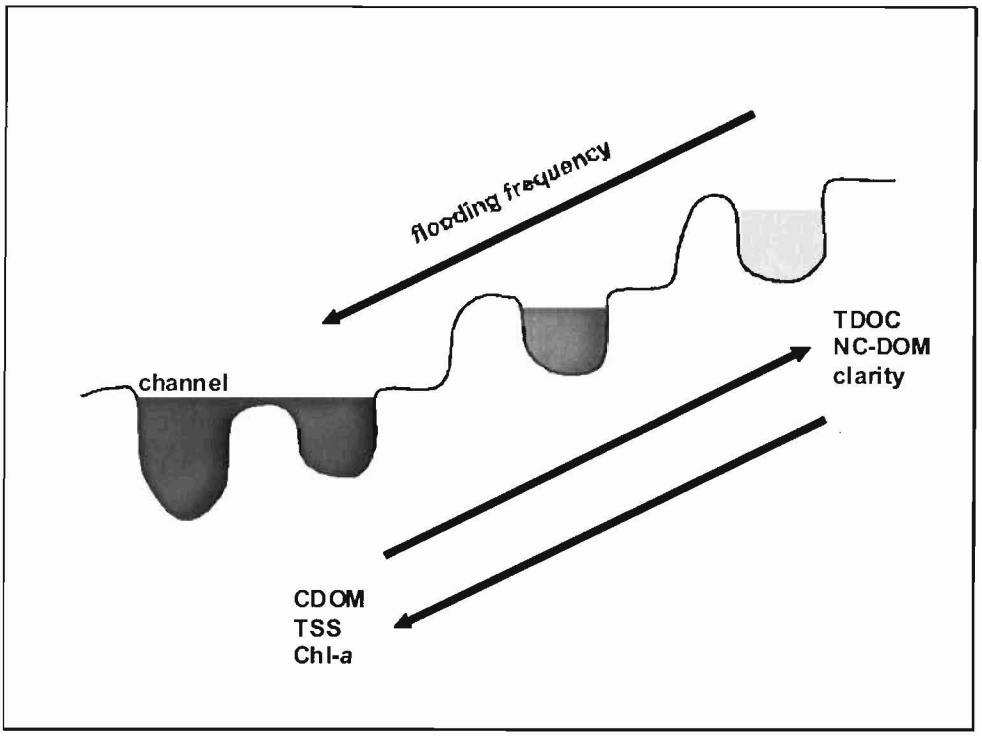

Figure 2.3 Sill elevations of individual lakes give rise to a gradient of flooding frequencies and water chemistry trends in the Mackenzie Delta. Concentrations of CDOM, TSS and Chl-*a* tend to increase with increasing flooding frequency, while concentrations of TDOC and non-chromophoric DOM (NC-DOM) tend to increase with decreasing flooding frequency. Lakes that are flooded less frequently also tend to have clearer water columns than those that are permanently connected to distributary channels.

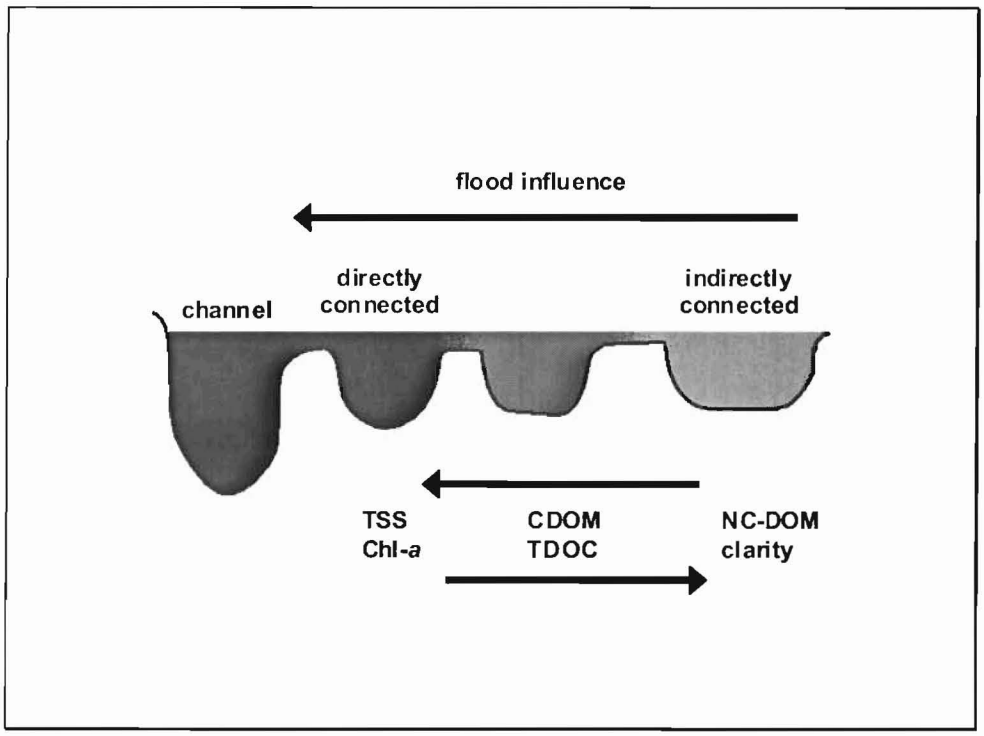

Figure 2.4 Sets of lakes that are joined in a chain exhibit a similar, but more variable, set of water chemistry gradients than do sill set lakes. Lakes that are closer to a channel connection receive greater inputs of floodwaters and tend to have higher concentrations of TSS and Chl-*a*. In contrast, lakes that are located further from a channel connection are clearer and tend to have higher concentrations of non-chromophoric DOM (NC-DOM). In the summer of 2004, lakes in the middle of the chain set had the highest concentrations of both CDOM and TDOC.

a)

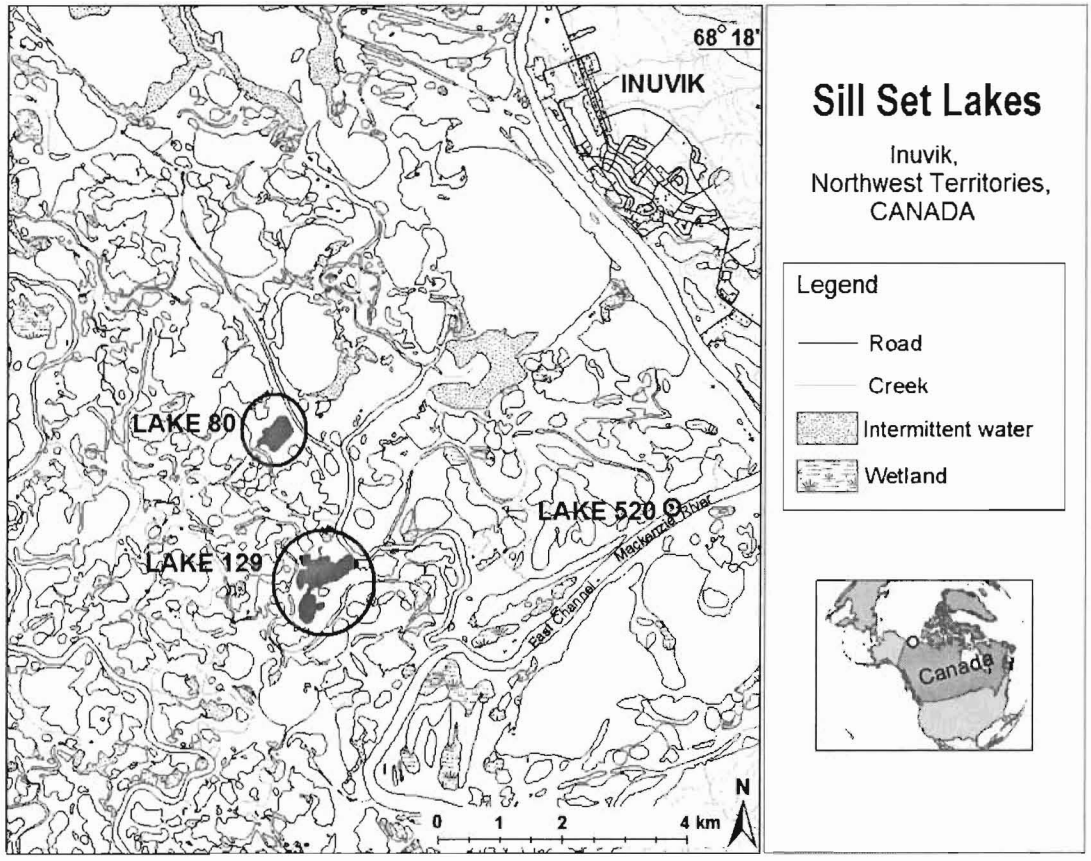

Figure 2.5 Location of sampling sites in the Mackenzie Delta: a) the sill set lakes, and b) the chain set sampling sites.

b)

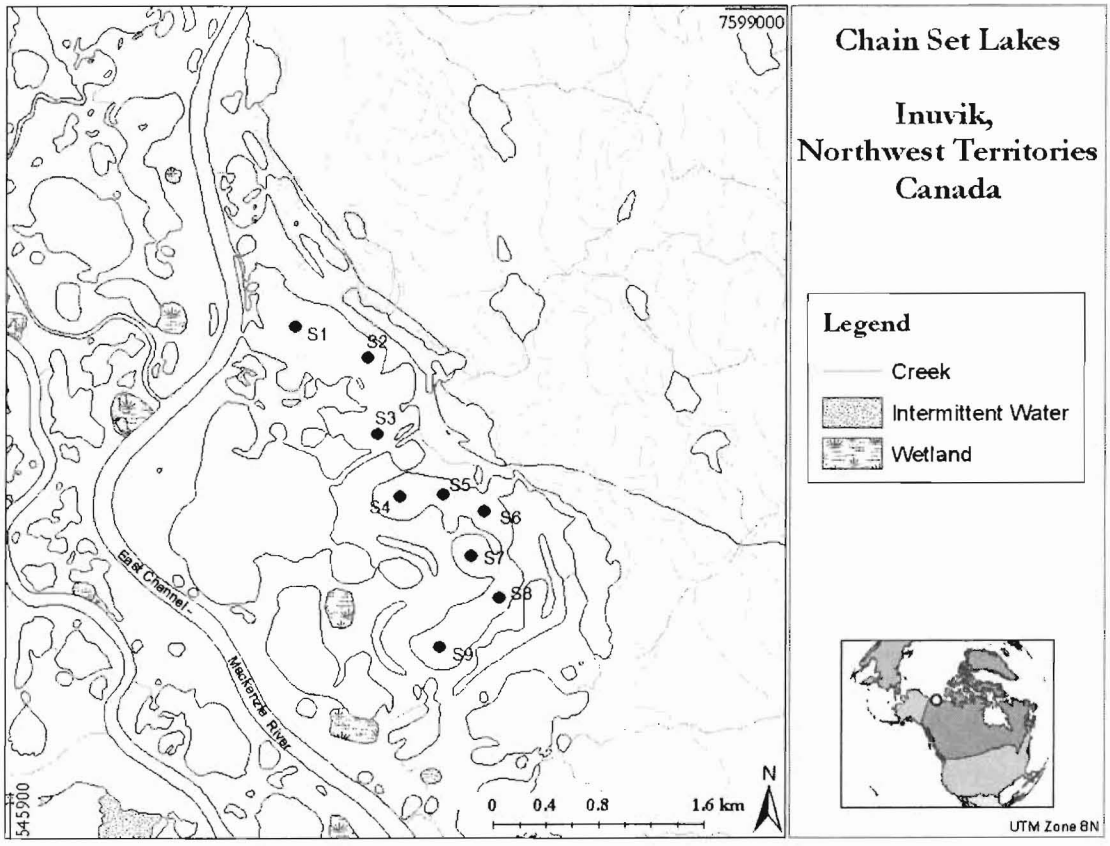
7599000
545900
S1
S2
S3
S4
S5
S6
S7
S8
S9
East Channel
Mackenzie River
0 0.4 0.8 1.6 km
N
Chain Set Lakes
Inuvik,
Northwest Territories
Canada
Legend
Creek
Intermittent Water
Wetland
UTM Zone 8N

Photo by author

Figure 2.6 The OL 754 portable high accuracy submersible UV-VIS scanning spectroradiometer (Optronics Laboratories), configured for field scans. The submersible integrating sphere and depth indicator can be seen to the right. The 3 m long parallel swing arm allowed the operator to position and hold the integrating sphere at a specific depth while a series of spectral scans were taken.

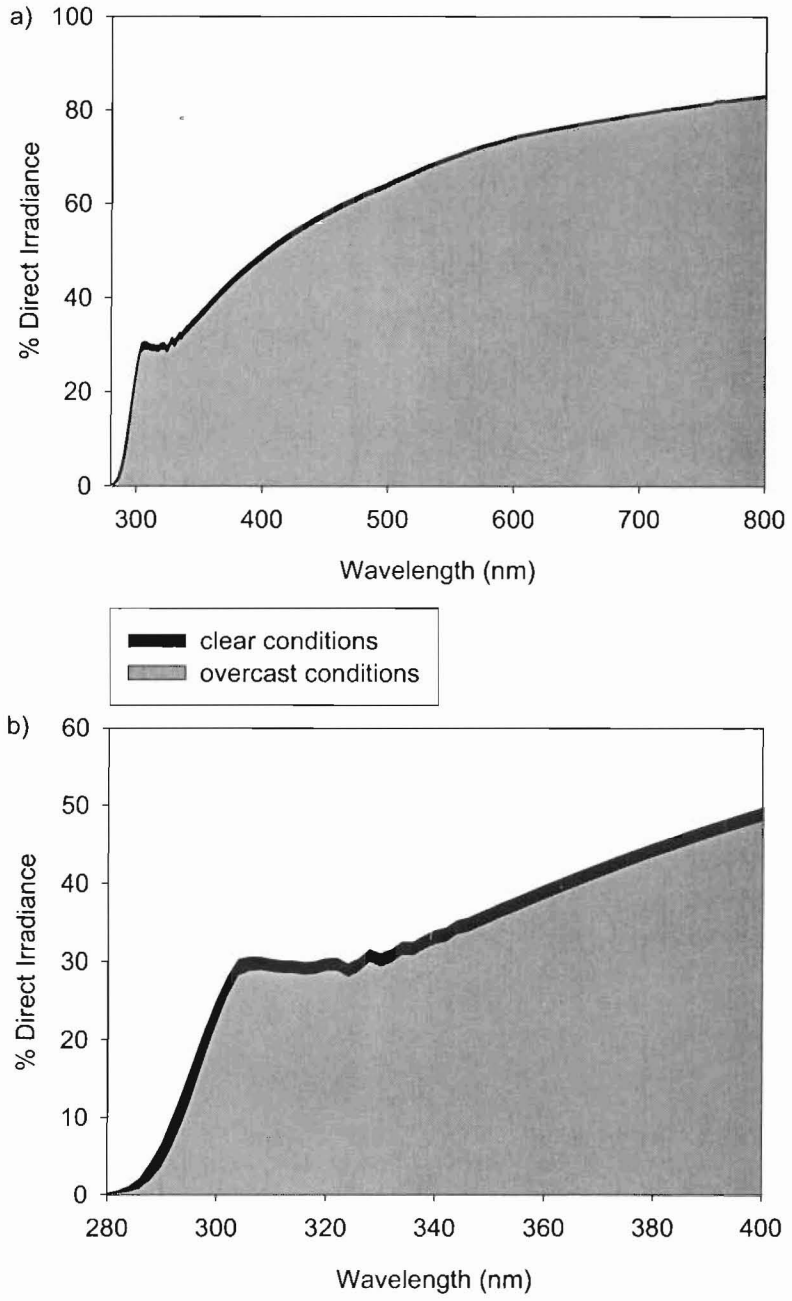

Figure 2.7 Proportion of the incident irradiance field that is direct, as opposed to diffuse, under both clear and overcast conditions. Both a) the full spectrum (280-800 nm) and b) the UV spectrum only (280-400 nm) are shown. Overcast conditions reduce the proportion of direct irradiance at all wavelengths. Data were collected using an OL 754 spectroradiometer. Calculation of the proportion of the measured irradiance field composed of direct irradiance was performed using the SMARTS2 model.

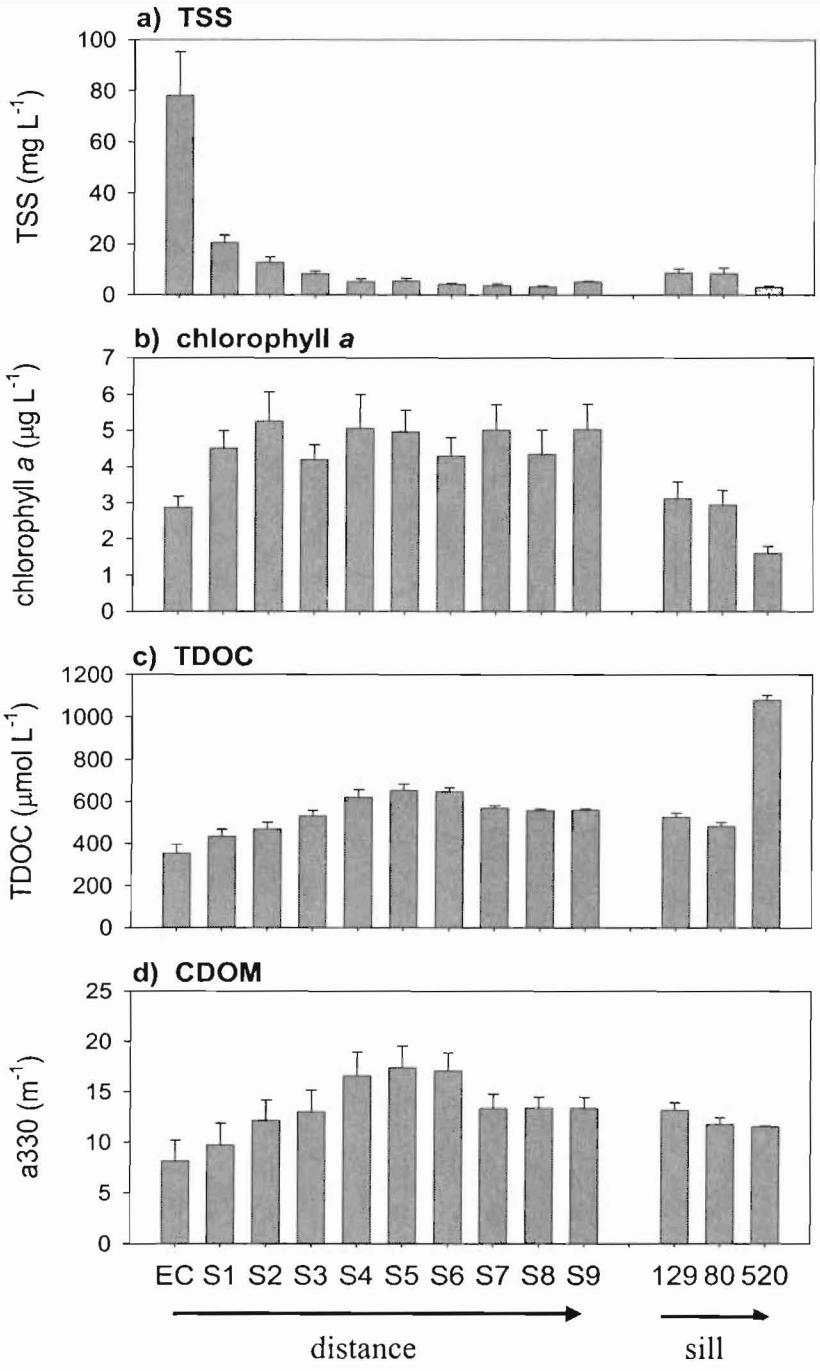

Figure 2.8 Water chemistry data pertaining to all sites sampled for irradiance attenuation during the summer of 2004. Data for both the chain set (S1-S9) and the sill set lakes (Lakes 129, 80 and 520) are shown, along with water chemistry data from the East Channel (EC) as a riverine reference. Mean values of a) TSS, b) Chl-*a*, c) TDOC, and d) CDOM over the open water season are displayed, with error bars representing one standard error of the mean.

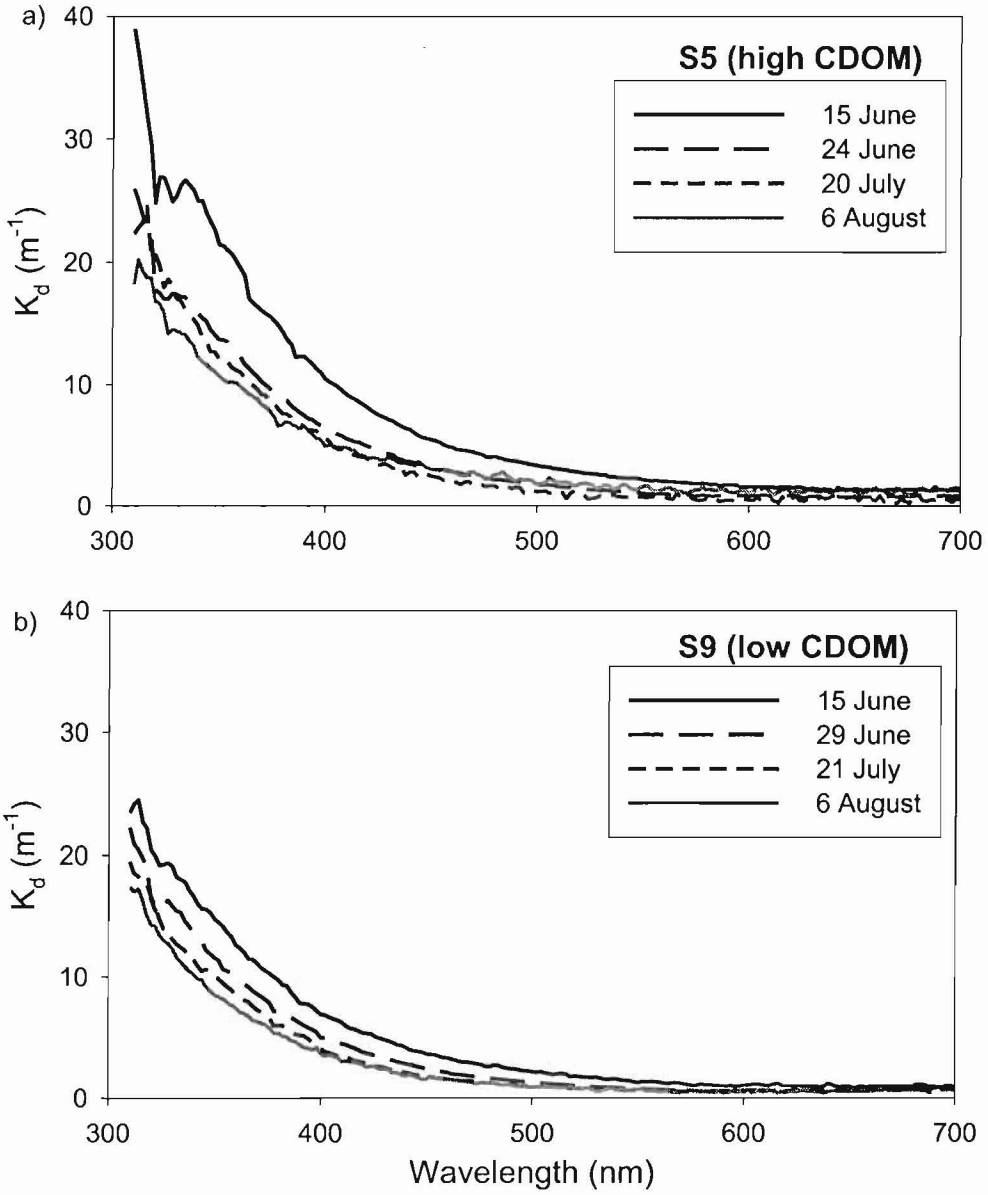

Figure 2.9 Time series of the decline in diffuse attenuation coefficients (K_d, m^{-1}) over the open water season of 2004 at a) S5, a high CDOM site, and b) S9, a low CDOM site. Most of the loss in attenuation capacity occurs in the UV wavebands due to CDOM photobleaching.

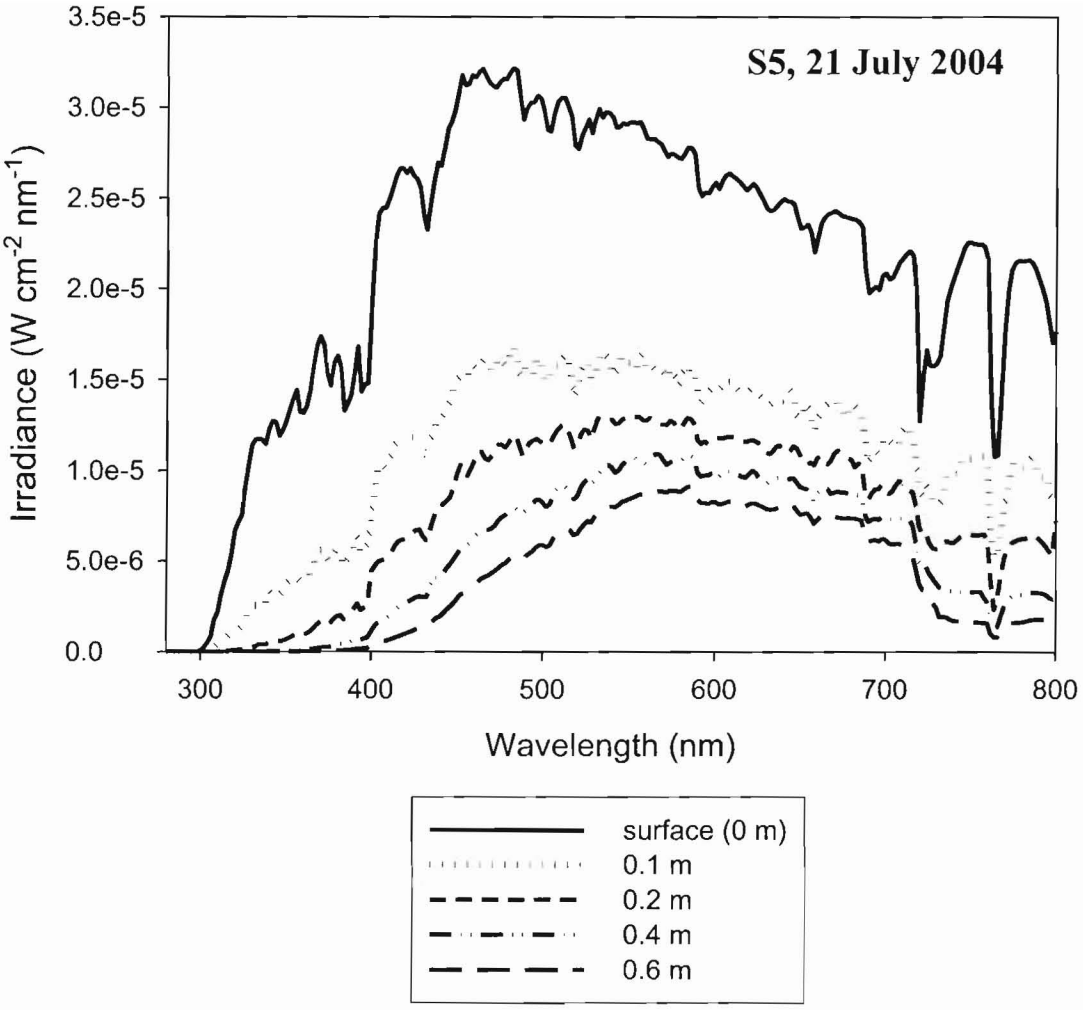

Figure 2.10 Decline in irradiance with increasing depth at sampling site S5 in the chain set lakes of the Mackenzie Delta. All scans were taken under constant sky conditions on 21 July 2004. The surface scan was taken with the sensor of the spectroradiometer positioned just above the surface of the lake, and is therefore a scan of the ambient irradiance conditions during the period of *in situ* scanning.

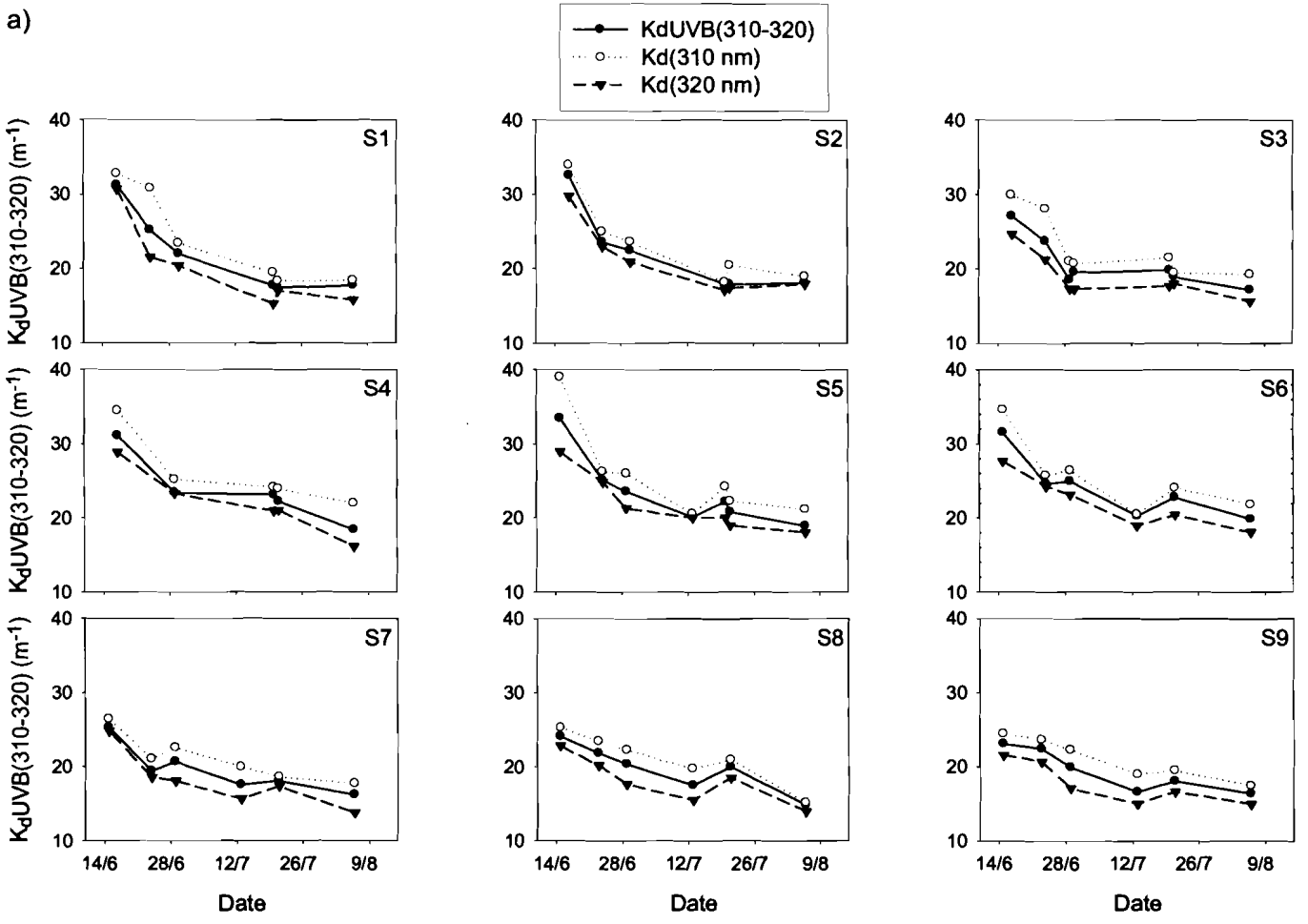

Figure 2.11 Diffuse attenuation coefficients for a) the UVB (310-320 nm) waveband, b) the UVA waveband, and c) the PAR waveband in the chain set lakes, and d) all wavebands in the sill set lakes, during the open water season of 2004. Average attenuation coefficients are shown along with attenuation coefficients at the waveband boundaries.

b)

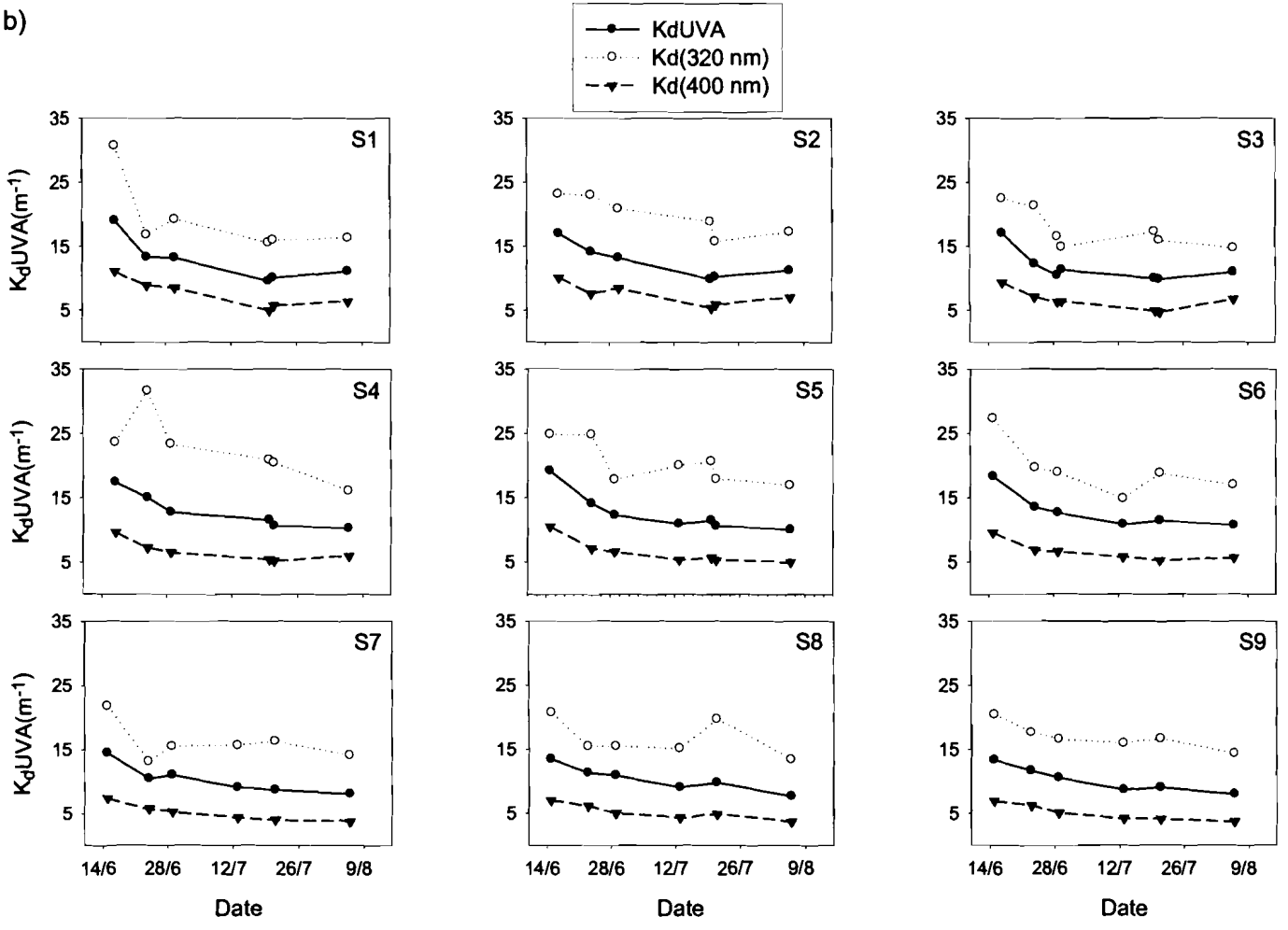
KdUVA
Kd(320 nm)
Kd(400 nm)
S1
S2
S3
S4
S5
S6
S7
S8
S9
KdUVA(m-1)
35
25
15
5
14/6
28/6
12/7
26/7
9/8
Date

c)

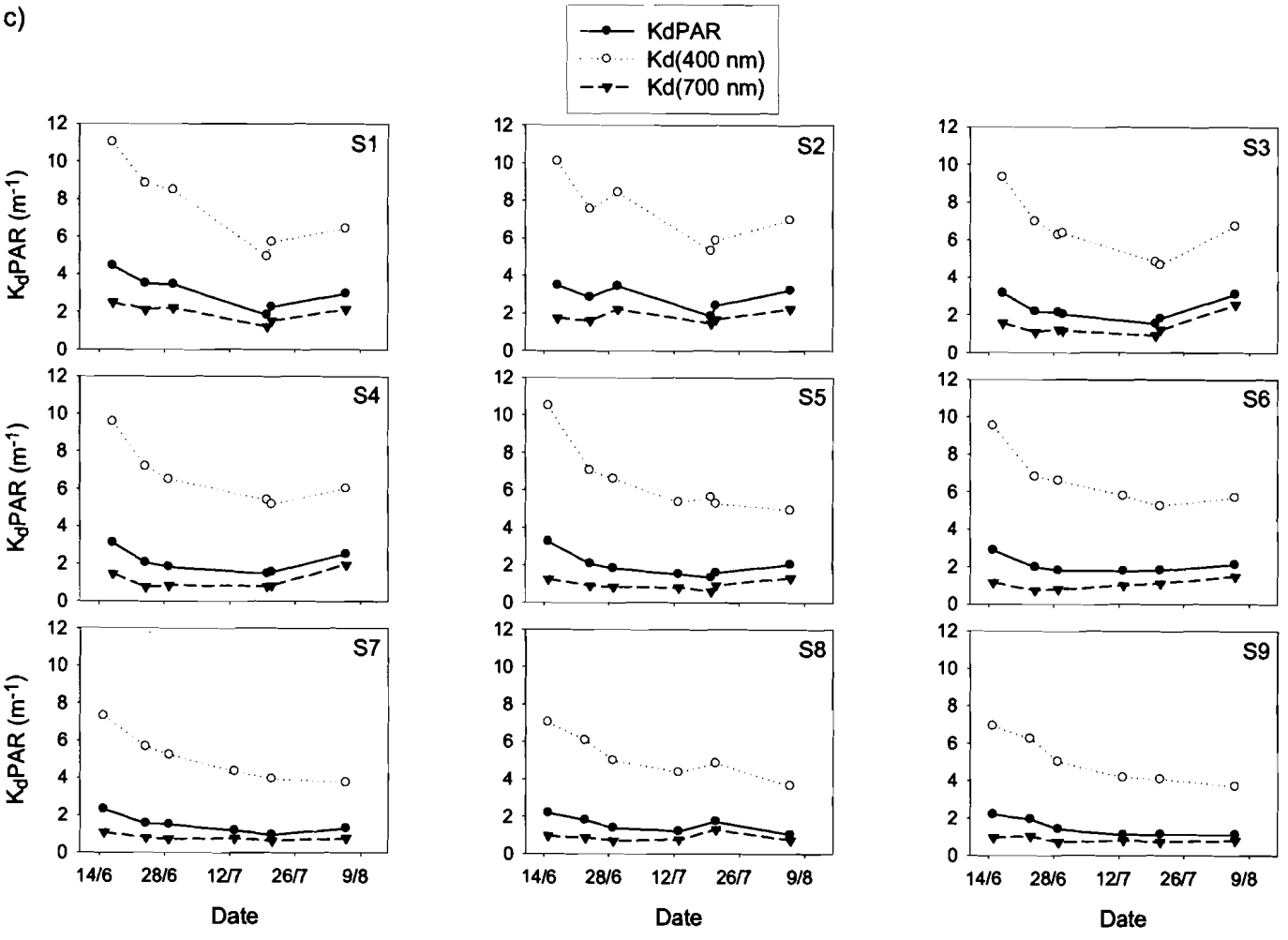
KdPAR
Kd(400 nm)
Kd(700 nm)
S1
S2
S3
S4
S5
S6
S7
S8
S9
$K_dPAR\ (m^{-1})$
0
2
4
6
8
10
12
14/6
28/6
12/7
26/7
9/8
Date

d)

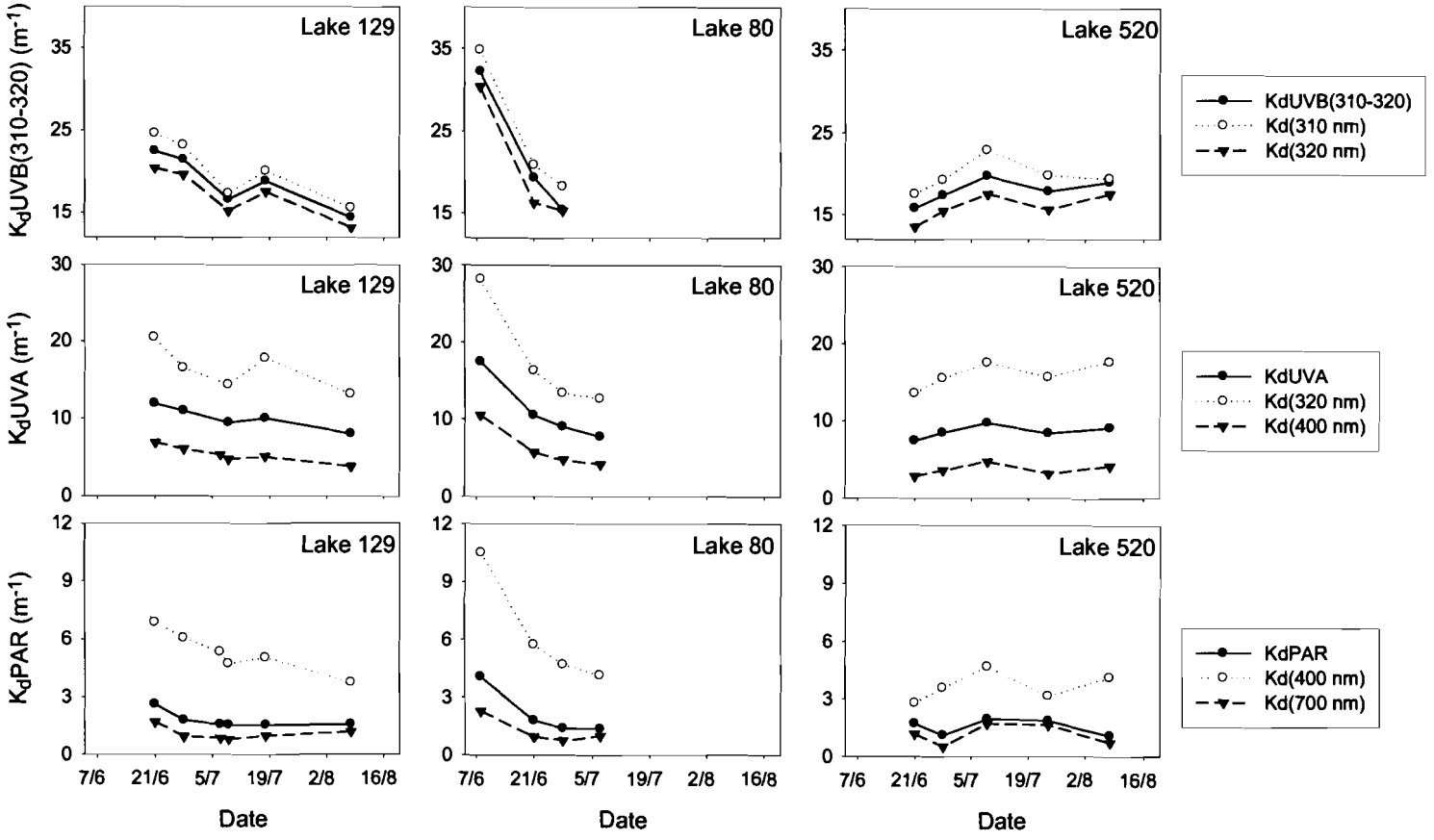
Lake 129
Lake 80
Lake 520
$K_dUVB(310-320)$ (m^{-1})
K_dUVA (m^{-1})
K_dPAR (m^{-1})
KdUVB(310-320)
Kd(310 nm)
Kd(320 nm)
KdUVA
Kd(320 nm)
Kd(400 nm)
KdPAR
Kd(400 nm)
Kd(700 nm)
7/6
21/6
5/7
19/7
2/8
16/8
Date

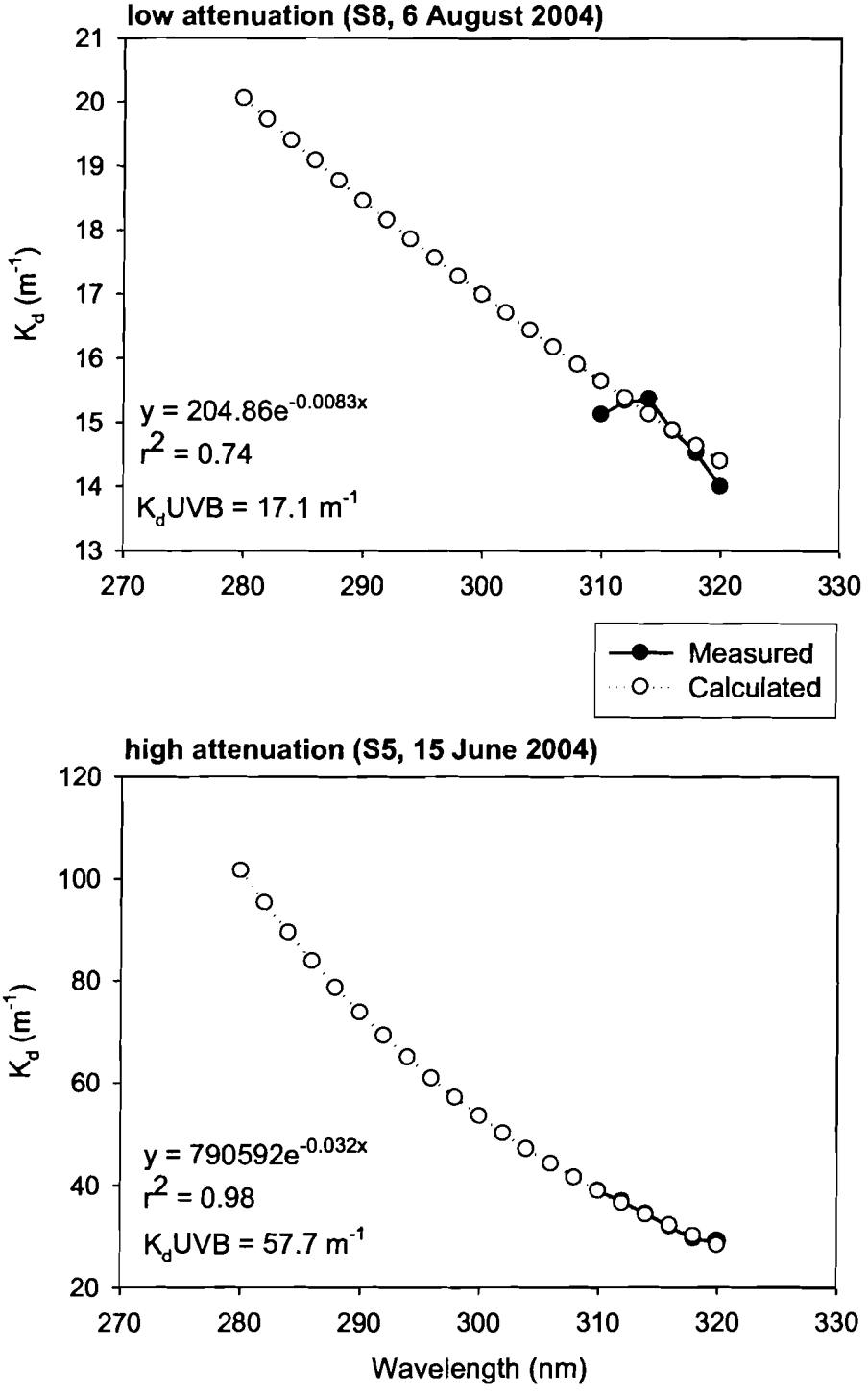

Figure 2.12 Extrapolation of *in situ* K_d (m^{-1}), measured from 310 to 320 nm, over the interval from 280 to 320 nm for examples of both low and high *in situ* attenuation. The exponential decline equations used to calculate the extrapolated data are shown.

a)

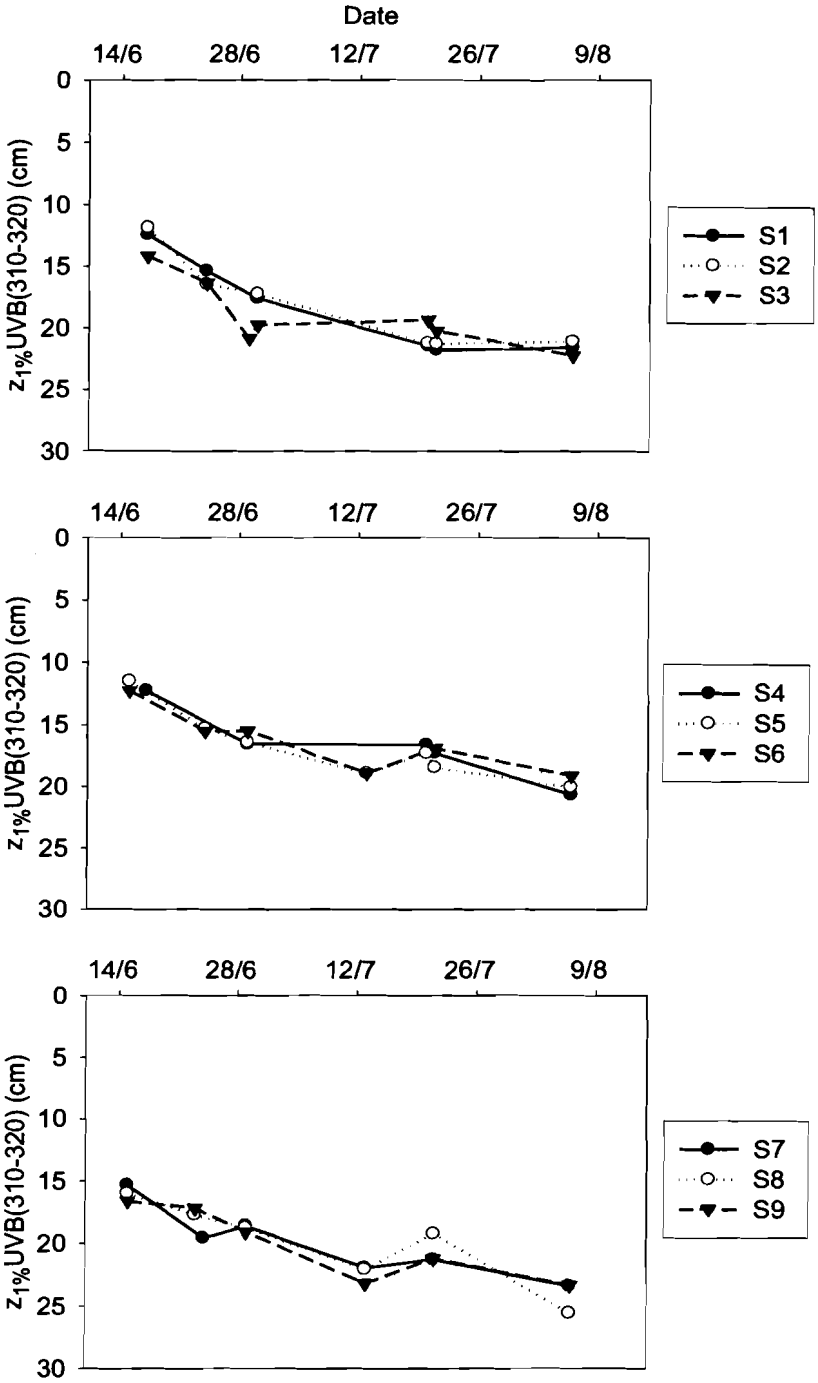

Figure 2.13 Average photic depths ($z_{1\%}$) for a) the UVB (310-320 nm) waveband, b) the UVA waveband, and c) the PAR waveband in the chain set lakes, and d) for all wavebands in the sill set lakes, during the open water season of 2004.

b)

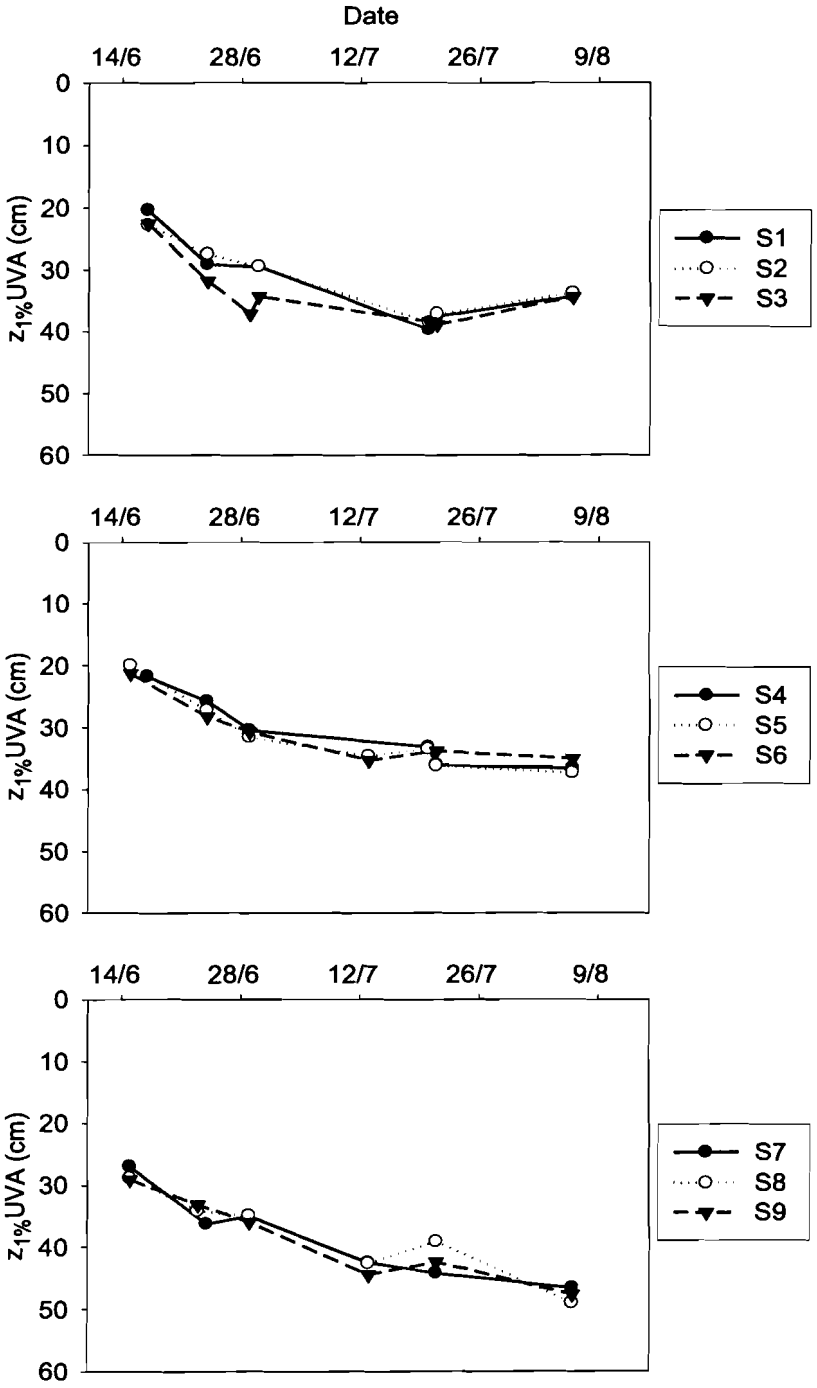
Date
14/6
28/6
12/7
26/7
9/8
0
10
20
30
40
50
60
$z_{1\%}$UVA (cm)
S1
S2
S3
S4
S5
S6
S7
S8
S9

c)

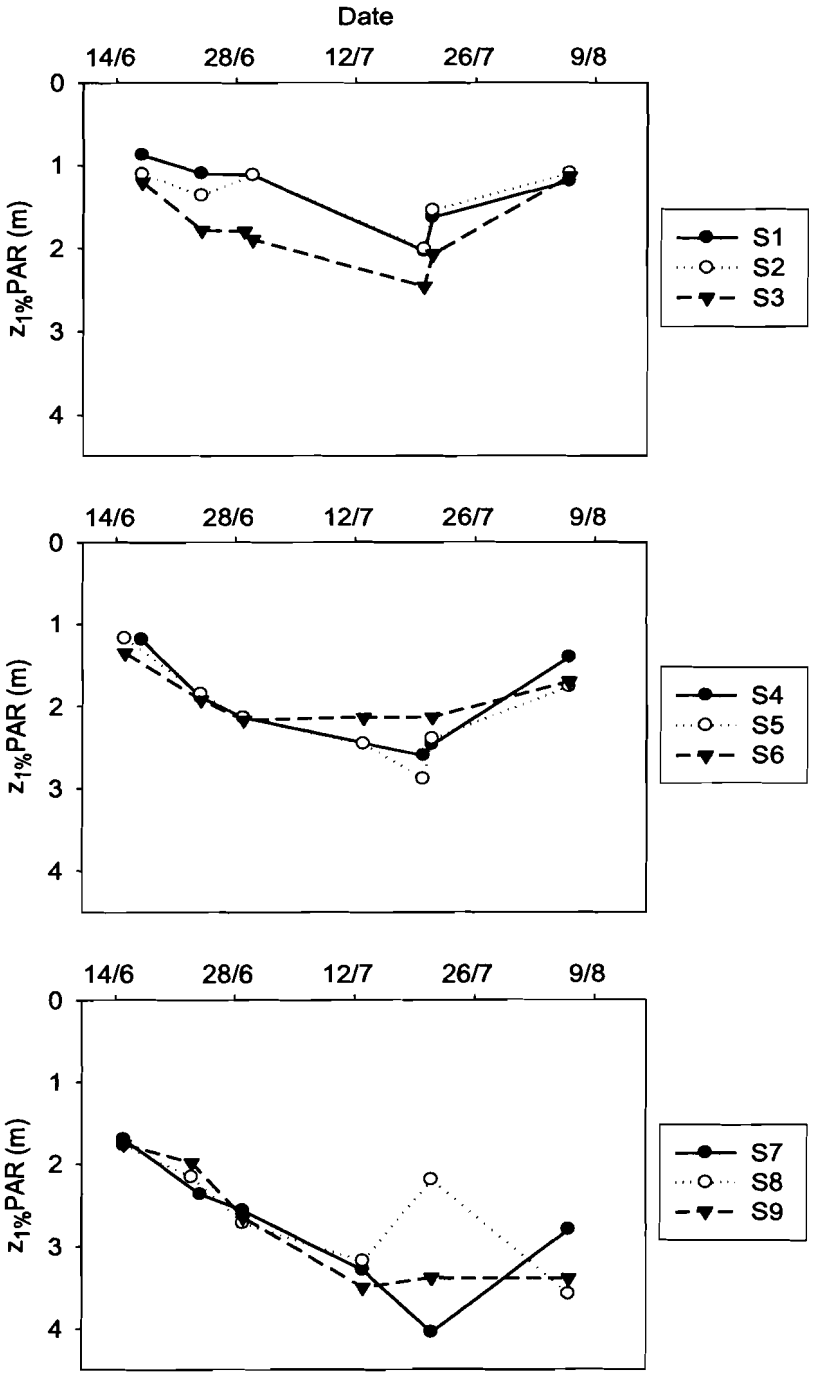

d)

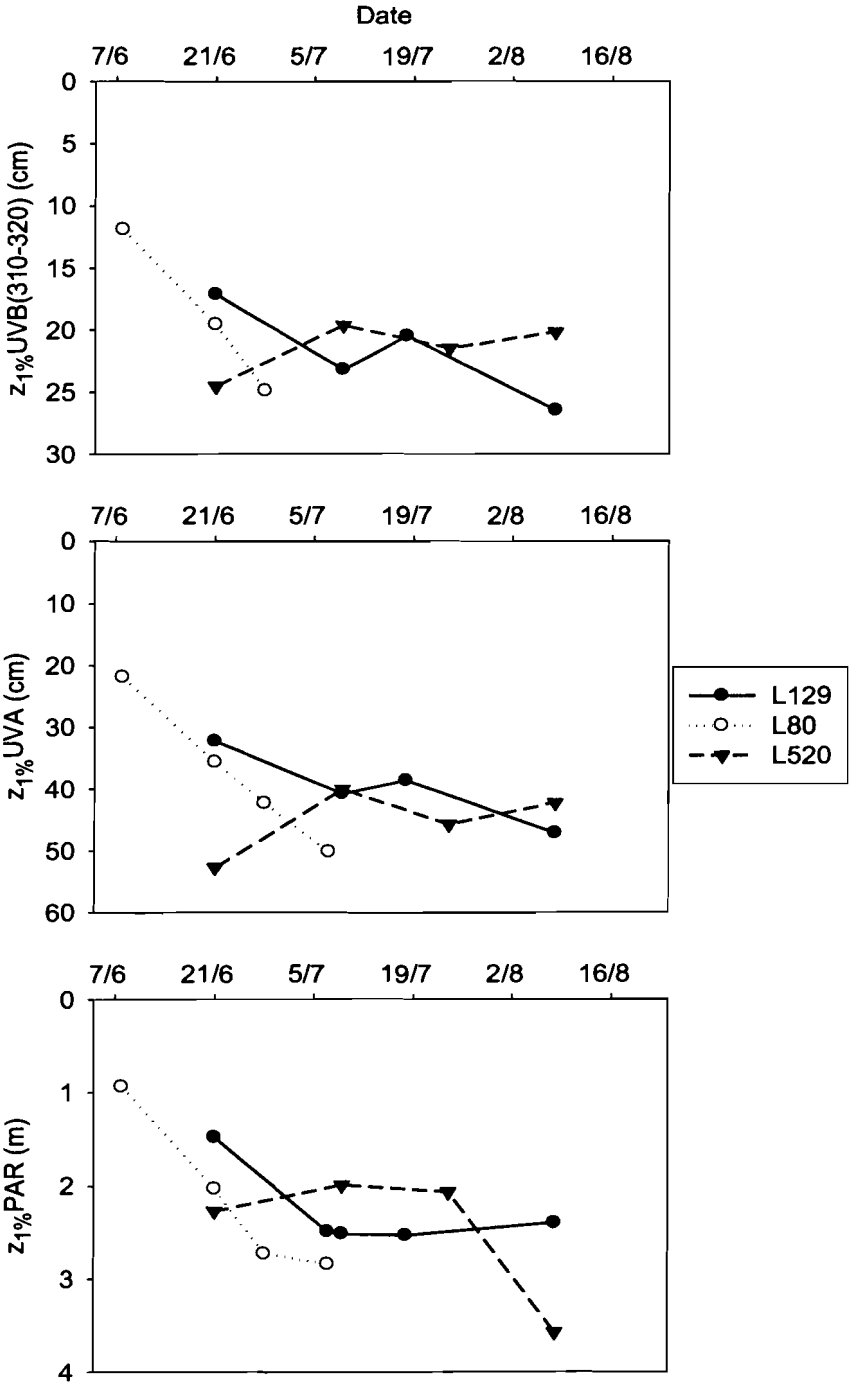
Date
7/6
21/6
5/7
19/7
2/8
16/8
$z_{1\%}$UVB(310-320) (cm)
0
5
10
15
20
25
30
$z_{1\%}$UVA (cm)
0
10
20
30
40
50
60
$z_{1\%}$PAR (m)
0
1
2
3
4
L129
L80
L520

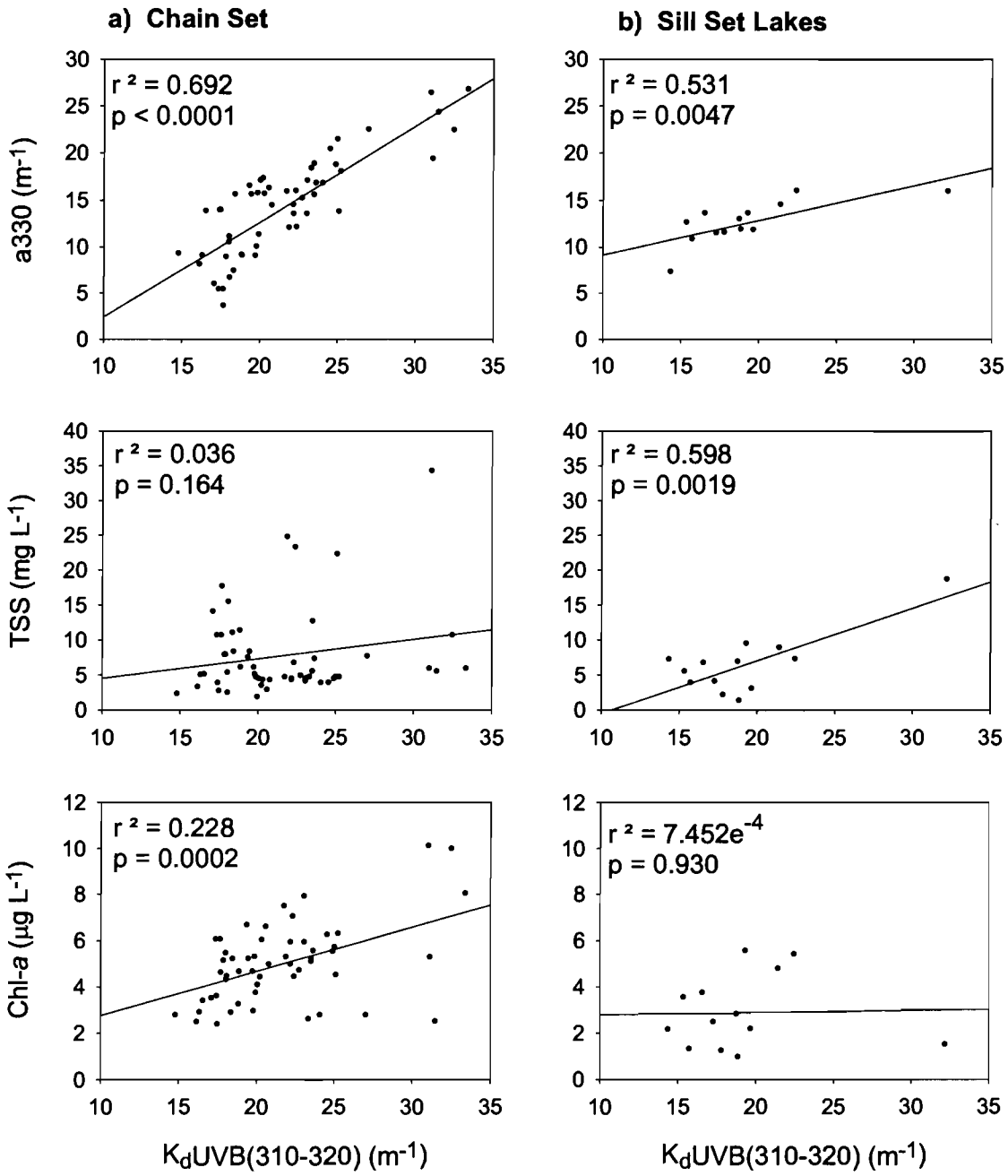

Figure 2.14 Diffuse attenuation coefficients for the UVB waveband ($K_dUVB(310\text{-}320)$, m^{-1}) plotted against CDOM (a330, m^{-1}), TSS and Chl-*a* in a) the chain set and b) the sill set lakes during the open water season of 2004. All regressions are simple linear regressions.

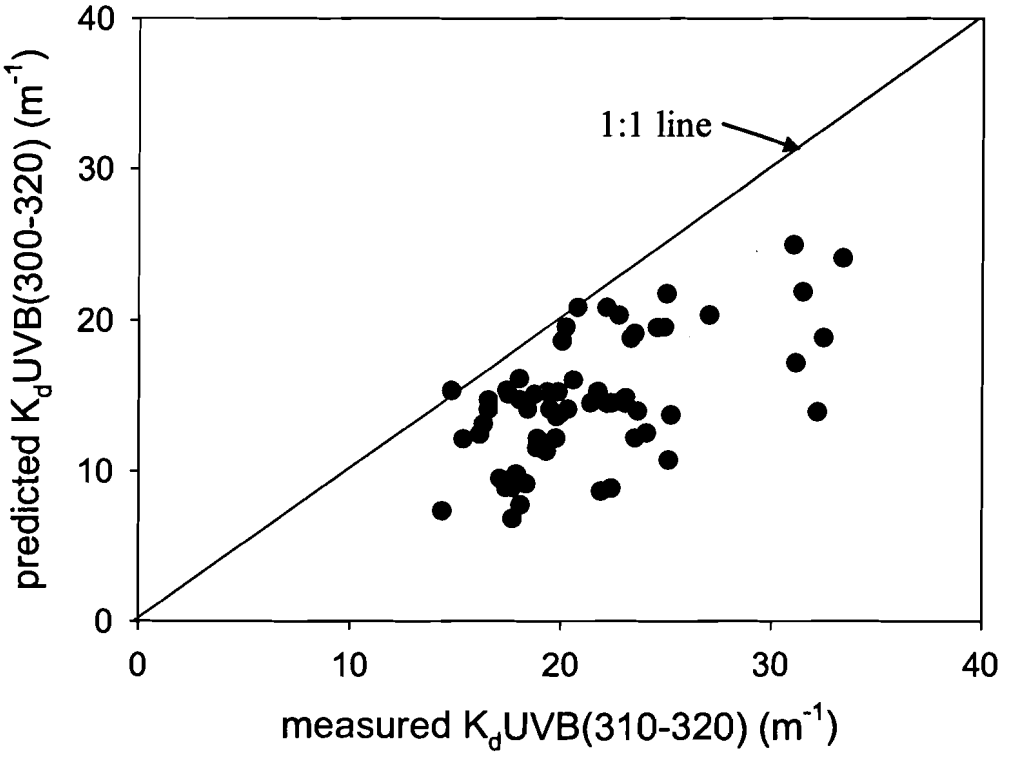

Figure 2.15 A comparison of measured *versus* calculated K_dUVB values for 12 sites in the Mackenzie Delta that were tracked throughout the summer of 2004. Measured K_dUVB(310-320) were obtained using a scanning spectroradiometer, while calculated K_dUVB(300-320) were obtained using the predictive power equation presented by Scully and Lean (1994; K_dUVB(300-320) = $0.42[DOC]^{1.86}$).

3 PHOTOBLEACHING OF DISSOLVED ORGANIC MATTER IN MACKENZIE DELTA LAKES

3.1 Introduction

Organic matter in aquatic ecosystems encompasses both living and dead material ranging in size from microscopic dissolved organic compounds to visible aggregates of particles (Wetzel and Likens 2000). The dissolved portion, known as dissolved organic matter (DOM), is defined operationally as the fraction of the organic pool that will pass through a filter with a pore size of 0.45 μm. It is composed of a heterogeneous group of organic molecules generally containing a large proportion of humic materials, along with a variety of smaller compounds such as fulvic acids and individual amino acids (Findlay et al. 2003). DOM is the predominant form of organic matter in most aquatic environments, and it plays a significant role in determining ecosystem function and structure (Obernosterer and Benner 2004).

3.1.1 Influence of DOM Origin on the Chemical and Optical Properties of Lakes

Quantities of DOM can vary by orders of magnitude among lakes, from less than 1 mg C L^{-1} to greater than 300 mg C L^{-1} (Molot et al. 2004), with a correspondingly wide variation of effects on the *in situ* environment. However, the quality of the DOM pool, as determined by the proportion of autochthonous *versus* allochthonous DOM, also has important implications for the chemical, optical and biological characteristics of a lake. The quantity and quality of DOM in inland waters together determine the availability of dissolved nutrients, modify the optical properties of the water column (see Chapter 2), and act as important regulators of aquatic food webs (Findlay et al. 2003). Additionally, processes that produce, consume, and transform DOM are important in determining the overall cycling of energy, carbon and nutrients in aquatic ecosystems (McKnight et al. 2003).

Aquatic DOM can be derived from one of two sources: within-lake photosynthetic production by phytoplankton and macrophytes (autochthonous DOM), or runoff containing leachates from the decomposition of terrestrial vegetation in the surrounding watershed (allochthonous DOM). Therefore, DOM molecules are either generated internally, or in the surrounding catchment where they are stored until they are flushed into water bodies by precipitation, flooding or snowmelt. This ties allochthonous DOM

supply and residence time to watershed hydrology and climate (Wrona et al. 2006, Curtis 1998).

Autochthonous DOM has a lower proportion of aromatic carbon rings in its molecular structure, making it more labile (bioavailable) than allochthonous DOM, which is predominantly derived from the decomposition of highly aromatic lignin. As a result, allochthonous DOM molecules are larger, more refractory and more resistant to biological degradation than are autochthonous DOM molecules. Lakes with predominantly allochthonous DOM pools, such as swamps or bogs, tend to be highly coloured or "stained". The high proportion of aromatic carbon ring structures contained in allochthonous DOM molecules act as strongly absorbing chromophores (photoreceptors) of UV wavelengths (McKnight et al. 2001). Therefore, allochthonous DOM is also known as chromophoric DOM (CDOM). Since autochthonous DOM contains a lower proportion of light absorbing chromophores, it absorbs lower amounts of both visible and UV irradiance and is also less coloured than allochthonous DOM. Lakes that primarily contain autochthonous DOM, such as those at high latitudes and altitudes where there is little vegetation within the surrounding watershed, generally have deeper photosynthetic compensation depths and clearer water columns than do lakes that primarily contain allochthonous DOM (Molot et al. 2004).

Although DOM origin plays a vital role in determining the chemical and optical properties of an aquatic system, with important implications for aquatic organisms and food webs, it can also be transformed *in situ* by a variety of processes. Bacterial degradation (Tranvik 1998), flocculation and sedimentation (Molot and Dillon 1997) and export via lake outflows (Gibson et al. 2001) can all alter the quantity and quality of DOM found within lakes. Additionally, the CDOM portion of the total DOM pool can be lost through photobleaching, a process that increases the transparency of the water column to UV irradiance (e.g. Osburn et al. 2001). As aromatic ring structures within CDOM molecules absorb wavelengths in the UV waveband, they are cleaved into smaller molecules with a reduced absorption capacity. Although very little of the total DOM pool is used directly as food by aquatic organisms, it is a major food source for bacterial populations when broken down by photochemical reactions into more labile forms (Kieber et al. 1989), further contributing to DOM losses from the system.

3.1.2 Indices of DOM Quality

It is possible to differentiate DOM that is primarily derived from terrestrial precursor material, such as soil or plant matter, from that primarily derived from within-lake microbial activity or precursor material (Lafrenière and Sharp 2004). The coloured allochthonous fraction of the DOM pool has optical properties that are commonly used to characterize both the quantity and quality of organic material present in aquatic ecosystems (e.g. Mopper and Shultz 1993, Coble et al. 1990, De Haan and De Boer 1987; Stewart and Wetzel 1980). Previous studies in Mackenzie Delta lakes have used only measurements of absorption at 330 nm normalized to an absorption coefficient over 1 m (a330, m^{-1}) to characterize the CDOM pool. However, this measurement is dependent on both the concentration and chemical nature of CDOM (Green and Blough 1994), whereas other commonly-used indices are independent of concentration and reflect only optical characteristics (Gibson et al. 2001).

Many analytical techniques that are used to examine DOM quality also have limitations such as poor sensitivity or the need for extractions or physical treatment before analysis, making the measurement of large numbers of samples impractical. This study examined several methods used to indicate DOM quality in other inland systems that require only simple measurements and little sample preparation, and which were independent of DOM concentration. These methods were used in order to determine the relative contributions of the spring flood, carrying allochthonous DOM, and within-lake production, generating autochthonous DOM, to the total DOM pool in individual lakes of the Mackenzie Delta. Given the large number of lakes in the delta and the short open water season, quick and accurate measurements of DOM quality could prove very valuable in future investigations of the DOM pool and the dependence of its quality on the annual flood, along with subsequent *in situ* changes in quality resulting from photochemical or biological activity.

Fulvic acids are the primary source of colour in most freshwater bodies; they comprise a heterogeneous class of moderate molecular weight, yellow-coloured organic acids that are present in some concentration in all natural waters (Klapper et al. 2002, McKnight et al. 1994). The fulvic acid content largely controls the absorption of UV irradiance in aquatic systems, as well as the generation of photoproducts (Laurion et al.

1997, Scully and Lean 1994). Variations in the chemical and optical characteristics of aquatic fulvic acids result from differences in precursor organic material and from geochemical processes acting on DOM (McKnight et al. 2001). These characteristics have given rise to several DOM diagnostics that use these properties to quantify or characterize organic fractions. The applicability of three indices requiring little sample preparation were assessed for Mackenzie Delta lakes during the summer of 2005.

Spectral Slope Coefficient

Typically, CDOM absorption spectra in the UV-visible ranges are featureless exponential declines with increasing wavelength (Figure 3.1; Tzortziou et al. 2007, McKnight et al. 2001). The spectral slope coefficient (S) expresses the rate of exponential decline in CDOM absorption with increasing wavelength, and lies between 10.0 and 23.0 μm^{-1} for most freshwater systems (Jerome and Bukata 1998, Laurion et al. 1997). Calculation of S for a water sample is a simple measurement requiring only filtration and a spectrophotometric scan of absorption over the relevant wavelength range.

A larger S coefficient indicates a steeper spectral slope in the UV region, corresponding to a greater loss in absorption with increasing wavelength (Whitehead et al. 2000). This indicates a more labile and bioavailable autochthonous DOM character, while a smaller S coefficient indicates a more refractory allochthonous character. This has been confirmed by studies that have found that S tends to be larger for fulvic acids than for more refractory humic acids, and tends to decrease with increasing molecular weight and aromaticity (Carder et al. 1989). However, changes in the absorption spectral slope as a result of photobleaching remain contradictory, with some studies indicating that exposure to solar irradiance causes an increase in S (e.g. Moran et al. 2000, Whitehead et al. 2000) and others indicating a decrease (e.g. Del Castillo et al. 1999, Gao and Zepp 1998, Morris and Hargreaves 1997). For this study, an increase in S coefficient was taken to indicate DOM photobleaching, since this corresponds to decreased UV absorbance, a less refractory DOM character and a lower average aromaticity of the DOM pool.

Specific Ultraviolet Absorbance

The specific ultraviolet absorbance (SUVA) is a measure of the "average" absorptivity of all DOM molecules in a water sample, and can therefore be used as a relative measure of DOM aromaticity (Weishaar et al. 2003). Since DOM derived from allochthonous sources contains a higher proportion of aromatic carbon due to the presence of degraded lignin (Mladenov et al. 2005), higher SUVA values indicating greater absorptivity also indicate a greater proportion of aromatic, allochthonous DOM in the total DOM pool. This measure is derived by dividing the total concentration of the DOM fraction (CDOM plus non-chromophoric DOM) by the absorptivity of the sample at a reference wavelength in the UV range, where allochthonous DOM absorption is highest. In this study, total dissolved organic carbon (TDOC) concentrations were used as proxies for total DOM concentrations, and absorption at the reference wavelength of 280 nm was used to indicate UV absorption.

Fluorescence Index

When molecules absorb photons, excess energy can result in the excitation of electrons. A variety of processes may then occur in order to dissipate the excitation energy and return electrons to the ground state. While most transitions occur via radiationless processes such as heat emission, fluorescence may also occur. Fluorescence is the radiative process in which light is emitted as an electron transitions from the lowest vibrational level of the excited state to the highest vibrational level of the ground state (Cory 2005). Fluorescence spectroscopy has been used extensively as a tool to characterize the source, reactivity and age of DOM since little sample preparation is required.

A method first proposed in a series of related papers (Hood et al. 2003, Klapper et al. 2002, McKnight et al. 2001) was followed in order to determine the predominant source of DOM present in Mackenzie Delta lakes. The development of this method stemmed from previous studies of DOM fluorescence (e.g. Coble 1996, Mobed et al. 1996) which indicated that differences in fluorescence properties were consistently related to structural characteristics of aquatic fulvic acids and could be used as an indicator of DOM source (McKnight et al. 2001). The proposed method ultimately

produces a Fluorescence Index (FI), a unitless ratio of fluorescence emissions that is indicative of the origin of the fulvic acid fraction of the sample. Samples which contain mostly autochthonous DOM will have higher FI values due to a greater decline in emission with increasing wavelength as compared to a sample of primarily allochthonous DOM (Klapper et al. 2002). The lower FI for allochthonous samples is a result of the higher proportion of aromatic carbon contained in these samples, which increases fluorescence emission at all wavelengths. Therefore, higher ratios indicate a generally more labile DOM character (Cory and McKnight 2005, McKnight et al. 2001) that is more likely to be taken up into microbial food webs.

Measuring FI requires minimal sample preparation (only filtration) and the samples can be measured rapidly, although a number of corrections must be applied to the resulting data. It may be used as a routine diagnostic tool when intercomparing DOM quality between widely different aquatic systems since FI measurements agree strongly between labs once analytical instruments are calibrated and standardized (Cory 2005).

3.1.3 Photochemical Breakdown of DOM

Exposure to UV irradiance subjects CDOM to photochemical degradation, which is accompanied by changes in optical properties that are commonly referred to as photobleaching (Morris and Hargreaves 1997). Photobleaching cleaves the aromatic rings that are the predominant feature of CDOM (Whitehead et al. 2000), and may result in either complete photomineralization to carbon dioxide and water, or in the cleavage of large organic molecules and aromatic structures into smaller, more labile units with lower molecular weight (Figure 3.2; Lindell et al. 1995). These lower molecular weight carbon compounds are used as a food source by bacteria, and an increase in their concentration can greatly stimulate community production. For instance, photochemical modification of CDOM on exposure to natural solar radiation, which includes the UV spectrum, has been shown to produce labile substrates that are consumed by microbes (Vähätalo et al. 2003) and which immediately stimulate sustained bacterial growth (Wetzel et al. 1995) that is propagated throughout aquatic foodwebs (Daniel et al. 2006). However, photobleached CDOM often has significantly reduced absorptivity in the UV range due to the destruction of chromophores. This results in a net increase in the transparency of the

water column to UVB (Osburn et al. 2001, Morris and Hargreaves 1997), which can have detrimental effects on all forms of aquatic life. Direct harmful effects can range from the cellular level of individual organisms, such as DNA damage and mutations, to the entire food web, such as alterations in species composition and declines in photosynthetic production (Wrona et al. 2006).

Photobleaching of CDOM in Mackenzie Delta Lakes

Annual flooding corresponding to ice break-up on north-flowing rivers such as the Mackenzie is an extreme event during which the majority of the year's discharge and corresponding biogeochemical fluxes occur. This annual peak in discharge is also the only time when lakes in the Mackenzie Delta receive appreciable inputs of water, nutrients and energy (Lesack et al. *submitted*). During a typical flooding event, river DOM concentrations increase dramatically at the onset of the melt and break-up, peak around the time of maximum river discharge, and then decrease to values close to those found before the melt by the end of the open water season (Hood et al. 2003). Floodwaters carry a high proportion of terrestrially-derived CDOM that is flushed from the river basin, and as such, it provides an important influx of photochemical substrate to delta lakes.

Floodplains in near-coastal regions, such as the Mackenzie Delta, have been indicated as important locations for CDOM photobleaching (Valentine and Zepp 1993). In these regions, photobleaching rates may be quite high due to high levels of CDOM in surface waters, the slow movement and long residence times of water within deltas, and high levels of exposure to UV irradiance (Mladenov et al. 2005). During the peak flood period following spring break-up, floodwater storage in Mackenzie Delta floodplains and lakes is estimated to be 47% (25.8 km^3 yr^{-1}) of peak Mackenzie River flow (55.4 km^3 yr^{-1}) (Emmerton et al. 2007). This floodwater is loaded with terrestrially-derived CDOM that originated in southern regions of the basin and can be pictured as a thin layer of water, approximately 2.3 m thick on average, spread out over the Mackenzie floodplain. During peak flood periods, which occur in late May or early June each year (Marsh and Hey 1994), this layer of water is exposed to continual solar irradiance during the period of 24 hour daylengths that occurs around the Arctic summer solstice, and is simultaneously in contact with flooded vegetation, both of which can substantially alter DOM quality.

Continual solar irradiance can lead to high rates of CDOM photobleaching, which reduces the UV-absorbing capacity of the water column. Therefore, as soon as the open water season commences, Mackenzie Delta water columns begin to photobleach and become more transparent to UV wavelengths. Conversely, flooded vegetation can leach additional allochthonous DOM into floodwaters (Mladenov et al. 2005), increasing the pool of photolytically-active CDOM and decreasing the transparency of the water column to UV, offsetting some effects of photobleaching. Although acting in opposition to one another, both factors can significantly alter the quality of the DOM pool as the Mackenzie River flows north through the delta to the Beaufort Sea, thereby seasonally altering the DOM composition of Mackenzie outflow. The very high CDOM levels observed immediately post-flood combined with 24 hour daylengths during the first half of the open water season indicate a large potential for CDOM photobleaching in the Mackenzie Delta.

The indirect effects of CDOM photobleaching on biota are also of interest. Toxic by-products of photobleaching such as hydrogen peroxide (H_2O_2), free radicals such as superoxides and hydroperoxides, and singlet oxygen are known to have detrimental effects on bacterial populations (Xenopoulos and Bird 1997, Cooper et al. 1989), thereby affecting the flow of energy into aquatic food webs. The production of H_2O_2, the longest lived of these harmful by-products, via UV-induced photobleaching has been examined in lakes of the Mackenzie Delta. The highest rates of H_2O_2 production were found in low-closure lakes which flood intermittently and may represent the optimal balance between UV irradiance penetration through the water column and concentrations of photochemical substrate (Febria et al. 2006). H_2O_2 concentrations as high as 4000 nmol L^{-1} were found in delta lakes around the time of the summer solstice, a level comparable to those found in temperate latitude lakes (Scully et al. 1996), with important implications for both chemical and biological processes (Cooper et al. 1994).

3.1.4 Research Objectives

The objectives of this chapter were: (1) to determine the quantity and quality of DOM present in Mackenzie Delta lakes using several diagnostic parameters that have been successfully used in similar environments, and (2) to determine photobleaching rates

for natural DOM pools exposed to different portions of the solar spectrum under conditions of continual irradiance around the time of the Arctic summer solstice.

Open water levels of both the total DOM pool (represented by TDOC in this study) and the chromophoric portion (CDOM) in representative Mackenzie Delta lakes were tracked during the summers of 2004 and 2005. Two sets of lakes with flooding frequencies determined by their sill elevations were studied in order to examine as full a range of DOM quantities and qualities as possible. During 2005, several measures of DOM quality were also investigated in order to assess their applicability to Mackenzie Delta lakes (FI, S coefficient, and $SUVA_{280}$). Although these parameters have been used to indicate DOM quality and source in other floodplain ecosystems (e.g. Mladenov et al. 2005) as well as in high altitude lakes (e.g. Laurion et al. 2000), to my knowledge they have never been extensively used in lakes within any Arctic delta. It was expected that lakes close to distributary channels that maintained their channel connection throughout the open water season (no-closure lakes) would have indices indicating a greater proportion of terrestrially-derived allochthonous DOM, since these lakes receive continual inputs of floodwater originating from runoff in more southerly, forested areas of the Mackenzie drainage basin during the open water period. Conversely, DOM indices were expected to indicate a higher proportion of autochthonous DOM in lakes that were located far from channel connections, or that were infrequently flooded due to high sill elevations (high-closure lakes). This was expected due to high production by macrophytes in these lakes, as well as lower inputs of floodwater carrying terrestrially-derived DOM. Also, as the residence time of water within a lake increased, DOM indices were expected to give a weaker allochthonous signal due to enhanced photobleaching resulting from long-term irradiance exposure.

The second objective of this chapter was to assess how natural DOM pools in lakes of the Mackenzie Delta photobleached when exposed to different portions of the solar spectrum. This was experimentally assessed using natural waters with differing proportions of chromophoric *versus* non-chromophoric DOM. The photobleaching rate was expected to be dependent on substrate levels, with higher proportions of CDOM in the total DOM pool of a lake leading to more rapid photobleaching. Also, the majority of the CDOM photobleaching that occurred under experimental conditions was expected to

be driven by UVA irradiance, similar to results found at lower latitudes. Although UVB photons are far more energetic when considered individually, they collectively account for less than 1% of the total irradiance flux reaching the Earth's surface (Vincent and Pienitz 1996). Fluxes of UVA are many times greater, and as a result, the UVA waveband is usually the dominant waveband driving photobleaching in freshwater systems (e.g. Osburn et al. 2001). This has important implications for future CDOM photobleaching rates in high latitude aquatic environments, since fluxes of ground-level UVB are expected to increase due to stratospheric ozone depletion while UVA fluxes remain unaltered.

3.2 Methods

3.2.1 Study Site and Design

The Mackenzie Delta (67-70° N, 133-137° W) is located between the Mackenzie River and its outlet to the Beaufort Sea (see Figure 2.1) and is the second largest delta in the circumpolar Arctic (approximately 13000 km^2). The delta is underlain by discontinuous permafrost up to 100 m thick, although sediments beneath lakes and channels remain unfrozen. It is an extremely lake-rich floodplain environment containing approximately 45000 permanent lakes (Emmerton et al. 2007) that are ice-covered for 7-8 months each year. On average, Mackenzie Delta lakes are small (area < 10 ha), shallow (mean depth < 2 m), and unstratified during the open water season from June to October (Squires 2002). These lakes are generally shallow enough to permit abundant macrophyte growth of species such as *Potamogeton*, *Chara* and *Ceratophyllum* during open water periods (Squires and Lesack 2003).

Since the Mackenzie River flows northwards towards polar latitudes, the freshet eventually encounters ice jams within the delta during the spring melt. This results in elevated water levels and flooding throughout much of the delta in late May and early June (Lesack et al. 1998, Rouse et al. 1997, Marsh and Hey 1989). The annual flood results in a single large pulse of sediment, nutrients and organic material entering many delta lakes over a relatively short period of time. During the remainder of the open water season, delta lakes experience a net loss of water due to evaporation, rapid drops in water levels following flooding, and near-desert levels of annual precipitation (Bigras 1990; Mackay 1963).

Mackenzie Delta lakes are flooded when water levels in distributary channels exceed that of the lake sill, the highest topographic point along the route followed by floodwaters as they flow from a distributary channel into a lake (Squires and Lesack 2003). Mackay (1963) proposed three classes of floodplain lakes in the Mackenzie Delta that were later quantified according to sill elevation by Marsh and Hey (1989; see Figure 2.2). No-closure lakes (sill elevation < 1.5 m asl; 12% of delta lakes) are permanently connected to distributary channels and remain flooded throughout the open water season;

low-closure lakes (1.5 m asl < sill elevation < 4.0 m asl; 55% of delta lakes) are flooded each spring but become isolated from distributary channels at some point during the open water season; and high-closure lakes (sill elevation > 4.0 m asl; 33% of delta lakes) which have sill elevations in excess of the average annual flood elevation and are therefore not flooded annually.

This delta-wide gradient in flooding frequency gives rise to predictable gradients in DOM, among other limnological variables (see Figure 2.3). TDOC and non-chromophoric dissolved organic matter (NC-DOM) concentrations tend to increase with decreasing flooding frequency due to abundant autochthonous macrophyte production in lakes with higher sill elevations. Conversely, CDOM absorbencies tend to increase with decreasing sill elevation due to continuous channel inputs of decomposing allochthonous organic matter.

Two sets of lakes near the town of Inuvik, NT (68°19' N, 133°29' W) were closely monitored during the summers of 2004 and 2005. Lakes were selected based on prior research in the Mackenzie Delta in order to represent a range of DOM quantities and qualities as determined by the sill elevations and corresponding flooding frequencies of individual lakes.

6 Lake Set

All lakes in the 6 lake set are located within 5 km to the southwest of Inuvik (Figure 3.3) and are accessible by motorboat. This lake set is comprised of six spatially discrete lakes that span the range of flooding frequencies as determined by sill elevation (Table 3.1a). The 6 lake set was sampled weekly for TDOC analysis during the summers of 2004 and 2005. Samples for CDOM analysis were taken more frequently in the six lake set during June of both years, when levels of incident solar irradiance were at an annual high and photobleaching potential was maximal. CDOM samples were taken up to three times weekly in the six lake set during June to capture this period of rapid photobleaching, with weekly sampling during the rest of the open water season.

40 Lake Set

The 40 lake set is comprised of 40 spatially discrete lakes spanning the range of flooding frequencies as determined by sill elevation (Figure 3.3, Table 3.1b). These lakes

were sampled three times during the open water periods of both 2004 (8 July, 26 July and 14 August) and 2005 (10 June, 2 July and 8 August). Unlike the 6 lake set, many lakes in the 40 lake set are inaccessible by boat and therefore sampling was conducted via helicopter.

3.2.2 Laboratory Analyses of Water Samples

Water Sampling

Water samples were taken from standard locations in each lake that were either marked with a float or found using GPS coordinates. All water samples for lab analyses were taken as subsurface dip samples from approximately 10 cm below the lake surface. All samples were collected in polyethylene bottles that were acid washed, copiously rinsed with distilled and deionized (DDI) water, and subsequently rinsed three times with sample water before being filled. All sample bottles were stored in dark coolers during transport to the Inuvik Research Centre, Inuvik, NT where samples were filtered appropriately within 10 hours of collection.

Total Dissolved Organic Carbon

Sample water was filtered through pre-combusted (450°C for 4 h) GF/F filters (nominal pore size 0.7 μm) under light vacuum and stored frozen in leached and rinsed 60 mL polyethylene bottles until analysis.

Samples were thawed and warmed to room temperature immediately prior to analysis. TDOC concentrations were measured on a Shimadzu TOC-Vcsh carbon analyzer equipped with an 8 port OCT-1 autosampler (Shimadzu, Kyoto, Japan) using high temperature catalytic oxidation and the non-purgeable organic carbon method. Briefly, this method requires acidifying each sample to between pH 2 – 3 by adding 0.5% (vol.) 2M HCl and then sparging for 5 minutes to remove all inorganic carbon. The sample is then combusted at 680°C, converting all organic carbon within the sample to CO_2, which is measured in a non-dispersive infrared gas analyzer. Replicate injections of each sample were run (minimum of 2 injections, maximum of 3) until the coefficient of variation fell below 2%. Calibration curves for TDOC analysis were constructed using standard dilutions of a 20 mg L^{-1} potassium hydrogen phthalate (KHP) solution. A NIST-

traceable KHP standard solution (8 mg L^{-1}) was used as a periodic check of instrument accuracy. DDI blanks were run every 12 samples, and all TDOC results were blank corrected following analysis.

TDOC results were generated in units of mg L^{-1}, but were later converted to units of μmol L^{-1} using the following conversion:

$$\text{TDOC } (\mu\text{mol L}^{-1}) = [\text{TDOC } (\text{mg L}^{-1}) / 12.011] * 1000$$

Chromophoric Dissolved Organic Matter

Sample water was vacuum filtered through DDI- and sample-rinsed 0.2 μm nitrocellulose Millipore filters and stored in leached and rinsed 60 mL polyethylene bottles at 4°C in the dark until analysis.

In 2004, CDOM absorbencies were measured spectrophotometrically on either a Spectronic 501 or Spectronic 301 (both instruments manufactured by Milton Roy, Ivyland, PA) using 10 cm optical glass cuvettes. Prefiltered (0.2 μm) DDI was used in the reference cuvette and to take blank measurements every 10 samples. CDOM absorbance was measured at 330 nm with another reading taken at 740 nm as an index of scatter. All measurements, including blanks, were scatter corrected as follows (Whitehead et al. 2000):

$$A_{330sc} = A_{330} - A_{740}\,(330/740)$$

where A_{330sc} denotes the scatter corrected absorbance readings at the reference wavelength of 330 nm and A_λ denotes sample absorbance at the designated wavelength. Sample CDOM absorbencies were further corrected by blank subtraction. CDOM absorption coefficients (a_{330}, m^{-1}) are expressed as natural logarithms normalized to one metre, and were calculated according to Kirk (1994):

$$a_{330} = 2.303 * A_{330sc} / l$$

where l denotes the optical pathlength (m).

In 2005, CDOM absorbencies were measured on a Genesys 5 scanning spectrophotometer (Milton Roy, Ivyland, PA) using a 5 cm quartz cuvette. Prefiltered (0.2 μm) DDI was used in the reference cuvette and to take blank scans every 12 samples.

CDOM absorbance was scanned from 250-750 nm in 1 nm increments. All scans, including blanks, were baseline corrected by subtracting the average absorbance over the interval 700-750 nm from the entire scan. Sample CDOM absorption scans were further corrected by subtraction of blank scans. CDOM absorption coefficients were then calculated for each wavelength as described above.

Spectral Slope Coefficient

Complete scans of CDOM absorbance in 2005 allowed for modeling of the spectral slope of the absorption curve from 300-600 nm following the methods of Markager and Vincent (2000) and Stedmon et al. (2000). The spectral slope coefficient (S) was calculated as follows:

$$a_\lambda = a_{\lambda 0} e^{S(\lambda 0 - \lambda)} + K$$

where a_λ is the absorption coefficient at a wavelength λ and $a_{\lambda 0}$ is the absorption coefficient at the reference wavelength of 330 nm. K is a background parameter that improves the fit of the model by minimizing systematic deviations that occur over the spectrum in its absence. S is the exponential slope parameter that characterizes the decrease in absorbance with increasing wavelength (expressed in units of nm^{-1}, or more conveniently, μm^{-1}).

Specific Ultraviolet Absorbance

Specific ultraviolet absorbance (SUVA) is defined as the UV absorbance of a water sample at a given wavelength normalized to the TDOC concentration of the sample. $SUVA_{280}$ (L mg C^{-1} m^{-1}) was calculated for all 2005 samples according to the methods of Mladenov et al. (2005):

$$SUVA_{280} = a_{280} / TDOC$$

where a_{280} is the corrected absorption coefficient at the reference UV wavelength of 280 nm (m^{-1}) and TDOC represents the total dissolved organic carbon concentration of the sample (mg L^{-1}).

Fluorescence Index

Sample water was vacuum filtered through 0.2 μm nitrocellulose Millipore filters, then stored in leached and rinsed 60 mL polyethylene bottles in the dark at 4°C until fluorescence measurements were taken. All samples were analysed on a Cary Eclipse fluorometer (Varian Inc., Palo Alto, CA) with a xenon flash lamp using a 1 cm quartz cell.

Samples for FI analysis were excited with light at 370 nm, while emission intensity was scanned from 400-550 nm in 1 nm increments with a 0.5 s integration time. Bandwidths were set to 5 nm for both the excitation and emission monochromator. DDI blanks were similarly scanned every 10 samples. In order to track any decay in lamp intensity over time and to standardize all emission scans to Raman units, three scans of the water Raman peak were taken daily (Cory 2005). Water Raman peaks were constructed by scanning a DDI blank under the same instrument parameters as above, with the exception of decreasing the excitation wavelength to 350 nm.

Data were imported to Microsoft Excel as ASCII files, in order to more easily manipulate emission readings during the required corrections. Following blank correction, all samples were corrected for emission intensity, which removes any variability in the emission readings that are a result of instrument-specific wavelength dependencies. This was accomplished using a correction file constructed by Varian Inc. Next, all strongly absorbing samples ($A_{370} > 0.02$ over a 1 cm pathlength) were corrected for inner filtering effects, or the decrease in fluorescence intensity resulting from sample absorbance of either excitation or emission light. Inner filter corrections were applied following the methods of McKnight et al. (2001). All data was then normalized to the daily Raman water intensity (equal to the area under the water Raman curve as measured at 350 nm excitation). The FI was calculated as follows (Cory 2005, McKnight et al. 2001):

$$FI = \frac{\text{Emission Intensity}_{470\ nm}}{\text{Emission Intensity}_{520\ nm}}$$

Reference standards were also measured as described above in order to assess autochthonous and allochthonous limits for FI on the Cary Eclipse fluorometer used in

this study. Suwannee River fulvic acid standard (International Humic Substances Society (IHSS), St. Paul, MN; product number 2S101F) was used as the allochthonous end-member, while Pony Lake fulvic acid reference (IHSS product number 1R109F) was used as the autochthonous end-member.

3.2.3 Photobleaching Experiments

Two short experiments were conducted during the summer of 2004 in order to examine lake water photobleaching rates under controlled conditions. Both experiments were conducted under ambient temperature conditions on the grounds of the Inuvik Research Centre, Inuvik NT, in outdoor incubators constructed of plywood, lined with black rubber pond liners, and filled with tap water (Figure 3.4). Lake water for both experiments was collected soon after break-up in order to capture post-flood CDOM absorbencies before appreciable *in situ* photobleaching had occurred. Dip samples were collected in acid washed and DDI rinsed 10 L carboys that were rinsed with sample water three times before being filled. Lake water was immediately GF/C filtered and stored at 4°C in the dark until experiments were conducted up to several weeks later. Immediately before experiments were begun, the GF/C filtered lake water was filtered through 0.2 μm nitrocellulose Millipore filters. Experimental lake water samples were placed in 1 L Acrylite OP-4 cylinders (GE Polymershapes, Burlington, ON; constructed by ASI Plastics, Coquitlam, BC) sealed with rubber or silicone stoppers. The Acrylite OP-4 microcosm walls allowed all wavelengths of incident solar irradiance to penetrate freely. During both experiments, half-hour average atmospheric PAR irradiances were logged using an underwater quantum sensor (LI-192SA) and battery powered data logger (LI-1000, both instruments manufactured by Li-Cor Biosciences, Lincoln, NB). Since the Li-Cor quantum sensors were calibrated for underwater use, all irradiance data was later adjusted to atmospheric measurements using an "in air" calibration multiplier. CDOM absorbency data were later converted to photobleaching rates expressing the average change in CDOM absorbance per unit incident PAR irradiance (m μmol^{-1}) over the course of the entire experiment.

A **DOM Composition Experiment** was conducted in order to assess the photobleaching capacity of lake water with a gradient of DOM compositions (ranging

from high CDOM/low TDOC to low CDOM/high TDOC). Two 24 h **Waveband Exclusion Experiments** were also conducted in order to assess the relative contributions of individual UV wavebands to CDOM photobleaching rates in lake water taken from two discrete lakes with opposing flooding frequencies and DOM compositions.

DOM Composition Experiment

Sites for this experiment were chosen from the chain set lakes, which exhibit strong gradients in DOM quality and water column clarity that are determined by distance from the channel connection (see section 2.3.1, Figures 2.4, 2.5b). Since the chain set lakes have a low sill elevation (1.500 m asl) they are classified as no-closure lakes and therefore maintain a channel connection throughout the open water season. In 2004, both CDOM absorbencies and TDOC concentrations were highest in the middle of the chain set (site S5), with absorbencies and concentrations decreasing both towards and away from the channel connection (Figure 2.9 c, d). A total volume of 10 L of sample water was collected from chain set sites S1, S3, S5, S7 and S9 on 17 June 2004.

Microcosms of sample water were placed under either 1) a full sun treatment (PAR+UVA+UVB; 4 replicates from each site) or 2) a dark control treatment (3 replicates from each site) at 12:00 PM MDT on 12 August 2004. Microcosms under the dark control treatment were wrapped in a layer of tin foil followed by two outer layers of black plastic, effectively excluding all irradiance. Subsamples were taken for CDOM analysis at 0, 4 and 8 h, and then at 24 h intervals until the conclusion of the experiment at 8:00 PM MDT on 17 August 2004. Ambient temperature varied from a low of 5.9°C to a high of 26.1°C during the course of the experiment (EC 2004). All microcosms were inverted several times each day to ensure that sample water remained well mixed throughout the experiment.

Waveband Exclusion Experiments

A total volume of 30 L of sample water was collected from both Lake 129 and Lake 520 on 15 June 2004. These lakes were chosen as representative end-members of the delta-wide flooding frequency and DOM composition gradients as determined by sill elevation. Lake 129 is a no-closure lake with a spring sill elevation of 1.500 m and therefore maintains its channel connection year round. As a result, it contains highly

coloured water with high CDOM absorbencies and low TDOC concentrations. In contrast, Lake 520 is a high-closure lake with a spring sill elevation of 5.169 m. Due to its high sill elevation, Lake 520 is not flooded annually and contains clear water with low CDOM absorbencies and high TDOC concentrations.

Three replicate microcosms of filtered sample water from each lake were placed under each of four treatments: 1) a full sun treatment (referred to as PAR+UVA+UVB), 2) an UVB removal treatment (referred to as PAR+UVA) under Mylar-D™ sheeting (GE Polymershapes, Burlington, ON), 3) an UV removal treatment (referred to as PAR) under Acrylite OP-2 sheeting (Cadillac Plastics, Coquitlam, BC) and 4) a dark control treatment in which microcosms were wrapped in a layer of tin foil and two outer layers of black plastic, effectively excluding all irradiance. Transmission properties of the screens used in the PAR+UVA and PAR treatments were confirmed on a sunny, cloudless day using a portable high accuracy UV-visible scanning spectroradiometer (OL 754-O-PMT; Optronics Laboratories, Orlando, FL). Although neither screen is completely effective, Mylar-D™ removes approximately 88% of incident UVB irradiance, while Acrylite OP-2 removes approximately 99% of incident UV irradiance (Figure 3.5).

Both experiments were conducted from 12:00 PM to 8:00 PM MDT, during the period around solar noon in Inuvik (approximately 3:00 PM MDT). Sample water from Lake 129 was experimentally photobleached on 25 July 2004 (ambient temperature between 21.0 – 23.1°C; EC 2004), while sample water from Lake 520 was photobleached on 7 August 2004 (ambient temperature between 17.2 – 22.5°C; EC 2004). Subsamples for CDOM analysis were taken every hour, while subsamples for TDOC analysis were taken at 0, 4, and 8 h. All microcosms were inverted hourly throughout the experiment to ensure that sample water remained well-mixed.

3.2.4 Statistical Analyses

All statistical analyses were performed using JMP 6.0.0 statistical software (SAS Institute, Cary, NC).

Preliminary analysis for the waveband exclusion experiment was performed using a two-way Analysis of Variance (ANOVA) randomized complete block design with lakes considered as a random effect in order to detect the presence of a significant difference (α

= 0.05) between waveband exposure treatments. Tukey HSD least squares mean difference analysis was subsequently used to perform pairwise comparisons to determine significant differences among treatments at $\alpha = 0.05$.

3.3 Results

3.3.1 Seasonal Patterns in DOM Quantity

Seasonal patterns in DOM quantity were monitored during the open water seasons of both 2004 and 2005 in representative lake sets within the Mackenzie Delta. Both the 40 and 6 lake sets contain lakes spanning the range of sill elevations found in mid-delta lakes. Both TDOC and CDOM have been measured in these lakes throughout previous open water seasons (e.g. Febria 2005, Riedel 2002, Spears 2002, Squires 2002, Teichreb 1999). However, the influence of the annual flood on delta lakes differs among years since the height of the peak flood and the duration of high water levels are variable and depend upon characteristics of the break-up period (Marsh and Hey 1994). Therefore, TDOC and CDOM are also variable among years and must be remeasured annually in order to track DOM quantity.

Since a lake's sill elevation determines the concentration of several constituents that are affected by or carried in floodwaters, water levels in the East Channel of the Mackenzie Delta were also monitored (Figure 3.6, data from WSC 2006). The annual spring flood differed in both magnitude and timing between the two open water seasons. In 2004, the peak flood occurred on 3 June when levels reached 5.52 m asl, while in 2005 the peak flood occurred on 24 May when levels reached 5.95 m asl. Also, in 2004 the flood receded more rapidly and reached lower levels by mid-summer than in 2005. Local weather also differed between the two open water seasons, with the summer of 2004 being generally warmer (see Appendix E) and sunnier (data not shown) than the summer of 2005.

6 Lake Set

TDOC concentrations in the 6 lake set generally increased slightly during the 2004 open water season in low- and high-closure lakes, while Lake 56 (no-closure) exhibited variable TDOC concentrations, with similar concentrations at the end of the open water season to those observed during early June (Figure 3.7). Over the 2005 open water season, most lakes in the 6 lake set exhibited a slight overall decline in TDOC

concentration. However, during both sampling periods, TDOC concentrations in Lake 520 increased rapidly during the open water season.

Evidence of photobleaching was seen during the open water periods of both 2004 and 2005, as CDOM absorbencies were high early in the open water season and generally declined until August (Figure 3.8). Lake 520 was an exception to this trend over the 2004 sampling period, with CDOM levels increasing slightly from 10.79 m^{-1} to 11.65 m^{-1}. However, in the summer of 2005 CDOM levels in Lake 520 declined from 14.45 m^{-1} to 12.62 m^{-1}, indicating significant inputs of floodwater containing CDOM at the beginning of the 2005 open water season. In 2004, initial CDOM absorbencies were highest in Lake 129 (no-closure) and Lake 87 (low-closure), while in 2005 initial CDOM absorbencies were highest in lakes that were most directly connected to distributary channels (Lakes 129, 87, 280 and 56).

Mean open water TDOC concentrations in the 6 lake set increased with increasing sill elevation during both open water periods (2004: $r^2 = 0.719$, $p = 0.033$; 2005: $r^2 = 0.319$, $p = 0.243$; Figure 3.9a). During both open water seasons, CDOM absorbencies decreased with increasing sill elevation (2004: $r^2 = 0.589$, $p = 0.075$; 2005: $r^2 = 0.319$, $p = 0.275$; Figure 3.9b). Correlations between either measure of DOM quantity and sill elevation were stronger in 2004 than in 2005. These relationships between DOM quantity and sill elevation were similar to those observed in previous years, in which gradients in TDOC concentration and CDOM absorbance ran counter to one another (Febria 2005, Spears 2002, Squires 2002).

40 Lake Set

The 40 lake set was sampled three times during each of the open water seasons of 2004 and 2005. Correlations were constructed between sill elevations and both TDOC concentrations and CDOM absorbencies. On each sampling date, TDOC concentration increased as sill elevation increased in a significant linear relationship ($p < 0.05$ in all cases; Figure 3.10a, 3.11a). However, CDOM absorbencies in the 40 lake set generally displayed either little correlation with sill elevation, or an increase with increasing sill elevation (Figure 3.10b, Figure 3.11b). This trend of increasing CDOM absorbency with increasing sill elevation was apparent later in both open water seasons, and approached a

significant linear relationship in 2004 ($r^2 = 0.074$, $p = 0.089$). On 10 June 2005, the 40 lake set also displayed an increase in CDOM absorbency as sill elevation increased.

3.3.2 Indices of DOM Quality

Fluorescence Index

FI was examined as a possible measure of DOM quality in the 6 lake set during the open water season of 2005. End member reference standards were also measured in order to determine the FI limits for autochthonous ($FI_{auto} = 1.45$) and allochthonous ($FI_{allo} = 1.17$) DOM. FI values among the 6 lakes were close in value in early June, immediately following the spring flood (FI = 1.35 to 1.38, Figure 3.12a), and indicated a slightly autochthonous DOM quality in all lakes. These values diverged throughout the summer, and by the end of the open water season, FI values had increased to the FI_{auto} limit in Lake 520, a high-closure lake with the highest sill elevation. FI values also increased in other high- and low-closure lakes, but declined in the no-closure lakes (Lakes 129 and 80) to ~1.30, intermediate between the limits for autochthonous and allochthonous DOM quality.

Mean open water FI values in the 6 lake set increased with increasing sill elevation in a significant linear relationship ($r^2 = 0.755$, $p = 0.025$; Figure 3.12b), indicating a more autochthonous DOM quality in high-closure lakes.

Spectral Slope Coefficient

The spectral slope coefficient is a measure of the decline in CDOM absorbance with increasing wavelength, and was also investigated in 2005 as a possible measure of DOM quality in Mackenzie Delta lakes. S coefficients among the 6 lake set were very similar in value immediately following the spring flood (S = 16.65 to 17.38 μm^{-1} on 1 June 2005; Figure 3.13a). All lakes experienced an increase in S coefficient over the open water season, indicating a greater decline in CDOM absorbance with increasing wavelength and the development of a more autochthonous DOM character. By the final sampling date, S coefficients had increased to between 20 and 21 μm^{-1} in most lakes in the 6 lake set, while Lake 520 had a S coefficient of 22.11 μm^{-1}, indicating a highly autochthonous DOM quality.

Mean open water S values in the 6 lake set increased with increasing sill elevation in a significant linear relationship ($r^2 = 0.721$, $p = 0.033$; Figure 3.13b), indicating a more autochthonous DOM quality in high-closure lakes. This relationship was also observed in the 40 lake set during the 2005 open water season (Figure 3.11c). Although the S coefficient was not significantly correlated with sill elevation during the 10 June survey, by mid-summer the correlation was highly significant ($r^2 = 0.374$, $p < 0.0001$) and it remained significant during the final survey on 8 August ($r^2 = 0.110$, $p = 0.037$).

Specific Ultraviolet Absorbance

The specific ultraviolet absorbance index ($SUVA_{280}$) is a measure of the average absorptivity of DOM at 280 nm per unit of TDOC in the sample, with lower $SUVA_{280}$ values indicating a more autochthonous DOM quality. $SUVA_{280}$ values were greatest on 1 June, immediately following break-up and the spring flood ($SUVA_{280}$ = 5.45 to 5.87 L mg C^{-1} m^{-1}; Figure 3.14a). Initial $SUVA_{280}$ values among the 6 lake set were also very similar to one another. Throughout the open water season, $SUVA_{280}$ values generally declined in all lakes, indicating photolytic breakdown of CDOM (Judd et al. 2007). By August, $SUVA_{280}$ values had diverged in the 6 lake set with the highest values found in no-closure Lakes 129 and 80, indicating a more allochthonous DOM quality in these lakes. $SUVA_{280}$ values in Lake 520, a high-closure lake, decreased rapidly during the first half of June and eventually plateaued, remaining below 3.50 L mg C^{-1} m^{-1} from 17 June until August.

Mean open water $SUVA_{280}$ values in the 6 lake set decreased with increasing sill elevation ($r^2 = 0.631$; Figure 3.14b), again indicating a more autochthonous DOM quality in high-closure lakes. The linear correlation also indicated a near-significant relationship between $SUVA_{280}$ and sill elevation in the 6 lake set ($p = 0.060$). This relationship was also observed in the 40 lake set during the 2005 open water season (Figure 3.11d). Although $SUVA_{280}$ values were not significantly correlated with sill elevation during the 10 June survey, by mid-summer the correlation was highly significant ($r^2 = 0.315$, $p = 0.0002$) and it remained significant during the final survey on 8 August ($r^2 = 0.114$, $p = 0.033$).

3.3.3 Experimental Analysis of Photobleaching Rates

Two experiments were conducted at the Inuvik Research Centre during the summer of 2004 in order to assess the influence of both DOM composition (predominantly autochthonous non-chromophoric DOM *versus* predominantly allochthonous CDOM) and waveband exposure (PAR *versus* PAR+UVA *versus* PAR+UVA+UVB) on photobleaching rates within Mackenzie Delta lakes.

DOM Composition Experiment

The influence of DOM composition on photobleaching rates was explored during a 5 day experiment from 12:00 PM on 12 August to 8:00 PM on 17 August, 2004. Lake water used in this experiment was taken from sites in the chain set lakes, located approximately 15 km north of Inuvik, NT off the East Channel of the Mackenzie River (see Figure 2.5b). This set of no-closure lakes exhibits a strong gradient in DOM quality and water column clarity as determined by distance from the channel connection (see section 2.3.1, Figure 2.4). Although the spatial trends in TDOC concentrations and CDOM absorbencies were different during the open water season of 2004 than those observed during previous studies (e.g. Squires 2002), the full gradient of DOM compositions was captured by sampling a range of chain set sites. Water from every second site in the chain set was used (sites S1, S3, S5, S7 and S9), with these sites capturing the gradient from high CDOM/low TDOC to low CDOM/high TDOC.

During the 5 days over which this experiment was conducted, sky conditions were clear with occasional clouds. Underwater integrated PAR measurements were recorded continuously throughout the experiment, showing maximum daily fluxes near solar noon (3:00 PM MDT; Figure 3.15). Although this experiment was conducted during a period of near-continuous daylight during the Arctic summer, PAR measurements declined to near zero each night (12:00 AM until 6:00 AM) due to low solar elevations at these times.

Microcosms placed under ambient irradiance conditions (PAR+UVA+UVB treatment) all experienced CDOM photobleaching (Figure 3.16a) while those under the dark treatment either exhibited constant CDOM absorbencies or slight increases (Figure 3.16b). An examination of photobleaching rates, expressed as the loss in CDOM absorbency per unit of incident PAR irradiance (m μmol^{-1}) revealed that photobleaching

rates were highest in microcosms from high CDOM sites (Figure 3.17). Photobleaching rates declined as initial CDOM absorbency declined, with S5 having the highest photobleaching rate (2.96 x 10^{-10} m μmol^{-1}) and S7 and S9 having the lowest rates (1.73 x 10^{-10} m μmol^{-1} and 1.71 x 10^{-10} m μmol^{-1}, respectively). Further statistical analysis was not possible due to insufficient replication of treatment microcosms.

Waveband Exclusion Experiments

The influence of waveband exposure on photobleaching rates in waters of differing non-chromophoric *versus* chromophoric DOM compositions was explored during two 8 hour experiments. Water from Lake 129, a high CDOM no-closure lake, was photobleached from 12:00 PM until 8:00 PM on 25 July 2004, and water from Lake 520, a low CDOM high-closure lake, was photobleached from 12:00 PM until 8:00 PM on 7 August 2004.

During the 2 days during which these experiments were conducted, sky conditions were clear and cloudless. Underwater integrated PAR measurements were recorded continuously throughout the experiments, showing maximum daily fluxes near solar noon (3:00 PM MDT; Figure 3.18).

For both Lake 129 and Lake 520, the greatest losses in CDOM absorbency occurred under the PAR+UVA+UVB treatment, followed by the PAR+UVA treatment (Figure 3.19). Both lakes experienced either no loss or a slight increase in CDOM absorbency under the PAR and dark treatments.

For each lake, average 8 hour changes in CDOM absorbency under each treatment were converted to photobleaching rates (expressed in units of m μmol^{-1}). This ensured that data from the two experiments, conducted on two days under slightly different irradiance conditions, were comparable. An examination of treatment photobleaching rates for each lake showed a similar response to waveband exclusion (Figure 3.20), in spite of differing initial CDOM absorbencies (14.98 m^{-1} in Lake 129 and 12.01 m^{-1} in Lake 520).

Two-way ANOVA statistical analysis, using a randomized complete block design with lakes considered as a random effect, examined the effects of waveband exclusion on photobleaching rates across both lakes. A significant difference in photobleaching rates between treatments was found ($p = 0.012$, Figure 3.21a). Further analysis revealed that,

across both lakes, there was no significant difference in photobleaching rates between microcosms exposed to PAR+UVA+UVB and those exposed to PAR+UVA (Figure 3.21b). Also, no significant difference in photobleaching rates was found between dark and PAR treatments, both of which exhibited a gain in CDOM absorbency during the experiment.

TDOC concentrations were also monitored at 0, 4 and 8 hours during both experiments. All treatments displayed a gain in TDOC during the course of the experiment (Figure 3.22). Gains were greatest under the PAR+UVA+UVB treatment in both lakes, with Lake 520 having a greater increase in TDOC concentration under each treatment than Lake 129.

3.4 Discussion

3.4.1 Seasonal Patterns in DOM Quantity and Quality

In both 2004 and 2005, seasonal open water patterns of DOM quantity and quality in Mackenzie Delta lakes generally followed patterns that had been observed in these lake sets during previous years (e.g. Lesack et al. *submitted*, Febria 2005, Riedel 2002, Spears 2002, Squires 2002, Teichreb 1999). During both open water seasons, TDOC concentrations either increased slightly or remained approximately constant in the 6 lake set (Figure 3.7), while CDOM absorbencies were generally highest immediately following peak flood (Figure 3.8), as expected since large amounts of CDOM are deposited in delta lakes during the annual period of break-up and high water. Also, CDOM absorbencies generally declined over both open water seasons (Figure 3.8), showing evidence of substantial *in situ* photobleaching in response to 24 hour daylengths in the delta following peak flood. Floodplains of large rivers have been indicated as hot spots of photochemical activity in other areas of the world, ranging from other deltas in the circumpolar Arctic (Neff et al. 2006) to tropical Africa (Mladenov et al. 2005) and South America (Amado et al. 2006). The Mackenzie Delta also appears to be a photochemical hot spot, with substantial changes in the quality and quantity of the DOM pool occurring within shallow flooded lakes exposed to continual irradiance during the open water season. This may substantially alter the DOM pool of the Mackenzie River before it is discharged to the Beaufort Sea, with implications for the off-shore optical and chemical environments.

The linear correlations between TDOC concentration and sill elevation, and CDOM absorbency and sill elevation, were stronger in the 6 lake set during 2004 than in 2005 (Figure 3.9). This may be due to the influence of two separate factors. First, the height of the peak flood was lower in 2004 than in 2005 (5.52 *versus* 5.95 m asl, respectively). As a result, delta lakes with high sill elevations were flooded for a shorter amount of time during the high water period of 2004. This would simultaneously maintain low levels of CDOM in high-closure lakes, which had become depleted through photobleaching during previous summers, as well as maintaining high concentrations of

TDOC, which had built up through autochthonous production and were not diluted by large inputs of low TDOC floodwater. Second, levels of incident irradiance during the open water period of 2005 were lower than during 2004 (data not shown). This likely resulted in lower CDOM photobleaching rates in delta lakes in 2005, leading to a weaker gradient of CDOM absorbencies with sill elevation than is usually observed.

An examination of DOM quality through the calculation of FI, S and $SUVA_{280}$ across the 6 lake set indicated the presence of floodwaters in all lakes during 2005. Similar values for all three parameters were found in all lakes during early June, immediately following peak water levels (Figures 3.12, 3.13, 3.14). This indicates a similar DOM quality in all 6 lakes at the beginning of the open water season, and therefore, the influence of the annual flood in each lake. It is interesting to note that although a floodwater DOM signature is present in all lakes during 2005, FI measurements indicate that this signature is less allochthonous than expected considering it originates in melt water from southern portions of the Mackenzie Basin located within the boreal forest (see Figure 3.12a). The floodwater signature completely overwhelms the existing DOM signature of the lake water that was stored under ice cover over the winter. This "reset" the DOM pool to a floodwater-DOM composition when individual lakes were inundated during the 2005 break-up.

During both summers, the 40 lake set displayed trends in CDOM absorbency that differed from those found in the 6 lake set. CDOM absorbency in the 40 lake set was not significantly correlated with sill elevation at any point during either open water season, and appeared to be either unrelated to sill elevation or to increase with increasing sill elevation (Figure 3.10, 3.11). This may be related to the connectivity of lakes in the 40 lake set to distributary channels. Many of these lakes are inaccessible by boat, and are therefore indirectly connected to main distributary channels through a series of shallow lakes and smaller channels. Along with sill elevation, connectivity determines the ease with which channel water will enter delta lakes during the annual flood. In any given year, lakes of any sill elevation that are far removed from a source of high-CDOM channel water may more closely resemble high-closure lakes in terms of DOM composition since the lateral extent of the annual flood may not reach them. In these lakes, precipitation and overland flow during the summer may contribute more

allochthonous DOM to the within-lake pool than the annual flood. Although the influence of sill elevation on limnological gradients has been well studied in Mackenzie Delta lakes, the influence of lake connectivity has been largely overlooked, and should be addressed in future studies of DOM quantity and quality.

3.4.2 Evaluation of DOM Quality Indices

Previous studies in the Mackenzie Delta have used absorption at a single reference wavelength (330 nm) to track the relative quantity of CDOM among lakes over the open water season (e.g. Febria 2005, Teichreb 1999). While using a reference wavelength is useful when comparing CDOM quantities among lakes of a single system, there are limitations inherent to this method. It is not possible to convert CDOM absorbencies to absolute DOM concentrations that can be compared among systems, since it is predominantly the intact allochthonous portion of the total DOM pool that is measured by commonly-used wavelengths in the UV or blue ranges such as 320 nm (e.g. Belzile et al. 2002) or 440 nm (e.g. Reche et al. 1999, Kirk 1994). By measuring only this portion, the contributions of autochthonous-derived DOM and photobleached CDOM to total DOM concentrations are not considered. This is problematic since within-lake production can contribute a variable amount to total DOM levels in individual lakes. Also, the ratio of chromophoric to non-chromophoric DOM (DOM quality) determines many important properties such as the lability of the DOM pool (Lindell et al. 1995) and its ability to complex trace metals (McKnight et al. 1992) and organic pollutants (Kukkonen and Oikari 1991), thus altering their uptake into aquatic food webs.

In a system such as the Mackenzie Delta, the development of simple indices to indicate DOM quality would provide valuable data regarding the composition of the DOM pool, as well as quantifiable measures indicating changes in DOM quality in response to flooding and photochemical processes. The delta contains tens of thousands of lakes that may be inundated with high-CDOM floodwater during the break-up period, substantially altering *in situ* DOM compositions. Once the flood begins to recede, DOM quality may be further altered by CDOM photobleaching, which can proceed at a rapid pace due to continual fluxes of solar irradiance around the summer solstice. The ability to capture these changes using indices requiring little sample preparation and simple

measurements is especially desirable since the ice free season in the delta is short (June – October) and all open water geochemical and biological processes occur rapidly during this time.

FI was used to determine the source of the DOM pool present within lakes of the Mackenzie Delta. Previous studies have used FI to distinguish autochthonous DOM ($FI_{auto} \sim 1.45$; for example, from photosynthetic or microbial production) from allochthonous DOM ($FI_{allo} \sim 1.17$; for example, from decomposing terrestrial vegetation via overland flow) (e.g. Kelton et al. 2007, Mladenov et al. 2005, Wolfe et al. 2002). FI values at the beginning of the 2005 open water season were very similar in all 6 lakes (FI = 1.35 to 1.38), indicating that all lakes had received inputs of floodwater which were dominating the DOM FI signal (Figure 3.12). Initial FI values in the 6 lake set indicated a far more autochthonous signal than was anticipated considering floodwater originates in more southerly portions of the Mackenzie basin, where boreal forest covers much of the landscape and the input of lignaceous DOM should be high. However, by the end of the open water season, FI values in the 6 lake set had diverged and displayed a gradient from almost entirely autochthonous in Lake 520 (FI = 1.45), to intermediate between autochthonous and allochthonous in no-closure Lakes 129 and 80 (FI ~ 1.30), which was similar to the initial FI values seen immediately after ice out. Values of FI in distributary channels fluctuated between 1.32 and 1.38 over the open water season (data not shown), indicating that no-closure lakes and distributary channels had DOM pools of similar origin.

Although FI values found during the open water season of 2005 were more autochthonous than expected, important processes affecting the DOM pool in delta lakes may be clarified by these results. For instance, FI results may indicate that water exchange during the spring flood is more complex than previously thought. Rather than floodwater simply entering delta lakes, flushing of lake water into delta distributary channels from floodplain lakes while they maintain channel connections during high water periods may also have important implications for the DOM pool. Lake water that was isolated from distributary channels for long periods during the previous open water season and then stored under ice over the winter may contain DOM that has been extensively photobleached, giving it a more autochthonous (non-aromatic) character.

Flooded conditions in the delta may mix lake water stored during the previous summer with floodwater, altering the floodwater DOM quality towards a more autochthonous character than if floodwaters consisted of only terrestrially-derived, allochthonous DOM. Examination of FI trends during future open water seasons should help elucidate the DOM quality and origin of floodwater in the Mackenzie Delta floodplain.

However, of the three indicators of DOM quality examined in this study, the measurement of FI requires the most intensive analysis and data correction. Conversely, both the spectral slope (S) coefficient and $SUVA_{280}$ are simple calculations requiring only a spectrophotometric scan of CDOM absorption, and in the case of $SUVA_{280}$, a measurement of TDOC concentration. Both indices gave good indications of DOM quality in the 6 and 40 lake sets throughout the open water seasons of 2005 (Figure 3.11c and d, 3.13 and 3.14). Both indicated a more allochthonous DOM quality due to the annual flood in early June, with similar values found in all lakes of the 6 lake set, and both appeared to capture changes in DOM quality in response to photobleaching over the open water season.

The S coefficient is a measure of the decline in DOM absorbance with increasing wavelength through the UV and blue wavelengths (in this study, 300-600 nm). Previous studies as well as this one have found that S increases upon exposure to natural irradiance, indicating a less aromatic and more autochthonous character (Obernosterer and Benner 2004, Del Vecchio and Blough 2002, Moran et al. 2000). On the other hand, $SUVA_{280}$ is a measurement of the average aromaticity of the entire DOM pool, with higher values indicating a more allochthonous vegetative character that has been found during high flow periods in other floodplain systems (e.g. Mladenov et al. 2005). During 2005, these indices both showed similar trends in DOM quality among the 6 lake set.

In Lake 129, the S coefficient indicated CDOM photobleaching over the open water season (S increased from 17.05 to 20.13 μm^{-1}), while $SUVA_{280}$ measurements indicated a decrease in DOM aromaticity ($SUVA_{280}$ decreased from 5.76 to 4.71 L mg C^{-1} m^{-1}). The magnitude of both indices changed by 18% over the open water season, indicating a shift toward a more autochthonous, less aromatic DOM quality by the end of the summer. By comparison, aromaticity declined much more sharply in Lake 520, a high-closure lake, over the open water season ($SUVA_{280}$ decreased from 5.71 to 2.87 L

mg C^{-1} m^{-1}) while S increased more sharply (16.65 to 22.11 μm^{-1}). Changes in magnitude for each index were 50% and 34% respectively. Although the changes in magnitude do not agree as well as do those for Lake 129, trends in both the S coefficient and $SUVA_{280}$ indicate substantial photobleaching in Lake 520. Since this is a high-closure lake, no additional inputs of high-CDOM channel water were received during the open water season to offset losses in aromaticity due to photobleaching, resulting in a very low average aromaticity of the total DOM pool by the end of the open water season. It can also be inferred that the CDOM pool in Lake 129, a no-closure lake, was photobleached over the open water season, but that the total DOM pool was composed of a higher proportion of allochthonous aromatic DOM which kept $SUVA_{280}$ values high. This may be a result of continual inputs of high-CDOM channel water over the open water season.

From the results of this study, it appears as though all three indices have merit in describing the origin and quality of the DOM pool in Mackenzie Delta lakes. These indices are very informative since they can be used to indicate not just differing DOM sources but also changing DOM qualities in response to *in situ* biogeochemical processes over the open water season. However, due to the ease of calculating the spectral slope coefficient and $SUVA_{280}$, these two indices may be the most practical for use in survey work in the delta. Since they are easily calculated for a large number of samples, they could be applied to a large number of Mackenzie Delta lakes and channels in order to gain a greater understanding of DOM quality.

3.4.3 Experimental CDOM Photobleaching Rates

In north-flowing rivers, the majority of the annual discharge and concurrent biogeochemical fluxes occur during the annual flood and the open water period that follows. When peak flood conditions occur in the Mackenzie Delta, floodwater becomes isolated in shallow lakes (< 2 m deep; Squires 2002) where it can undergo significant changes in water chemistry driven by reduced flows and increased irradiance exposure during the period of 24 hour daylengths immediately following break-up (Emmerton 2006). High-CDOM floodwater is structurally and chemically altered via photobleaching reactions driven by UV absorption over the duration of the open water season. This results in an increased transparency of the water column to all wavelengths of irradiance

(Osburn et al. 2001) and also alters the bioavailability of the DOM pool (Vähätalo et al. 2003), with important implications for aquatic biota.

Measurement of CDOM absorbency at 330 nm (a330, m^{-1}) in the 6 lake set indicated strong *in situ* photobleaching in some lakes throughout the open water seasons of 2004 and 2005 (Figure 3.8). Additionally, measurements of the S coefficient and $SUVA_{280}$ in the 6 lake set during 2005 also indicated significant CDOM photobleaching and corresponding changes in the quality of the DOM pool (Figure 3.13a, 3.14a). However, many different factors may also contribute to reductions in CDOM absorbencies, such as biotic activity and dilution due to precipitation or inputs of channel water. Therefore, in an effort to more closely examine the influence of DOM composition and UV exposure on photobleaching rates in lakes of the Mackenzie Delta, large volume water samples were taken soon after peak flood when CDOM levels were at an annual high, and were later used to conduct controlled photobleaching experiments.

Many other experimental examinations of CDOM photobleaching have used water samples irradiated by artificial light sources, and additionally, many have used solutions in small reaction vessels, giving optically thin samples that are only directly comparable to the upper few centimetres of a natural water column. Although these experiments may clarify some aspects of the photochemical reaction mechanism, they are not applicable to *in situ* processes where changes in the irradiance field, either through natural fluctuations or as a function of increasing depth, play a role (Whitehead et al. 2000). Therefore, the experiments in this study used natural solar irradiance as a light source, and also used microcosms that were approximately 15 cm in depth in order to more accurately simulate the portion of the water column that would be affected by UV-driven photochemical processes *in situ*.

Both experiments conducted in this study indicated that measurable amounts of DOM photobleaching can occur under local solar fluxes over very short time periods. Measureable losses in CDOM absorbency were observed over periods as short as an hour. This agrees with findings from lower latitudes, where instantaneous irradiance fluxes are far higher. For instance, evidence of photobleaching was found over several hours in a subarctic lake in Quebec (Gibson et al. 2001). However, the discovery of such high rates in an Arctic floodplain was somewhat surprising since the proportion of diffuse irradiance

in the UV spectrum is much higher at polar latitudes (ACIA 2005). Photobleaching rates were higher when levels of photochemical substrate were higher (Figure 3.17) but regardless of the initial DOM composition, the energy used to drive CDOM photobleaching was mostly derived from the absorption of photons in the UVA waveband (Figure 3.20). For both high-CDOM water taken from Lake 129 and low-CDOM water taken from Lake 520, no significant difference in photobleaching rate was found between the PAR+UVA+UVB and PAR+UVA treatments following 8 hours of exposure to natural solar fluxes (Figure 3.21b). Additionally, there was no significant difference between the photobleaching rates found under the dark and PAR treatments. Photons within the UVB waveband are more highly energetic, and therefore have a greater photobleaching capacity per photon, than do UVA photons. However, ground-level fluxes of UVA are several times higher than are UVB fluxes (Laurion et al. 1997), and therefore the cumulative photobleaching potential of the UVA waveband is far higher than is that for the UVB waveband. For instance, Osburn et al. (2001) found that over 50% of total photobleaching was due to UVA irradiance in 4 lakes in Pennsylvania and Argentina, and a similar result was also found in several lakes in Sweden and Brazil (Granéli et al. 1998). UVB fluxes are expected to increase for the next several decades due to stratospheric ozone depletion over the Arctic (IPCC 2007) while UVA fluxes remain unaltered. In spite of this anticipated increase in UVB, cumulative fluxes of UVA will continue to be far higher and it therefore seems unlikely that CDOM photobleaching rates will increase substantially in response to further ozone loss.

Experimental photobleaching rates are likely much higher than rates that would be observed *in situ*. Within the water column of Mackenzie Delta lakes processes such as CDOM dilution via channel inputs, runoff from the lake catchment or larger Mackenzie basin following precipitation events, and wind-induced mixing bringing fresh photobleaching substrate to the surface, would all combine to reduce photobleaching rates. Therefore, a logical next step in the study of photobleaching in Mackenzie Delta lakes would be to examine *in situ* photobleaching rates. Large-scale enclosures that isolate a large volume water sample within the lake could be constructed, thereby exposing the enclosure to local irradiance fluxes while removing the influence of dilution, runoff and mixing. Losses in CDOM absorbency within the enclosure over time could be

compared to the surrounding lake water in order to determine the influence of *in situ* processes on photobleaching.

Increases in TDOC concentrations throughout the course of both waveband exclusion experiments may be a result of phytoplankton production of low molecular weight carbohydrates, proteins or lipids. These may be transformed into larger molecular weight DOM molecules through abiotic or microbial processes (Tranvik 1993), thereby increasing the TDOC pool while simultaneously increasing the amount of photobleaching substrate in all treatments. This would account for the increase in CDOM absorbency over the course of the experiments in UV excluded treatments, where photobleaching did not occur.

3.4.4 Potential Effects of Climate Change Stressors on DOM Pools in Mackenzie Delta Lakes

The Mackenzie Delta, located in the western Canadian Arctic, is a biogeochemical "hot spot" containing approximately 45000 lakes (Emmerton et al. 2007) which will likely be affected by multiple co-occurring climate change stressors (Lesack et al. *submitted*). In combination, the effects of permafrost melting, increased vegetative cover, longer ice-free seasons, and lower annual flood levels will exert a large influence on the DOM pool within delta lakes and, consequently, the Beaufort Sea.

Temperature increases due to climate change are predicted to be especially severe in the western Canadian Arctic. Mean annual temperatures in this region are expected to increase by between 3-5°C over the 1981-2000 baseline by the period 2071-2090 (IPCC 2007, ACIA 2005). This is approximately twice the anticipated increase in global mean annual temperature over the same time period (ACIA 2005). Increased temperatures will have a range of impacts on sensitive northern aquatic ecosystems, many of which will alter characteristics of the *in situ* DOM pool. The quantity and quality of DOM present in an aquatic ecosystem determines its optical and chemical characteristics, as well as the availability of food to support aquatic biota. Therefore, any change in the DOM pool can alter species composition (Molot et al. 2004), ecosystem productivity (Bothwell et al. 1994) or rates of biogeochemical cycling (Vähätalo et al. 2003).

As temperatures increase, the depth and extent of permafrost is expected to decrease while active layers deepen (Prowse et al. 2006). The Mackenzie Delta is underlain by permafrost up to 100 m deep, although sediments under lakes and channels may remain unfrozen (Squires and Lesack 2003). If permafrost melts in response to rising temperatures, large amounts of terrestrially-derived aromatic CDOM that are currently sequestered in permafrost will be released to surface waters. A similar effect will result from increased vegetative cover within the Mackenzie basin. DOM is negatively correlated with latitude and decreases with increasing distance from the treeline (Vincent and Pienitz 1996, Pienitz and Smol 1994). Over the next several decades, the North American treeline is expected to move further northwards as temperatures increase and growing seasons lengthen (Pienitz and Vincent 2000). Increased fluxes of allochthonous CDOM will be flushed into the delta from both sources during the spring melt, increasing loads deposited in delta lakes during the annual flood. This will increase *in situ* irradiance absorption, particularly in the UV wavebands, thereby shielding the water column from the effects of UV exposure. This increased sunscreening capacity will likely far outweigh increased *in situ* UVB fluxes due to stratospheric ozone depletion (Schindler 1996).

However, future UVB fluxes within Mackenzie Delta lakes will increase in response to longer periods of open water each year. The delta is currently ice-free from June to October (Emmerton et al. 2007), with this period expected to lengthen in response to increased temperatures (Wrona et al. 2006). A longer open water period will expose delta lakes to increased UVB fluxes for longer periods, increasing photoreaction rates (Whitehead et al. 2000) and water column transparency. A longer ice-free season will also result in higher rates of wind mixing in delta lakes, increasing CDOM turnover within the water column and limiting the extent of *in situ* sunscreening.

The CDOM pool will also be altered due to lower peak flood heights and shorter flood durations resulting from fewer instances of ice-jamming during the annual break-up. The formation of ice-jams in the Mackenzie Delta requires a north-south temperature differential that sends melt water from more southerly, upstream regions of the basin into still-frozen channel ice in the delta, resulting in widespread flooding (Prowse et al. 2006, Lesack and Marsh *in press*). Peak annual water levels in the central delta have decreased

by 0.47 m since 1964, corresponding to a decreased frequency of ice-jamming during the spring melt (Lesack and Marsh *in press*). Further decreases are predicted as a result of diminished differences in air temperature between the southern and northern parts of the Mackenzie basin. As ice-jamming events decrease, a lower proportion of delta lakes will be flooded each year since the peak flood height will not exceed the sills of high-closure lakes. As a result, flood-borne loads of CDOM to delta lakes will likely decrease, also decreasing the absorption capacity of the water column and increasing its transparency to UV wavelengths (Arts et al. 2000). Additionally, as the period between water renewal events in high-closure lakes lengthens, water columns will become increasingly clear as within-lake stores of CDOM are photobleached and are not replenished by floodwater.

Once it has passed through the lakes and channels of the Mackenzie Delta, the Mackenzie River eventually discharges to the Beaufort Sea basin of the Arctic Ocean. The Arctic receives about 10% of the total world river discharge (Häder et al. 1998) and is an important global sink for terrestrial DOM, receiving more DOM per unit volume than any other ocean basin (Opsahl et al. 1999). Therefore, the highly-productive Arctic Ocean ecosystem may also experience substantial changes in optical and chemical characteristics due to changing DOM pools carried in the outflow of major circumpolar rivers such as the Mackenzie.

3.5 Conclusions and Recommendations

Relative CDOM quantity in a subset of Mackenzie Delta lakes has been monitored for several years using measurements of absorbency at a single reference wavelength. However, the bioavailability and reactivity of DOM is not just determined by how much is present, but also by its quality. Three indices of DOM quality were applied to water samples from discrete delta lakes during the summer of 2005, all of which produced results that were significantly (FI and S coefficient) or near-significantly ($SUVA_{280}$) correlated with sill elevation. As well, all three indices captured important changes in the quality of the DOM pool resulting from photobleaching over the open water season. However, due to the simplicity of measuring the S coefficient and $SUVA_{280}$ index as compared to FI, these parameters may be better suited to use in systems such as the Mackenzie Delta. Since the open water season is short and the system contains more than 45000 lakes in total, informative but quick measurements are necessary in order to adequately assess the quality of the DOM pool.

Strong evidence that UVA wavelengths overwhelmingly control CDOM photobleaching was found in two delta lakes with opposing DOM compositions resulting from differing frequencies of spring flooding. The removal of UVB wavelengths (PAR+UVA treatment) produced photobleaching rates in microcosms of lake water that did not differ significantly from those found under full solar spectra (PAR+UVA+UVB treatment), while the removal of the entire UV waveband (PAR treatment) produced significantly lower rates. Therefore, further stratospheric ozone depletion over Arctic latitudes, which will only increase fluxes of UVB at ground level, will likely exert only a small influence on *in situ* photobleaching rates. However, changing climatic conditions in the Arctic are likely to reduce the period of ice cover each year, exposing lakes in the Mackenzie Delta to increased seasonal fluxes of all wavelengths over the open water season, including the photolytically-dominant UVA waveband. Additionally, in response to future climate change, peak flood heights are expected to decrease while CDOM loads to those delta lakes that are flooded in a given year are predicted to increase. These factors all have the potential to alter both the quantity and quality of DOM in delta lakes, with implications for nutrient uptake into microbial food webs, the underwater irradiance

environment, rates of biogeochemical cycling, and the fate of metals and contaminants within delta waterways.

Further investigation is necessary to determine rates of *in situ* photobleaching in delta lakes. Currently, dilution of the DOM pool by fresh inputs of channel water, especially during storm surge events, is an unknown quantity. Also, photobleaching experiments performed using microcosms in incubators do not adequately account for the effects of lake turnover by wind mixing, which likely acts to reduce photobleaching rates when compared to experimental values. Within-lake macrocosms could be used to isolate some lake water while allowing the surrounding waters to mix with fresh inputs from distributary channels, while DOM indices are monitored in both. However, this study represents an important step towards a better understanding of DOM quality and dynamics in Mackenzie Delta lakes.

3.6 References

Amado, A.M., V.F. Farjalla, F.D. Esteves, R.L. Bozelli, F. Roland and A. Enrich-Prast. 2006. Complementary pathways of dissolved organic carbon removal pathways in clear-water Amazonian ecosystems: photochemical degradation and bacterial uptake. FEMS Microbiology Ecology 56: 8-17.

Arctic Climate Impact Assessment (ACIA). 2005. Arctic climate impact assessment: scientific report. Cambridge University Press, New York, USA. 1042 pp.

Arts, M.T., R.D. Robarts, F. Kasai, M.J. Waiser, V. Tumber, A. Plante, H. Rai and H.J. deLange. 2000. The attenuation of ultraviolet radiation in high dissolved organic carbon waters of wetlands and lakes on the northern Great Plains. Limnology and Oceanography 45: 292-299.

Belzile, C., J.A.E. Gibson and W.F. Vincent. 2002. Colored dissolved organic matter and dissolved organic carbon exclusion from lake ice: implications for irradiance transmission and carbon cycling. Limnology and Oceanography 47: 1283-1293.

Bigras, S.C. 1990. Hydrological regime of lakes in the Mackenzie Delta, Northwest Territories, Canada. Arctic Alpine Research 22: 163-174.

Bothwell, M.L., D.M.J. Sherbot and C.M. Pollock. 1994. Ecosystem response to solar ultraviolet-B radiation: influence of trophic level interactions. Science 265: 97-100.

Carder, K.L., R.G. Steward, G.R. Harvey and P.B. Ortner. 1989. Marine humic and fulvic acids: their effects on remote sensing of ocean chlorophyll. Limnology and Oceanography 34: 68-81.

Coble, P.G. 1996. Characterization of marine and terrestrial DOM in seawater using excitation-emission matrix spectroscopy. Marine Chemistry 51: 325-346.

Coble, P.G., S.A. Green, N.V. Blough and R.B. Gagosian. 1990. Characterisation of dissolved organic matter in the Black Sea by fluorescence spectroscopy. Nature 348: 432-435.

Cooper, W.J., C. Shao, D.R.S. Lean, A.S. Gordon and F.E. Scully Jr. 1994. Factors affecting the distribution of H2O2 in surface waters In Environmental chemistry of lakes and reservoirs, advances in chemistry series 237. Baker, L.A. (ed.). American Chemical Society, Washington D.C., USA. pp 391-422.

Cooper, W.J., R.G. Zika, R.G. Petasne, and A.M. Fischer. 1989. Sunlight-induced photochemistry of humic substances in natural waters: major reactive species. *In* Aquatic humic substances: influence on fate and treatment of pollutants. American Chemical Society, Denver, USA. pp. 333-362.

Cory, R.M. 2005. Photochemical and redox reactivity of dissolved organic matter. Ph.D. Thesis, University of Colorado. 252 pp.

Cory, R.M. and D.M. McKnight. 2005. Fluorescence spectroscopy reveals ubiquitous presence of oxidized and reduced quinines in dissolved organic matter. Environmental Science and Technology 39: 8142-8149.

Curtis, P.J. 1998. Climatic and hydrologic control of DOM concentration and quality in lakes. *In* Aquatic Humic Substances, D.O. Hessen and L.J. Tranvik (eds.). Springer-Verlag, Berlin, Germany. pp 93-106.

Daniel, C., W. Graneli, E.S. Kritzberg and A.M. Anesio. 2006. Stimulation of metazooplankton by photochemically modified dissolved organic matter. Limnology and Oceanography 51: 101-108.

De Haan, H. and T. De Boer. 1987. Applicability of light absorbance and fluorescence as measures of concentration and molecular size of dissolved organic carbon in humic lake Tjeukemeer. Water Resources 21: 731-734.

Del Castillo, C.E., P.G. Coble, J.M. Morell, J.M. Lopez and J.E. Corredor. 1999. Analysis of the optical properties of the Orinoco River plume by absorption and fluorescence spectroscopy. Marine Chemistry 66: 35-51.

Del Vecchio, R. and N.V. Blough. 2002. Photobleaching of chromophoric dissolved organic matter in natural waters: kinetics and modeling. Marine Chemistry 78: 231-253.

Emmerton, C.A. 2006. Downstream nutrient changes through the Mackenzie River Delta and Estuary, western Canadian arctic. M.Sc. Thesis, Simon Fraser University. 181 pp.

Emmerton, C.A., L.F.W. Lesack and P. Marsh. 2007. Lake abundance, potential water storage, and habitat distribution in the Mackenzie River Delta, western Canadian Arctic. Water Resource Research 43: W05419, doi:10.1029/2006WR005139.

Environment Canada (EC). 2004. [Online]. Climate data online. Available: http://www.climate.weatheroffice.ec.gc.ca/climateData/hourlydata_e.html.

Febria, C.M. 2005. Patterns of hydrogen peroxide among lakes of the Mackenzie Delta and potential effects on bacterial production. M.Sc. Thesis, Simon Fraser University. 124 pp.

Febria, C.M., L.F.W. Lesack, J.A.L. Gareis and M.L. Bothwell. 2006. Patterns of hydrogen peroxide among lakes of the Mackenzie Delta, western Canadian Arctic. Canadian Journal of Fisheries and Aquatic Sciences 63: 2107-2118.

Findlay, S.E.G., R.L. Sinsabaugh, W.V. Sobczak and M. Hoostal. 2003. Metabolic and structural response of hyporheic microbial communities to variations in supply of dissolved organic matter. Limnology and Oceanography 48: 1608-1617.

Gao, H.Z. and R.G. Zepp. 1998. Factors influencing photoreactions of dissolved organic matter in a coastal river of the southeastern United States. Environmental Science and Technology 32: 2940-2946.

Gibson, J.A.E., W.F. Vincent and R. Pienitz. 2001. Hydrologic control and diurnal photobleaching of CDOM in a subarctic lake. Archiv für Hydrobiologie 152: 143-159.

Granéli, W., M. Lindell, M. Bias and F. Esteves. 1998. Photoproduction of dissolved inorganic carbon in temperate and tropical lakes – dependence on wavelength band and dissolved organic carbon concentration. Biogeochemica 43: 175-195.

Green, S.A. and N.V. Blough. 1994. Optical absorption and fluorescence properties of chromophoric dissolved organic matter in natural waters. Limnology and Oceanography 39: 1903-1916.

Häder, D.-P., H.D. Kumar, R.C. Smith and R.C. Worrest. 1998. Effects on aquatic ecosystems. Journal of Photochemistry and Photobiology B: Biology 46: 53-68.

Hood, E., D.M. McKnight and M.W. Williams. 2003. Sources and chemical character of dissolved organic carbon across an alpine/subalpine ecotone, Green Lakes Valley, Colorado Front Range, United States. Water Resources Research 39: doi:10.1029/2002WR001738.

Intergovernmental Panel on Climate Change (IPCC). 2007. Climate Change 2007: The Physical Science Basis. Contribution of Working Group I to the Fourth Assessment Report of the Intergovernmental Panel on Climate Change. Solomon, S., D. Qin, M. Manning, Z. Chen, M. Marquis, K.B. Avery, M. Tignor and H.L. Miller (eds.). Cambridge University Press; Cambridge, UK and New York, USA. 996 pp.

Jerome, J.H. and R.P. Bukata. 1998. Tracking the propagation of solar ultraviolet radiation: dispersal of ultraviolet photons in inland waters. Journal of Great Lakes Research 24: 666-680.

Judd, K.E., B.C. Crump and G.W. Kling. 2007. Bacterial responses in activity and community composition to photo-oxidation of dissolved organic matter from soil and surface waters. Aquatic Sciences 69: 96-107.

Kelton, N., L.A. Molot and P.J. Dillon. 2007. Spectrofluorometric properties of dissolved organic matter from Central and Southern Ontario streams and the influence of iron and irradiation. Water Research 41: 638-646.

Kieber, D.J., J. McDaniel and K. Mopper. 1989. Photochemical source of biological substrates in sea-water – implications for carbon cycling. Nature 341: 637-639.

Kirk, J.T.O. 1994. Light and photosynthesis in aquatic ecosystems, 2nd edition. Cambridge University Press, Cambridge, UK. 509 pp.

Klapper, L., D.M. McKnight, J.R. Fulton, E.L. Blunt-Harris, K.P. Nevin, D.R. Lovely and P.G. Hatcher. 2002. Fulvic acid oxidation state detection using fluorescence spectroscopy. Environmental Science and Technology 36: 3170-3175.

Kukkonen, J. and A. Oikari. 1991. Bioavailability of organic pollutants in boreal waters with varying levels of dissolved organic material. Water Research 25: 455-463.

Lafrenière, M.J. and M.J. Sharp. 2004. The concentration and fluorescence of dissolved organic carbon (DOC) in glacial and nonglacial catchments: interpreting hydrological flow routing and DOC sources. Arctic, Antarctic, and Alpine Research 36: 156-165.

Laurion, I., M. Ventura, J. Catalan, R. Psenner and R. Sommaruga. 2000. Attenuation of ultraviolet radiation in mountain lakes: factors controlling the among- and within-lake variability. Limnology and Oceanography 45: 1274-1288.

Laurion, I., W.F. Vincent and D.R.S. Lean. 1997. Underwater ultraviolet radiation: development of spectral models for Northern high latitude lakes. Photochemistry and Photobiology 65: 107-114.

Lesack, L.F.W., and P. Marsh. *In Press*. Lengthening plus shortening of river-to-lake connection times in the Mackenzie River Delta respectively via two global change mechanisms along the arctic coast. Geophysical Research Letters.

Lesack, L.F.W., M. Squires, P. Marsh, C. Emmerton, C. Febria, J. Gareis, A. Riedel, B. Spears, C. Teichreb and M. Bothwell. *Submitted*. Ecology of lakes in the Mackenzie River Delta: potential responses to global change.

Lesack, L.F.W., P. Marsh and R.E. Hecky. 1998. Spatial and temporal dynamics of major solute chemistry among Mackenzie Delta lakes. Limnology and Oceanography 43: 1530-1543.

Lindell, M.J., W. Granéli and L. Tranvik. 1995. Enhanced bacterial growth in response to photochemical transformation of dissolved organic matter. Limnology and Oceanography 40: 195-199.

Mackay, J.R. 1963. The Mackenzie Delta area, N.W.T., Canada. Canadian Department of Mines and Technical Surveys, Geographical Branch Memoir 8. 202 pp.

Markager, S. and W.F. Vincent. 2000. Spectral light attenuation and the absorption of UV and blue light in natural waters. Limnology and Oceanography 45: 642-650.

Marsh, P. and M. Hey. 1989. The flooding hydrology of Mackenzie Delta lakes near Inuvik, N.W.T., Canada. Arctic 42: 41-49.

Marsh, P. and M. Hey. 1994. Analysis of spring high water events in the Mackenzie Delta and implications for lake and terrestrial flooding. Geografiska Annaler 76A: 221-234.

McKnight, D.M., E.D. Andrews, S.A. Spaulding and G.R. Aiken. 1994. Aquatic fulvic acids in algal-rich Antarctic ponds. Limnology and Oceanography 39: 1972-1979.

McKnight, D.M., K.E. Bencala, G.W. Zellweger, G.R. Aiken, G.L. Feder and K.A. Thorn. 1992. Sorption of dissolved organic carbon by hydrous aluminium and iron oxides occurring at the confluence of Deer Creek with the Snake River, Summit County, Colorado. Environmental Science and Technology 26: 1388-1396.

McKnight, D.M., E.W. Boyer, P.K. Westerhoff, P.T. Doran, T. Kulbe and D.T. Andersen. 2001. Spectrofluorometric characterization of dissolved organic matter for indication of precursor organic material and aromaticity. Limnology and Oceanography 46: 38-48.

McKnight, D.M., E. Hood and L. Klapper. 2003. Trace organic moieties of dissolved organic material in natural waters *In* Aquatic Ecosystems Interactivity of DOM, Findlay, S.E.G. and R.L. Sinsabaugh (eds.). Academic Press, San Diego, USA.

Mladenov, N., D.M. McKnight, P. Wolski and L. Ramberg. 2005. Effects of annual flooding on dissolved organic carbon dynamics within a pristine wetland, the Okavango Delta, Botswana. Wetlands 25: 622-638.

Mobed, J.J., S.L. Hemmingsen, J.L. Autry and L.B. McGown. 1996. Fluorescence characterization of IHSS humic substances: total luminescence spectra with absorption correction. Environmental Science and Technology 30: 3061-3065.

Molot, L.A. and P.J. Dillon. 1997. Photolytic regulation of dissolved organic carbon in northern lakes. Global Biogeochemical Cycles 11: 357-365.

Molot, L.A., W. Keller, P.R. Leavitt, R.D. Robarts, M.J. Waiser, M.T. Arts, T.A. Clair, R. Pienitz, N.D. Yan, D.K. McNicol, Y.T. Prairie, P.J. Dillon, M. Macrae, R. Bello, R.N. Nordin, P.J. Curtis, J.P. Smol and M.S.V. Douglas. 2004. Risk analysis of dissolved organic matter-mediated ultraviolet B exposure in Canadian inland waters. Canadian Journal of Fisheries and Aquatic Sciences 61: 2511-2521.

Mopper, K. and C.A. Shultz. 1993. Fluorescence as a possible tool for studying the nature of water column distribution of DOC components. Marine Chemistry 41: 229-238.

Moran, M.A., W.M. Sheldon Jr. and R.G. Zepp. 2000. Carbon loss and optical property changes during long-term photochemical and biological degradation of estuarine dissolved organic matter. Limnology and Oceanography 45: 1254-1264.

Morris, D.P. and B.R. Hargreaves. 1997. The role of photochemical degradation of dissolved organic carbon in regulating the UV transparency of three lakes on the Pocono Plateau. Limnology and Oceanography 42: 239-249.

Neff, J.C., J.C. Finlay, S.A. Zimov, S.P. Davydov, J.J. Carrasco, E.A.G. Schuur and A.I. Davydova. 2006. Seasonal changes in the age and structure of dissolved organic carbon in Siberian rivers and streams. Geophysical Research Letters 33: Art. No. L23401.

Obernosterer, I. and R. Benner. 2004. Competition between biological and photochemical processes in the mineralization of dissolved organic carbon. Limnology and Oceanography 49: 117-124.

Opsahl, S., R. Benner and R.M.W. Amon. 1999. Major flux of terrigenous dissolved organic matter through the Arctic Ocean. Limnology and Oceanography 44: 2017-2023.

Osburn, C.L., H.E. Zagarese, D.P. Morris, B.R. Hargreaves and W.E. Cravero. 2001. Calculation of spectral weighting functions for the solar photobleaching of chromophoric dissolved organic matter in temperate lakes. Limnology and Oceanography 46: 1455-1467.

Pienitz, R. and J.P. Smol. 1994. The ecology and physicochemical characteristics of lakes in the subarctic and arctic regions of the Yukon Territory, Fennoscandia (Finland, Norway), the Northwest Territories and Northern Quebec. *In* Proceedings of the fourth Arctic-Antarctic diatom symposium. Hamilton, P.B. (ed.), Canadian Technical Report of Fisheries and Aquatic Sciences No. 1957, Fisheries and Oceans, Ottawa, Canada.

Pienitz, R. and W.F. Vincent. 2000. Effect of climate change relative to ozone depletion in subarctic lakes. Nature 404: 484-487.

Prowse, T.D., F.J. Wrona, J.D. Reist, J.J. Gibson, J.E. Hobbie, L.M.J. Lévesque and W.F. Vincent. 2006. Climate change effects on hydroecology of Arctic freshwater ecosystems. Ambio 35: 347-358.

Reche, I., M.L. Pace and J.J. Cole. 1999. Relationship of trophic and chemical conditions to photobleaching of dissolved organic matter in lake ecosystems. Biogeochemistry 44: 259-280.

Riedel, A.J. 2002. Zooplankton composition and control of heterotrophic flagellates among lakes of the Mackenzie Delta. M.Sc. Thesis, Simon Fraser University. 99 pp.

Rouse, W.R., Douglas, M.S.V., Hecky, R.E., Hershey, A.E., Kling, G.W., Lesack, L., Marsh, P., McDonald, M., Nicholson, B.J., Roulet, N.T., and J.P. Smol. 1997. Effects of climate change on the freshwaters of arctic and subarctic North America. Hydrological Processes 11: 873-902.

Scully, N.M. and D.R.S. Lean. 1994. The attenuation of ultraviolet radiation in temperate lakes. Archiv für Hydrobiologie 43: 135-144.

Spears, B.M. 2002. Effects of nutrient limitation on heterotrophic bacterial productivity and edible phytoplankton biomass among lakes of the Mackenzie Delta, Western Canadian arctic. M.Sc. Thesis, Simon Fraser University. 159 pp.

Squires, M.M. 2002. The distribution and abundance of autotrophs among lakes of the Mackenzie Delta, western Canadian arctic. PhD Thesis, Simon Fraser University. 195 pp.

Squires, M.M. and L.F.W. Lesack. 2003. Spatial and temporal patterns of light attenuation among lakes of the Mackenzie Delta. Freshwater Biology 48: 1-20.

Stedmon, C.A., S. Markager and H. Kaas. 2000. Optical properties and signatures of chromophoric dissolved organic matter (CDOM) in Danish coastal waters. Estuarine, Coastal and Shelf Science 51: 267-278.

Stewart, A.J. and R.G. Wetzel. 1980. Fluorescence-absorbance ratios – a molecular weight tracer of dissolved organic-matter. Limnology and Oceanography 25: 559-564.

Teichreb, C.J. 1999. Effects of dissolved organic carbon as a bacterial growth substrate and as an ultraviolet-B radiation sunscreen for aquatic microbial foodwebs in Mackenzie Delta lakes, Northwest Territories. M.Sc. Thesis, Simon Fraser University. 196 pp.

Tranvik, L.J. 1998. Degradation of dissolved organic matter in humic waters by bacteria. *In* Aquatic Humic Substances, D.O. Hessen and L.J. Tranvik (eds.). Springer-Verlag, Berlin, Germany. pp 259-283.

Tranvik, L.J. 1993. Microbial transformations of labile dissolved organic matter into humic-like matter in seawater. FEMS Microbiological Ecology 12: 177-183.

Tzortziou, M., C.L. Osburn and P.J. Neale. 2007. Photobleaching of dissolved organic material from a tidal marsh-estuarine system of the Chesapeake Bay. *In press*.

Vähätalo, A.V., K. Salonen, U. Münster, M. Järvinen and R.G. Wetzel. 2003. Photochemical transformation of allochthonous organic matter provides bioavailable nutrients in a humic lake. Archiv für Hydrobiologie 156: 287-314.

Valentine, R.L. and R.G. Zepp. 1993. Formation of carbon monoxide from the photodegradation of terrestrial dissolved organic carbon in natural waters. Environmental Science and Technology 27: 409-412.

Vincent, W.F., and R. Pienitz. 1996. Sensitivity of high-latitude freshwater ecosystems to global change: temperature and solar ultraviolet radiation. Geoscience Canada 23: 231-236.

Water Survey of Canada (WSC). 2006. [Online]. Data products and services. Available: http://scitech.pyr.ec.gc.ca/waterweb/formnav.asp?lang=0.

Weishaar, J.L., G.R. Aiken, B.A. Bergamaschi, M.S. Fram, R. Fujii and K. Mopper. 2003. Evaluation of specific ultraviolet absorbance as an indicator of the chemical composition and reactivity of dissolved organic carbon. Environmental Science and Technology 37: 4702-4708.

Wetzel, R.G., P.G. Hatcher and T.S. Bianchi. 1995. Natural photolysis by ultraviolet irradiance of recalcitrant dissolved organic matter to simple substrates for rapid bacterial metabolism. Limnology and Oceanography 40: 1369-1380.

Wetzel, R.G. and G.E. Likens. 2000. Composition and biomass of phytoplankton *In* Limnological Analyses, 3rd edition. Springer-Verlag New York, USA. pp 163-169.

Whitehead, R.F., S. de Mora, S. Demers, M. Gosselin, P. Monfort and B. Mostajir. 2000. Interactions of ultraviolet-B radiation, mixing, and biological activity on photobleaching of natural chromophoric dissolved organic matter: A mesocosm study. Limnology and Oceanography 45: 278-291.

Wolfe, A.P., S.S. Kaushal, J.R. Fulton and D.M. McKnight. 2002. Spectrofluorescence of sediment humic substances and historical changes of lacustrine organic matter provenance in response to atmospheric nutrient enrichment. Environmental Science and Technology 36: 3217-3223.

Wrona, F.J., T.D. Prowse, J.D. Reist, J.E. Hobbie, L.M.J. Lévesque, R.W. Macdonald and W.F. Vincent. 2006. Effects of ultraviolet radiation and contaminant-related stressors on Arctic freshwater ecosystems. Ambio 35: 388-401.

Xenopoulos, M.A. and D.F. Bird. 1997. Effect of acute exposure to hydrogen peroxide on the production of phytoplankton and bacterioplankton in a mesohumic lake. Photochemistry and Photobiology 66: 471-478.

3.7 Tables

Table 3.1 Physical data pertaining to all sites sampled during the open water seasons of 2004 and 2005 in a) the 6 lake set and b) the 40 lake set.

a) 6 lake set

Lake No.	Spring Sill (m asl)	Connection	Coordinates North	Coordinates West	Lake Area (ha)
129	2.363	direct	68 18.330'	133 50.566'	37.8
80	2.631	direct	68 19.399'	133 52.324'	19.3
87	3.389	indirect	68 19.047'	133 52.435'	3.9
280	3.838	indirect	68 19.248'	133 50.375'	2.4
56	4.623	direct	68 19.394'	133 50.817'	3.1
520	5.169	indirect	68 18.816'	133 42.854'	0.2

b) 40 lake set

Lake No.	Spring Sill (m asl)	Connection	Coordinates North	Coordinates West	Lake Area (ha)
302a	1.500	direct	68 21.012'	133 47.368'	853.0
15a	2.177	direct	68 20.513'	133 48.437'	437.6
4	2.363	indirect	68 20.015'	133 53.978'	330.5
85a	2.363	direct	68 18.982'	133 51.552'	50.6
129	2.363	direct	68 18.238'	133 51.145'	37.8
79a	2.631	indirect	68 19.393'	133 53.078'	34.6
80	2.631	indirect	68 19.428'	133 52.160'	19.3
148a	2.631	direct	68 16.928'	133 50.517'	28.4
302b	2.631	indirect	68 19.492'	133 48.707'	18.9
501	2.631	indirect	68 20.254'	133 43.529'	126.9
85b	2.990	indirect	68 19.289'	133 51.747'	1.7
107	2.990	direct	68 18.041'	133 52.404'	16.7
272	2.990	direct	68 18.772'	133 47.680'	27.3
300	2.990	direct	68 18.900'	133 49.630'	34.4
301a	2.990	indirect	68 19.487'	133 47.755'	36.6
58	3.389	indirect	68 19.784'	133 52.049'	13.7
87	3.389	indirect	68 19.015'	133 52.460'	3.9
141	3.389	indirect	68 17.878'	133 50.090'	17.2
148b	3.389	indirect	68 17.098'	133 52.062'	94.8
511	3.389	indirect	68 19.763'	133 43.617'	1.6
111	3.671	direct	68 17.964'	133 53.095'	5.3
184	3.671	direct	68 17.773'	133 53.662'	17.7
272b	3.671	indirect	68 18.747'	133 46.492'	2.1
11	3.838	indirect	68 20.612'	133 52.864'	105.4
538	3.838	indirect	68 18.568'	133 45.843'	37.9
131	4.077	indirect	68 18.065'	133 51.065'	1.2
148f	4.077	indirect	68 16.747'	133 51.307'	12.4
287	4.077	indirect	68 19.145'	133 46.632'	9.8
517	4.077	indirect	68 19.377'	133 43.662'	72.9
56	4.623	direct	68 19.394'	133 50.817'	3.1
115	4.623	direct	68 18.673'	133 53.980'	2.3
134	4.623	direct	68 18.218'	133 48.047'	3.4
261	4.623	indirect	68 17.922'	133 47.145'	48.5
275	4.768	direct	68 18.672'	133 49.112'	5.9
522	4.913	direct	68 19.257'	133 41.518'	22.5
143	5.169	indirect	68 17.425'	133 50.205'	2.1
181	5.169	indirect	68 17.298'	133 53.688'	0.8
186	5.169	indirect	68 18.418'	133 53.840'	1.0
521	5.169	direct	68 19.033'	133 41.802'	0.1
527a	5.169	indirect	68 18.957'	133 43.530'	8.5

3.8 Figures

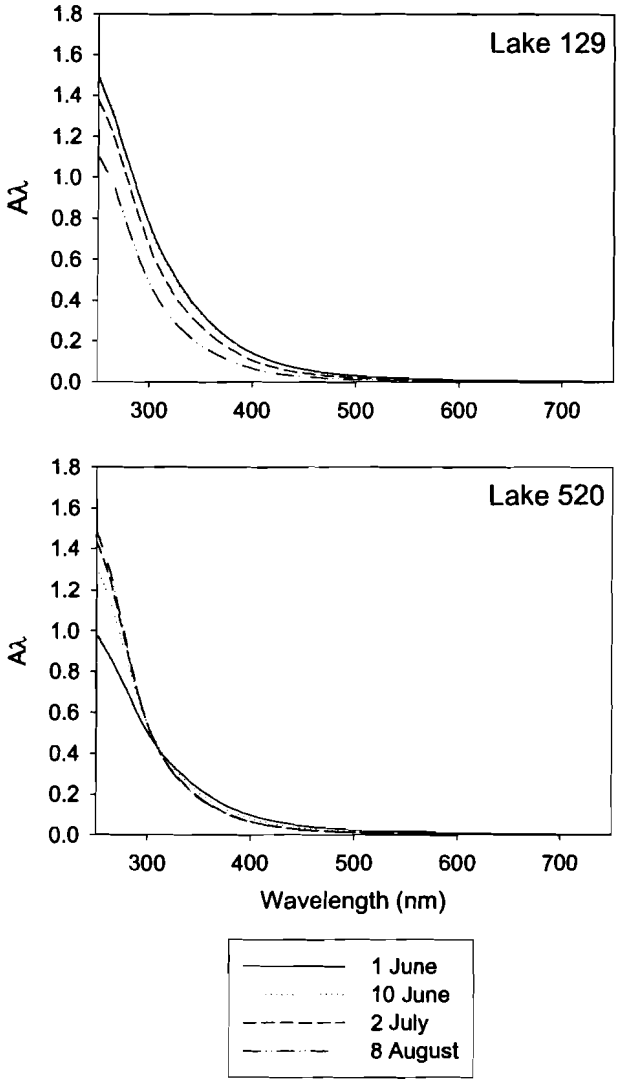

Figure 3.1 CDOM absorption (Aλ) declines as wavelengths increase and become less energetic. Lake 129 is a no-closure lake with a high proportion of allochthonous DOM, and therefore has higher CDOM absorption than does Lake 520, a high-closure lake with a high proportion of autochthonous DOM. CDOM absorption changes over the open water season in response to altered DOM compositions following the flood and CDOM photobleaching, as shown by the decline in absorption over the course of the open water season.

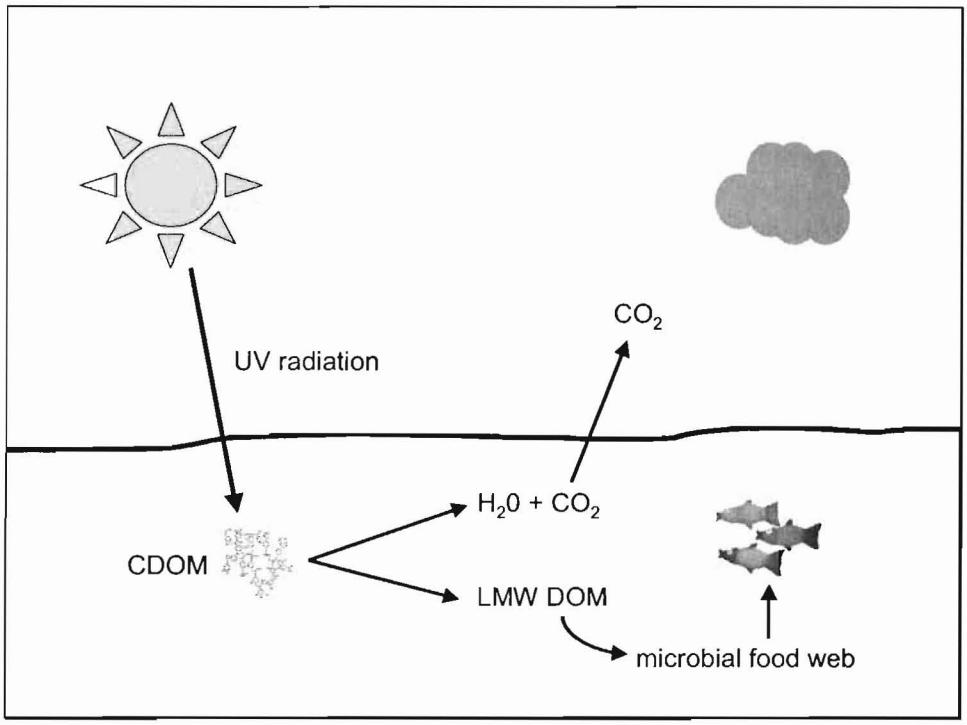

Figure 3.2 Schematic of the photobleaching process in lakes. UV radiation enters a lake and is intercepted by CDOM molecules. Aromatic carbon rings within the CDOM molecules absorb UV photons and are broken down ("photobleached"), resulting in either complete or incomplete mineralization of the CDOM molecule. Complete mineralization produces water (H_20) and carbon dioxide (CO_2) molecules; the latter may be released to the atmosphere if the lake is CO_2-saturated. Incomplete mineralization produces lower molecular weight (LMW) DOM containing a reduced proportion of aromatic C rings. LMW DOM is an important source of food for the aquatic microbial food web, which in turn supports the higher trophic levels within the lake.

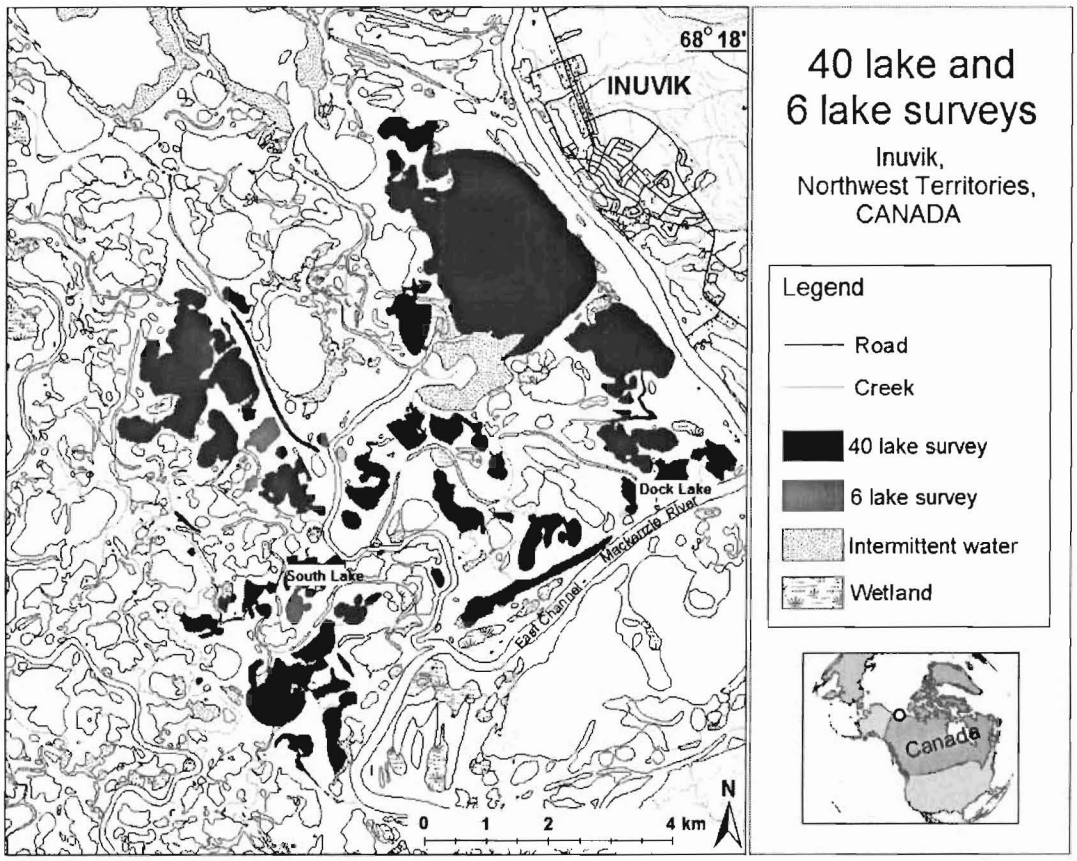

Figure 3.3 Location of lakes comprising the 40 lake and 6 lake sets in the Mackenzie Delta.

a)

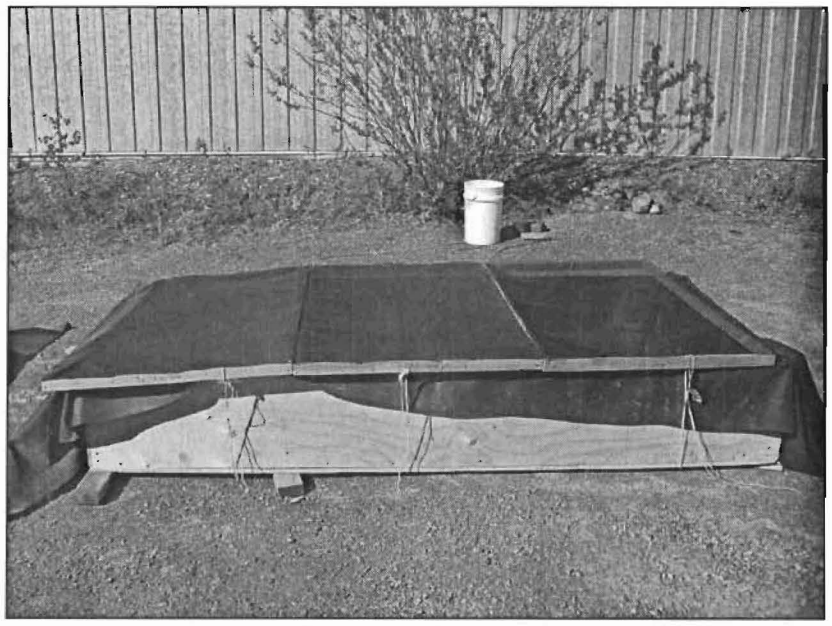

b)

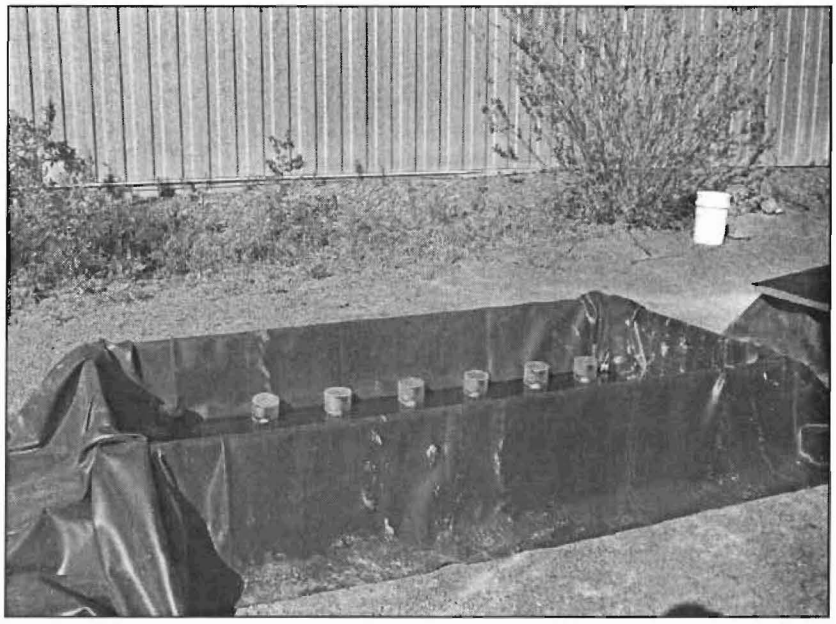

Photos by author

Figure 3.4 Experimental set-up of outdoor incubators used in all photobleaching experiments. One-litre microcosms were placed either a) under different UV filters held in place using wooden frames and rope or b) in an open incubator. Incubators were placed in an area of the Inuvik Research Centre grounds that was in direct sunlight between 9:00 AM and 9:00 PM, MDT.

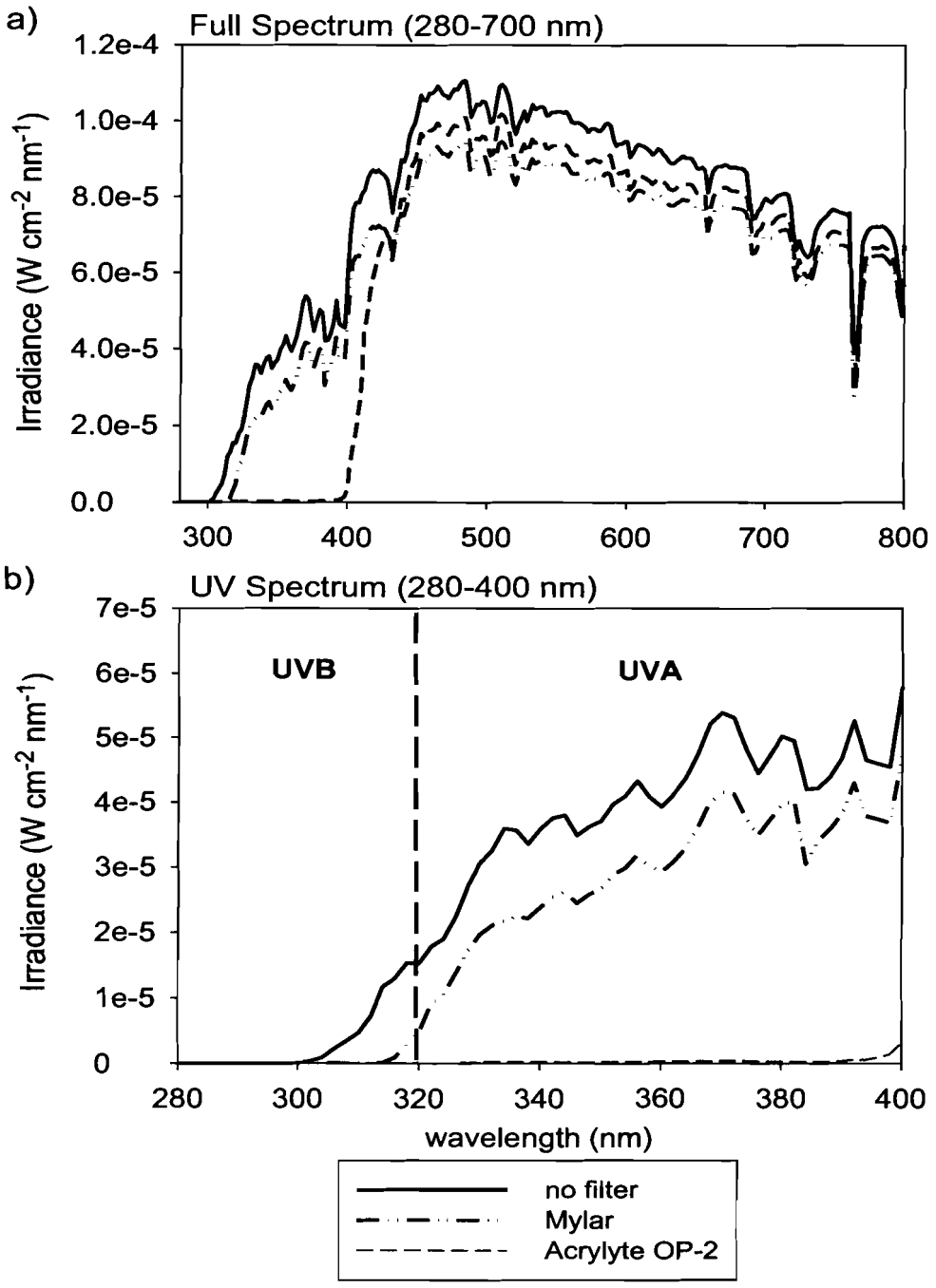

Figure 3.5 Transmission of solar irradiance through UV filters during clear, cloudless conditions. a) Both Mylar and Acrylyte OP-2 filters reduce total incident irradiance at all wavelengths from 280-700 nm. b) The Mylar filter transmits approximately 12% of solar irradiance in the UVB spectrum, while the Acrylyte OP-2 filter transmits only about 1% of solar irradiance in the entire UV spectrum. All scans were taken using an OL 754 spectroradiometer (Optronics Laboratories, Orlando FL).

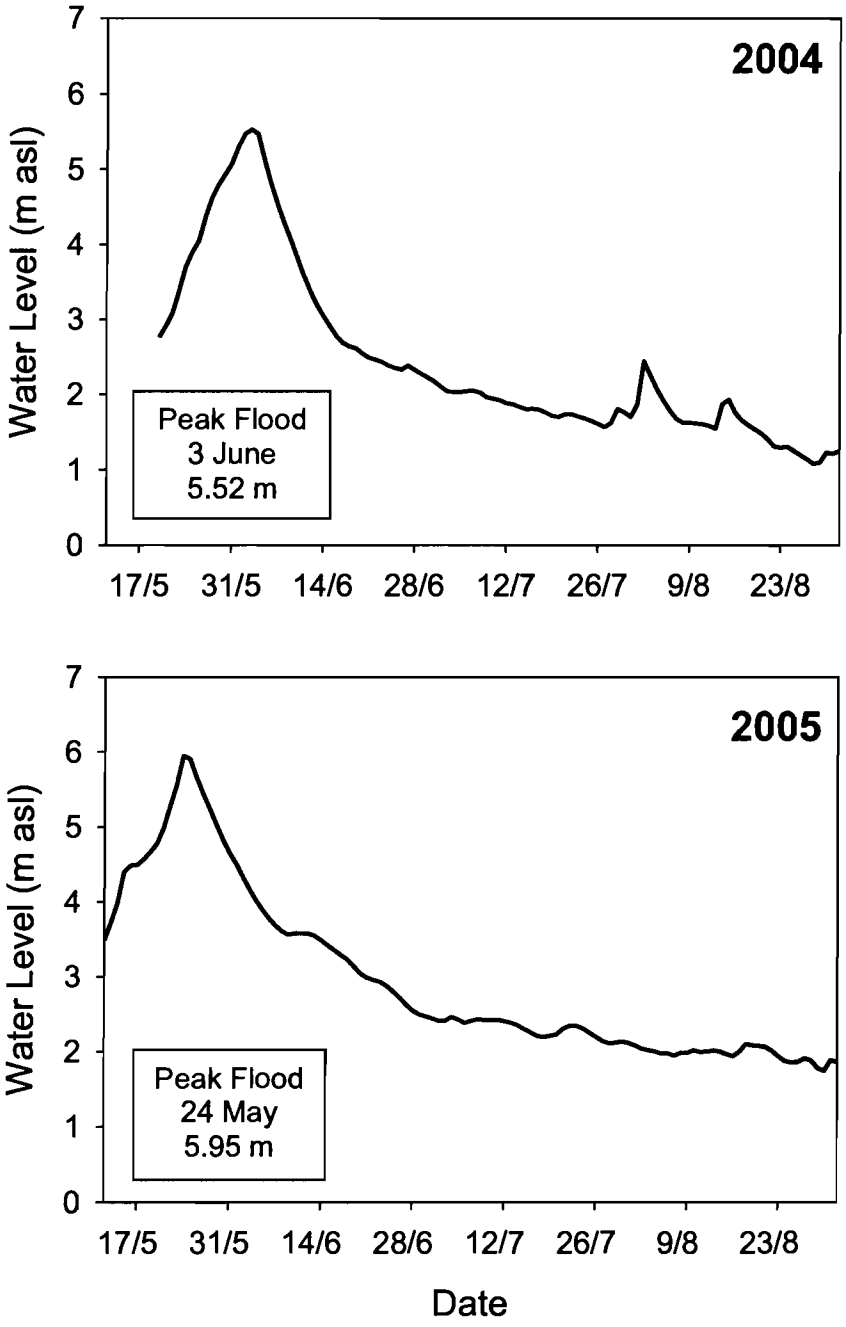

Figure 3.6 Water levels (m asl) in the Mackenzie Delta East Channel during the open water seasons of 2004 and 2005 as measured at the town of Inuvik (data provided by Water Survey of Canada).

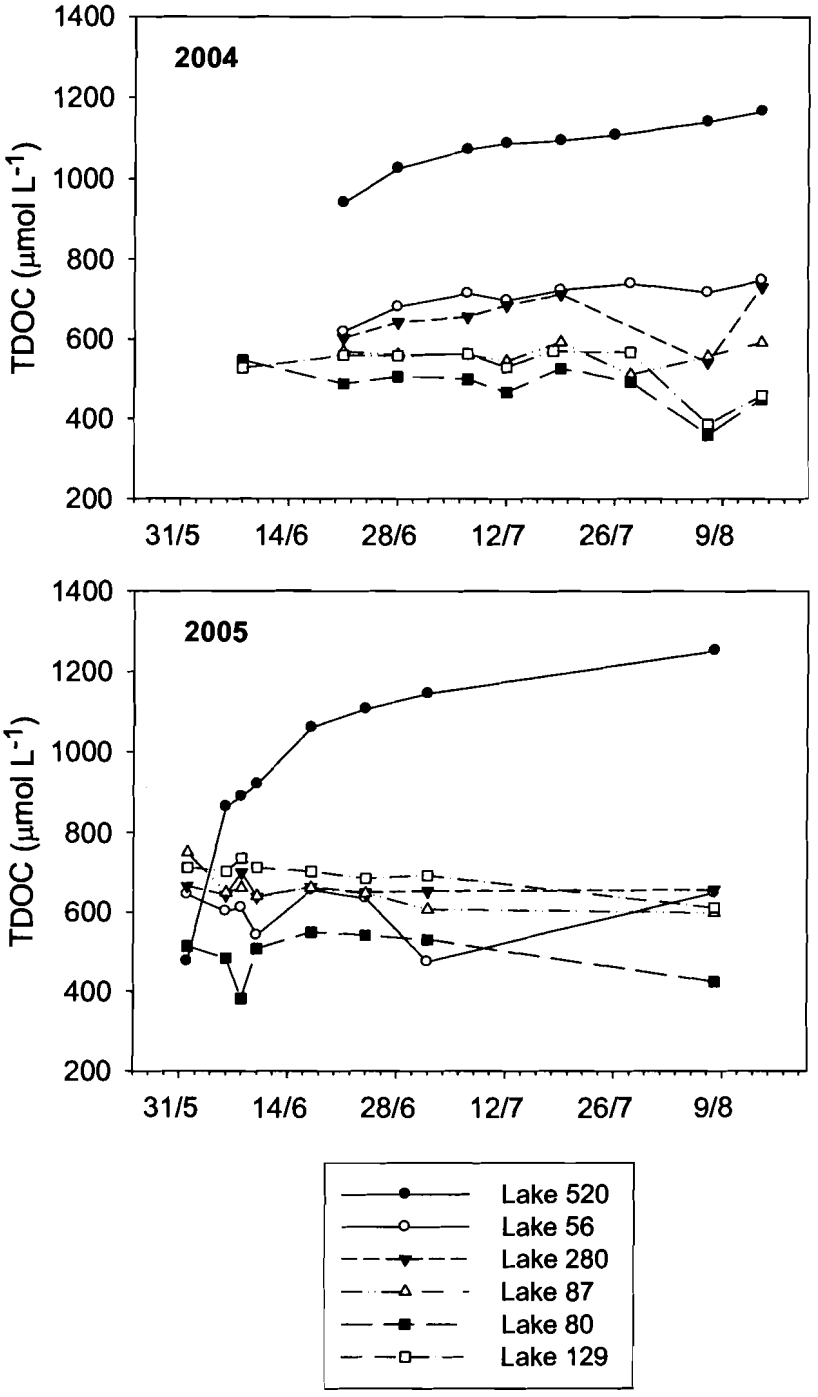

Figure 3.7 Seasonal patterns of TDOC concentrations (µmol L^{-1}) within the 6 lake set during the open water periods of 2004 and 2005.

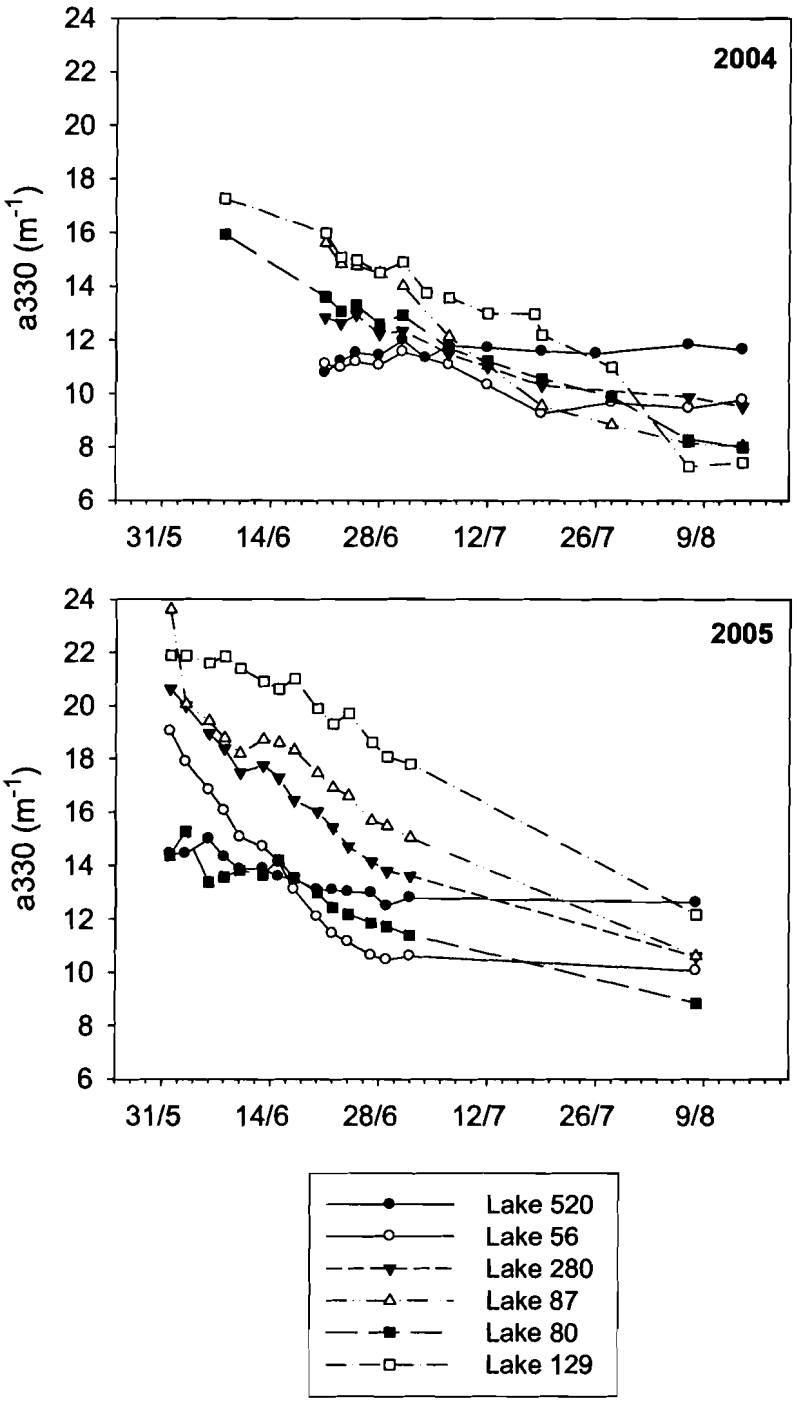

Figure 3.8 Seasonal patterns in CDOM absorbencies (a330, m^{-1}) within the 6 lake set during the open water periods of 2004 and 2005.

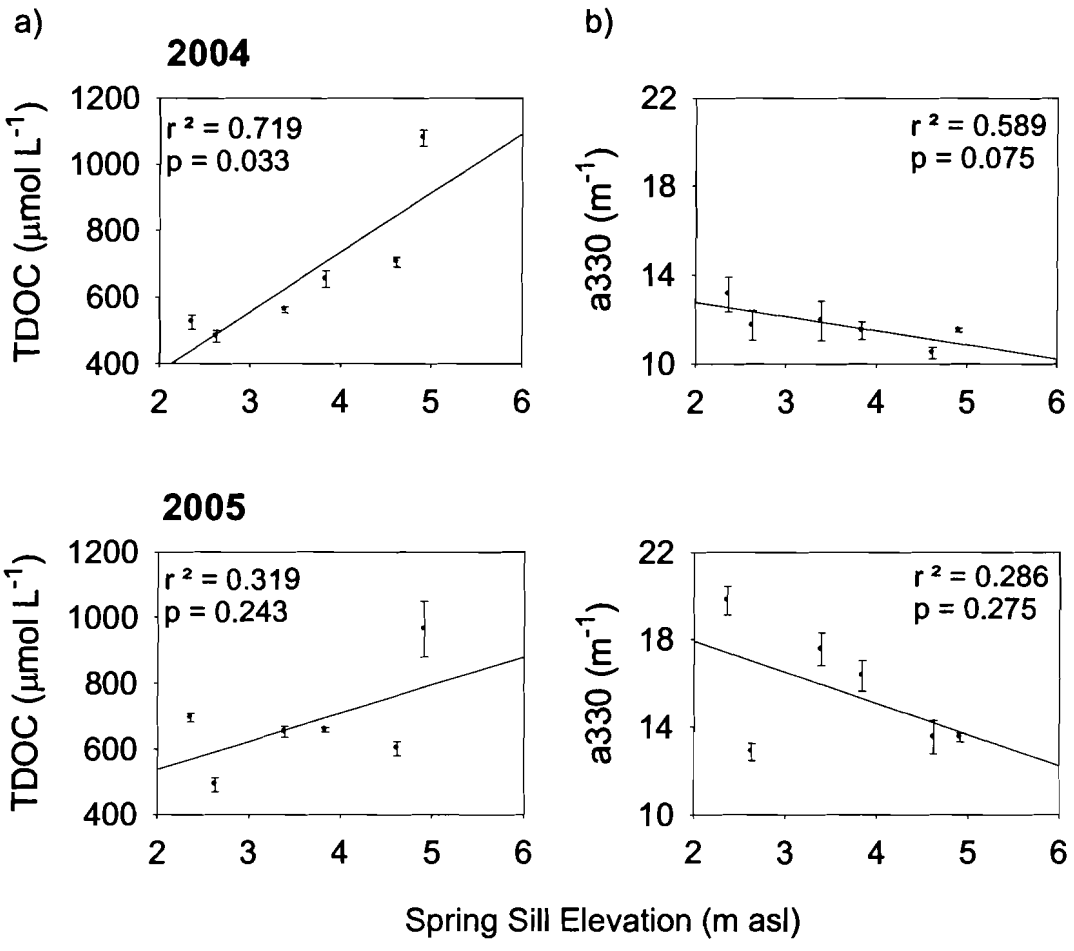

Figure 3.9 Relationship between spring sill elevation (m asl) and a) TDOC concentration (µmol L^{-1}), and b) CDOM absorbency (a330, m^{-1}), for the 6 lake set during the open water seasons of 2004 and 2005. Reported are mean values for the open water season from mid-lake dip samples, with error bars indicating one standard error of the mean.

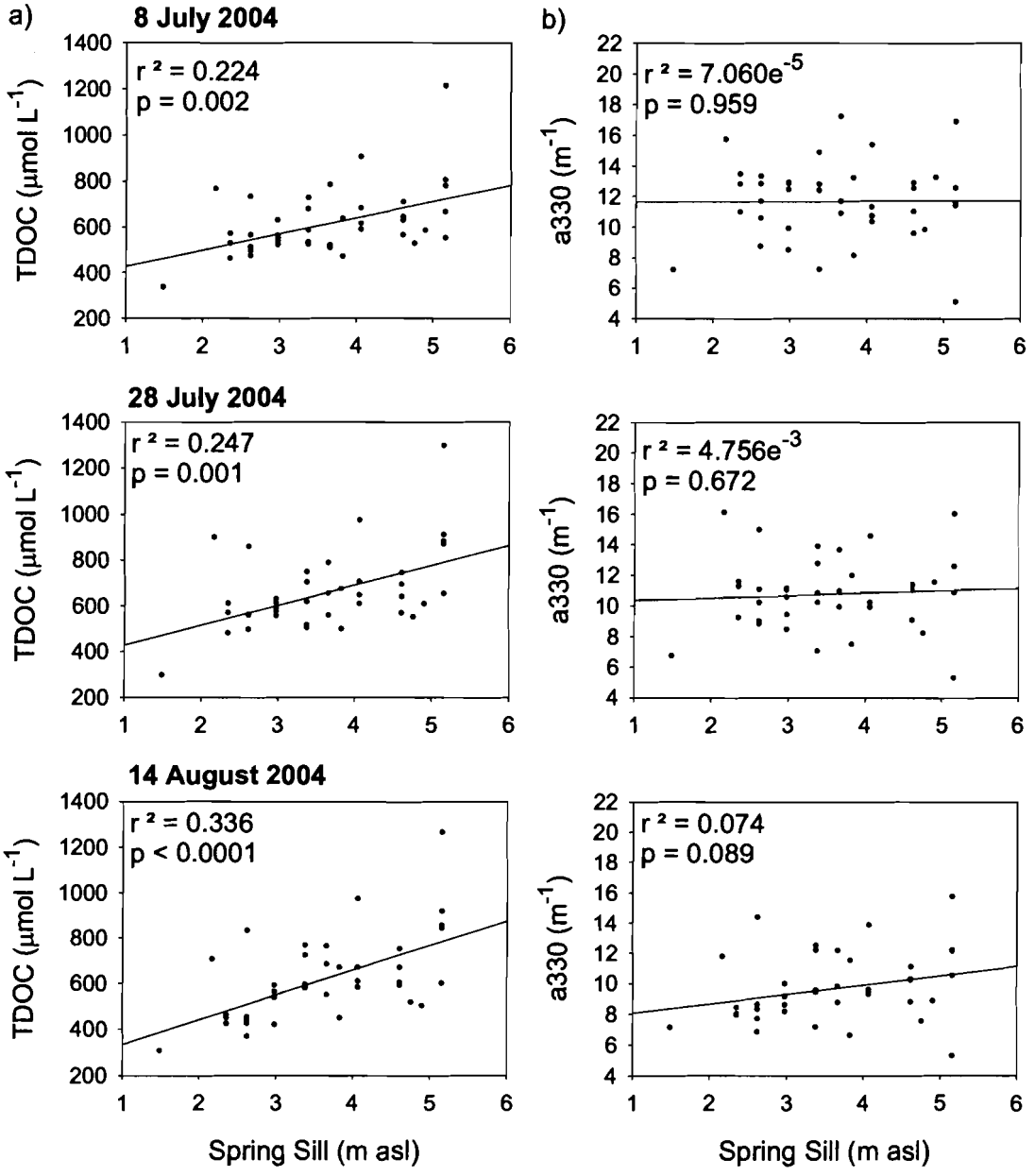

Figure 3.10 Relationships between spring sill elevation (m asl) and a) TDOC concentration (µmol L^{-1}), and b) CDOM absorbency (a330, m^{-1}), for forty spatially discrete lakes near Inuvik, NT, sampled three times during the open water season of 2004.

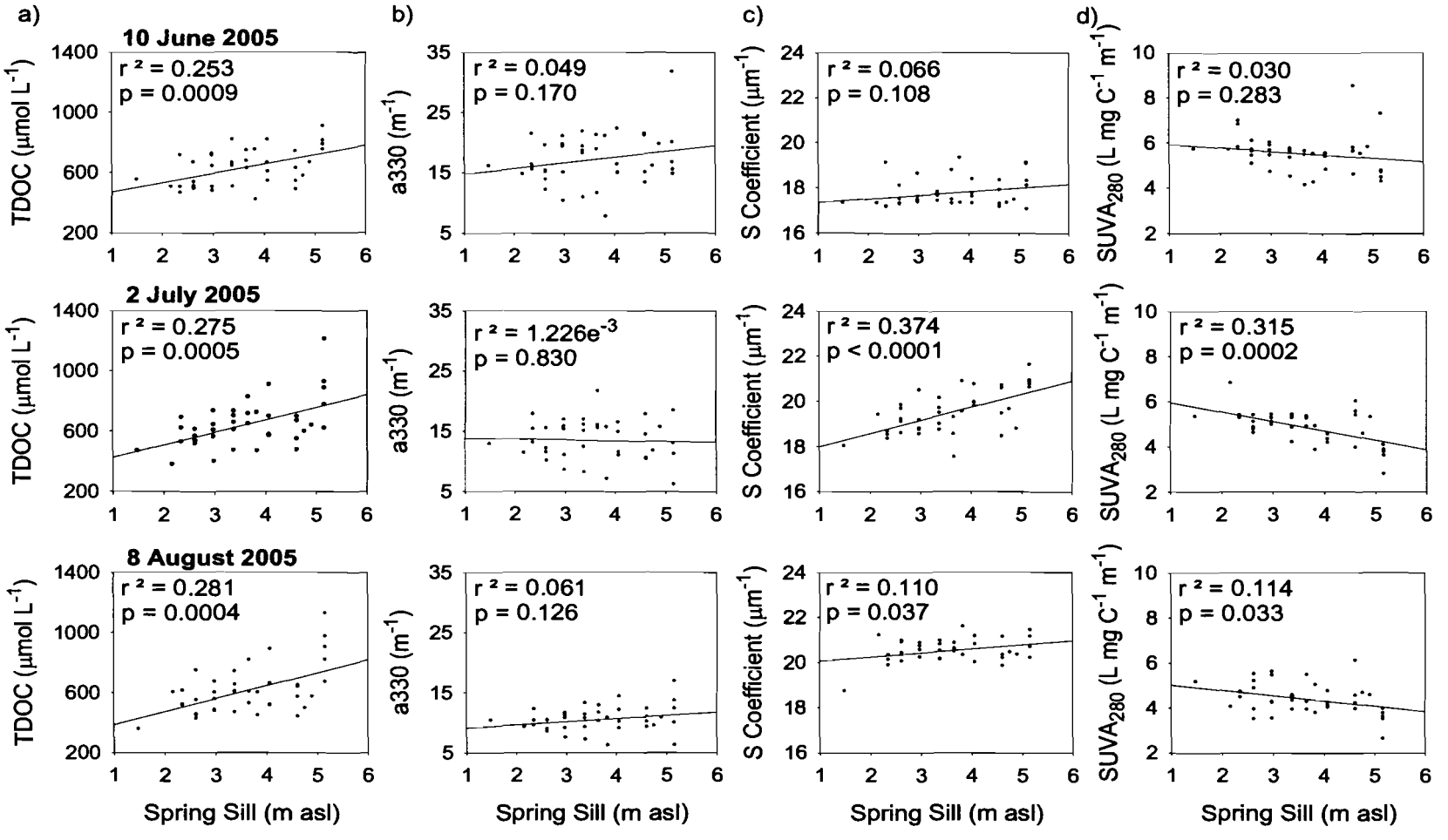

Figure 3.11 Relationships between spring sill elevation (m asl) and a) TDOC concentration (µmol L^{-1}), b) CDOM absorbency (a330, m^{-1}), c) spectral slope (S) coefficient (μm^{-1}), and d) $SUVA_{280}$ (L mg C^{-1} m^{-1}) for forty spatially discrete lakes near Inuvik, NT, sampled three times during the open water season of 2005.

a)

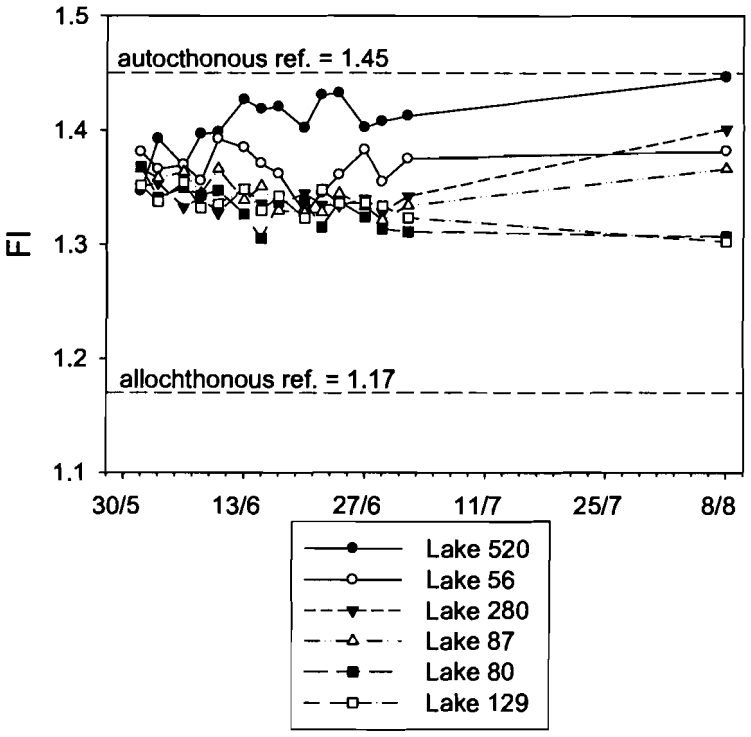

b)

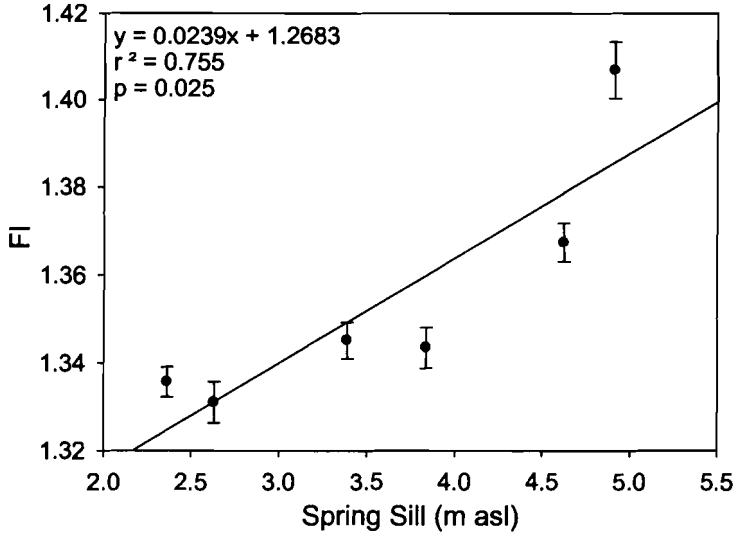

Figure 3.12 a) Seasonal patterns in fluorescence index (FI) values within the 6 lake set during the open water season of 2005. Reference lines indicate measured autochthonous and allochthonous standard fulvic acid solutions.
b) Relationship between FI and spring sill elevation (m asl) in the 6 lake set during the open water season of 2005. Reported are mean values for the open water season from mid-lake dip samples, with error bars indicating one standard error of the mean.

a)

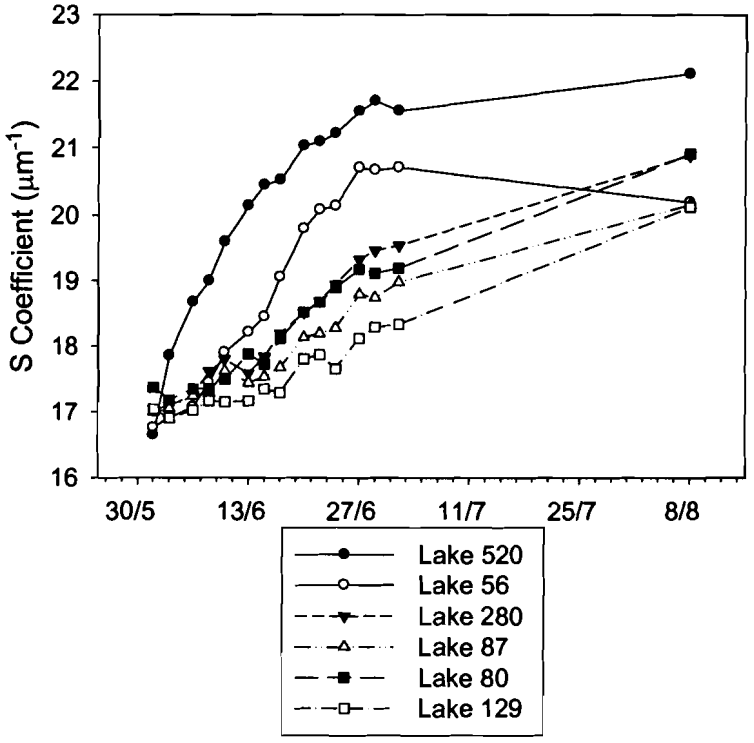

b)

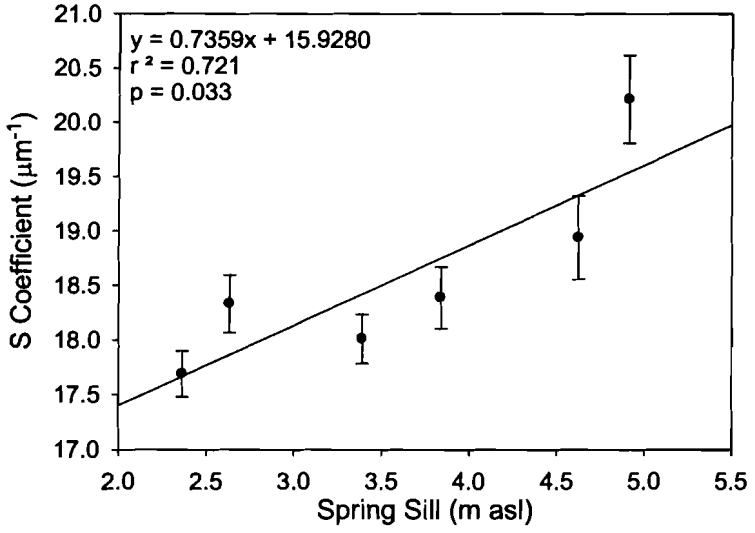

Figure 3.13 a) Seasonal patterns in the spectral slope coefficient (S, μm^{-1}) within the 6 lake set during the open water season of 2005. b) Relationship between S (μm^{-1}) and spring sill elevation (m asl) in the 6 lake set during the open water season of 2005. Reported are mean values for the open water season from mid-lake dip samples, with error bars indicating one standard error of the mean.

a)

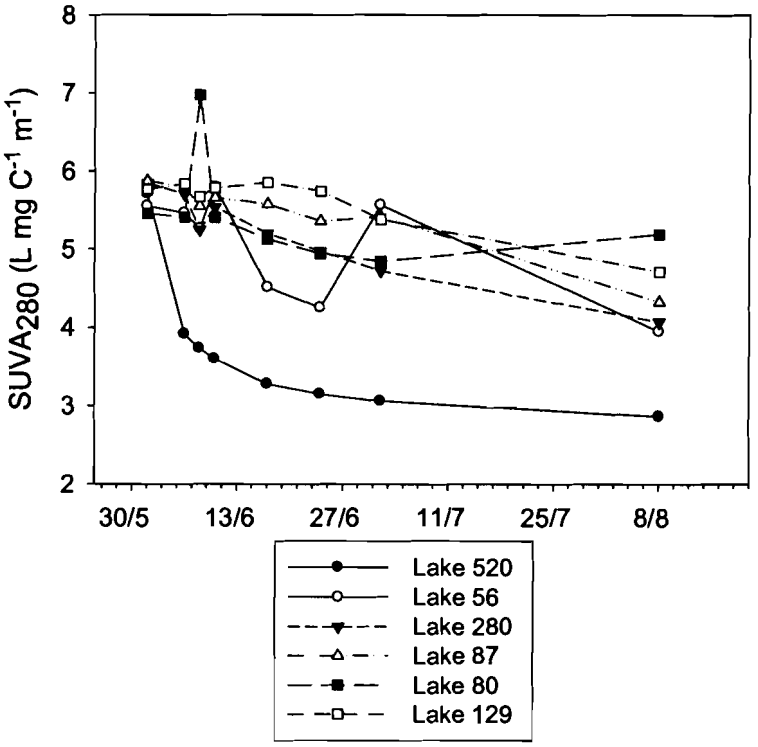

b)

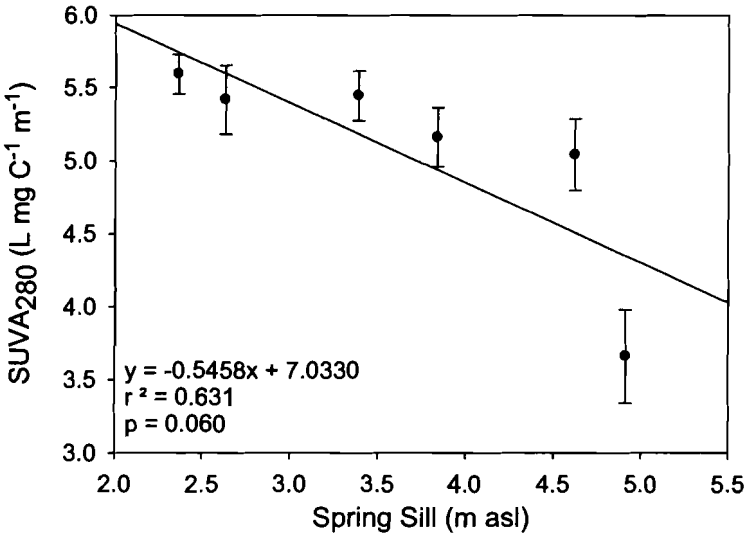

Figure 3.14 a) Seasonal patterns in $SUVA_{280}$ (L mg C^{-1} m^{-1}) within the 6 lake set during the open water season of 2005. b) Relationship between $SUVA_{280}$ (L mg C^{-1} m^{-1}) and spring sill elevation (m asl) in the 6 lake set during the open water season of 2005. Reported are mean values for the open water season from mid-lake dip samples, with error bars indicating one standard error of the mean.

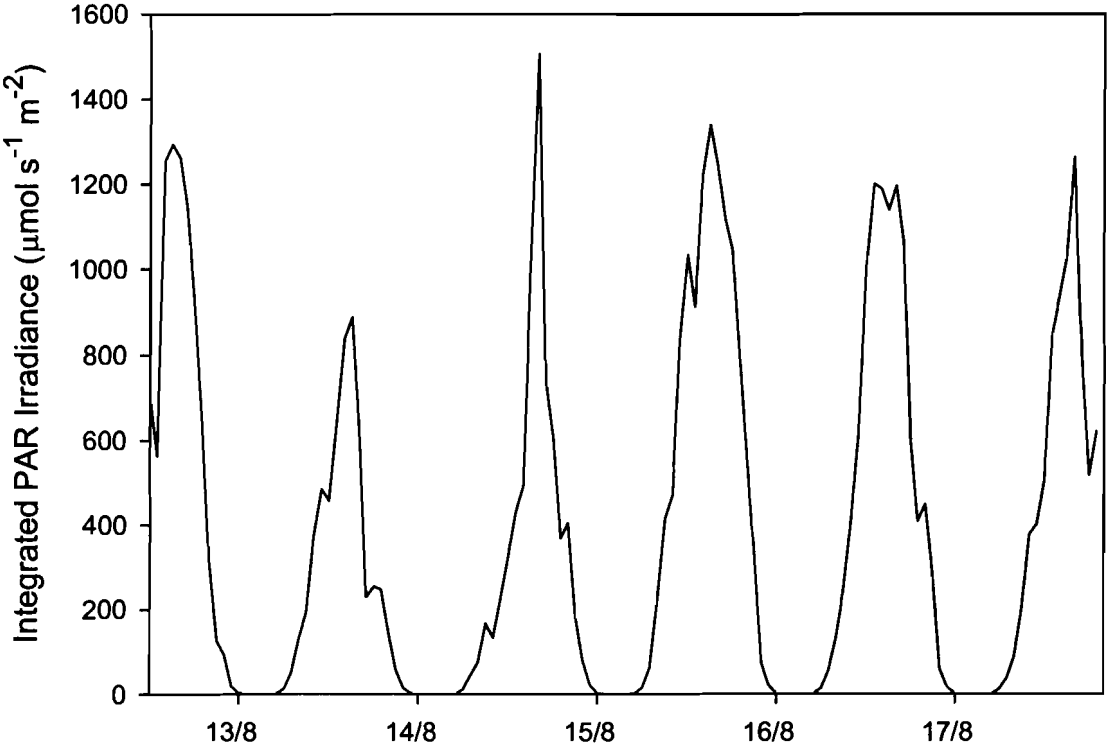

Figure 3.15 Integrated PAR fluxes during the DOM composition outdoor incubator experiment conducted from 12:00PM on 12 August to 8:00PM on 17 August, 2004. Integrated measurements were averaged for every hour interval.

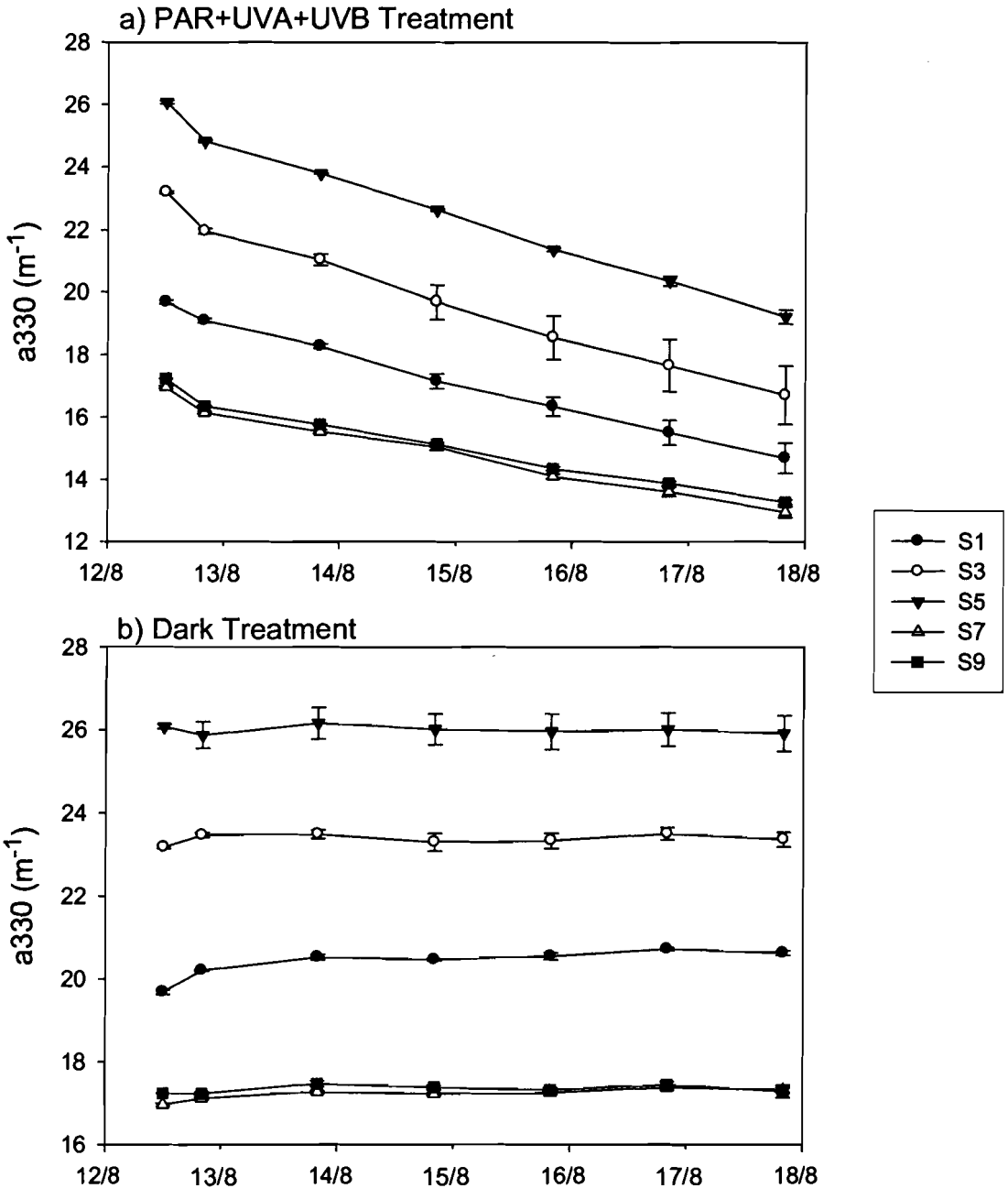

Figure 3.16 Measurements of CDOM absorbency (a330, m^{-1}) during the DOM composition outdoor incubator experiment conducted from 12:00PM on 12 August to 8:00PM on 17 August, 2004. Error bars represent one standard error of the mean.

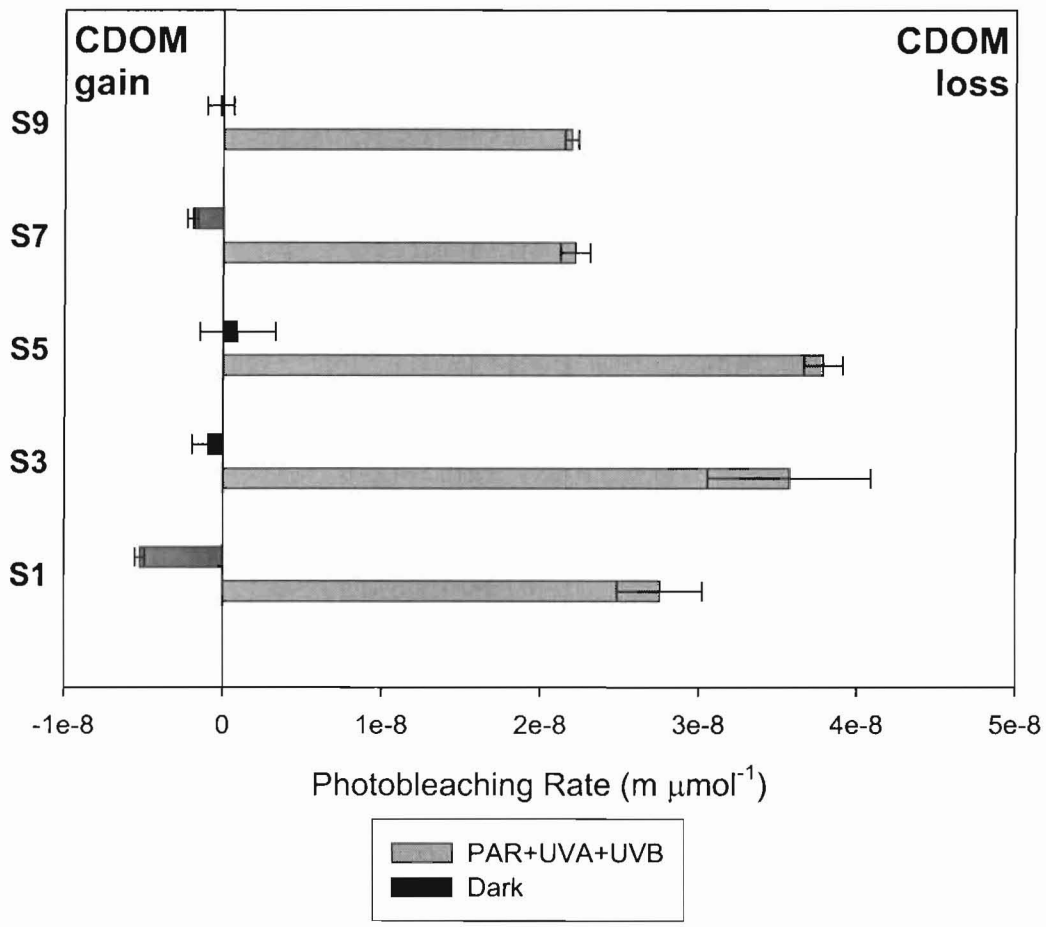

Figure 3.17 Average photobleaching rates (m μmol^{-1}) during the DOM composition outdoor incubator experiment conducted from 12:00PM on 12 August to 8:00PM on 17 August, 2004. Error bars represent one standard error of the mean.

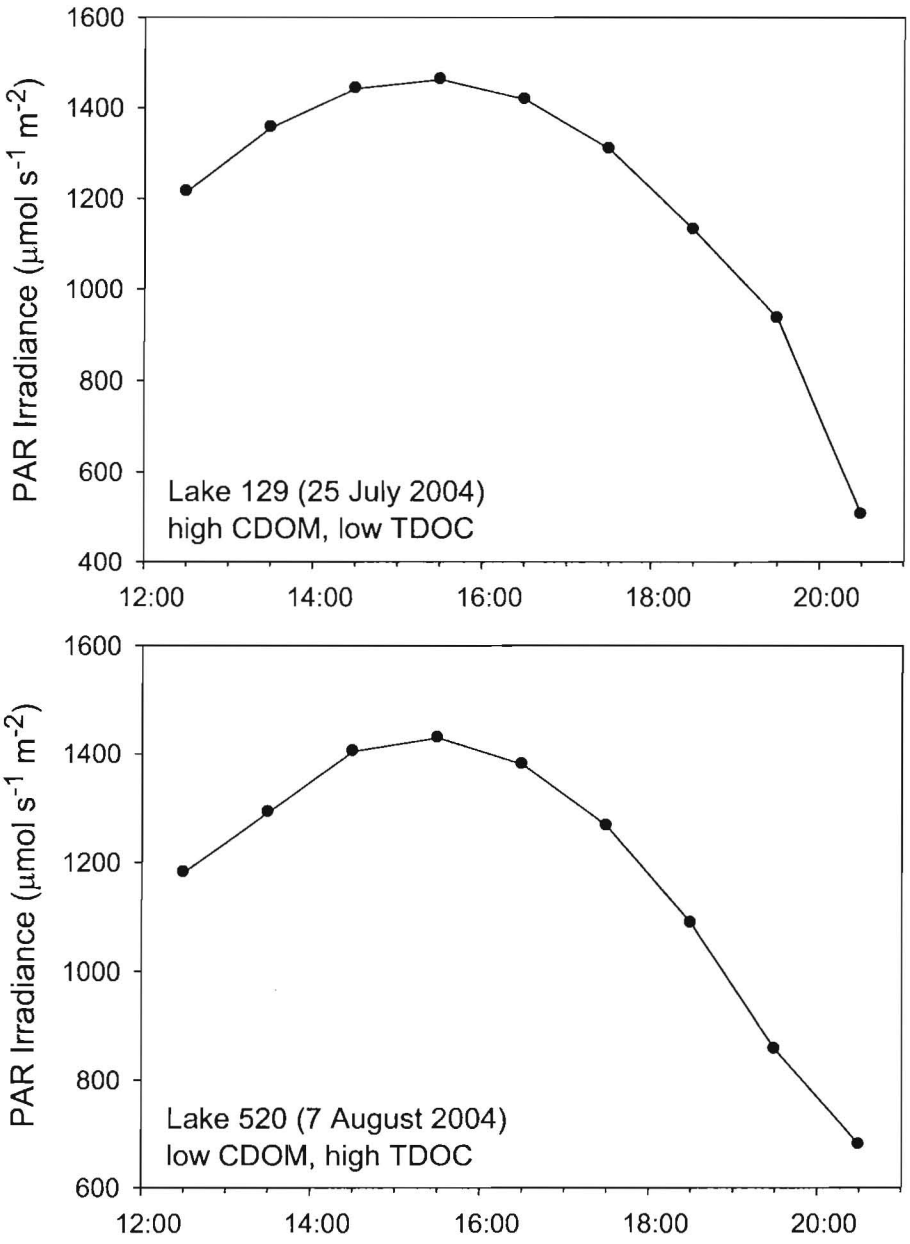

Figure 3.18 Integrated PAR irradiance fluxes during the waveband exclusion outdoor incubator experiments conducted from 12:00PM to 8:00PM on 25 July 2004 (Lake 129) and 7 August 2004 (Lake 520). Integrated PAR measurements were averaged for every hour interval.

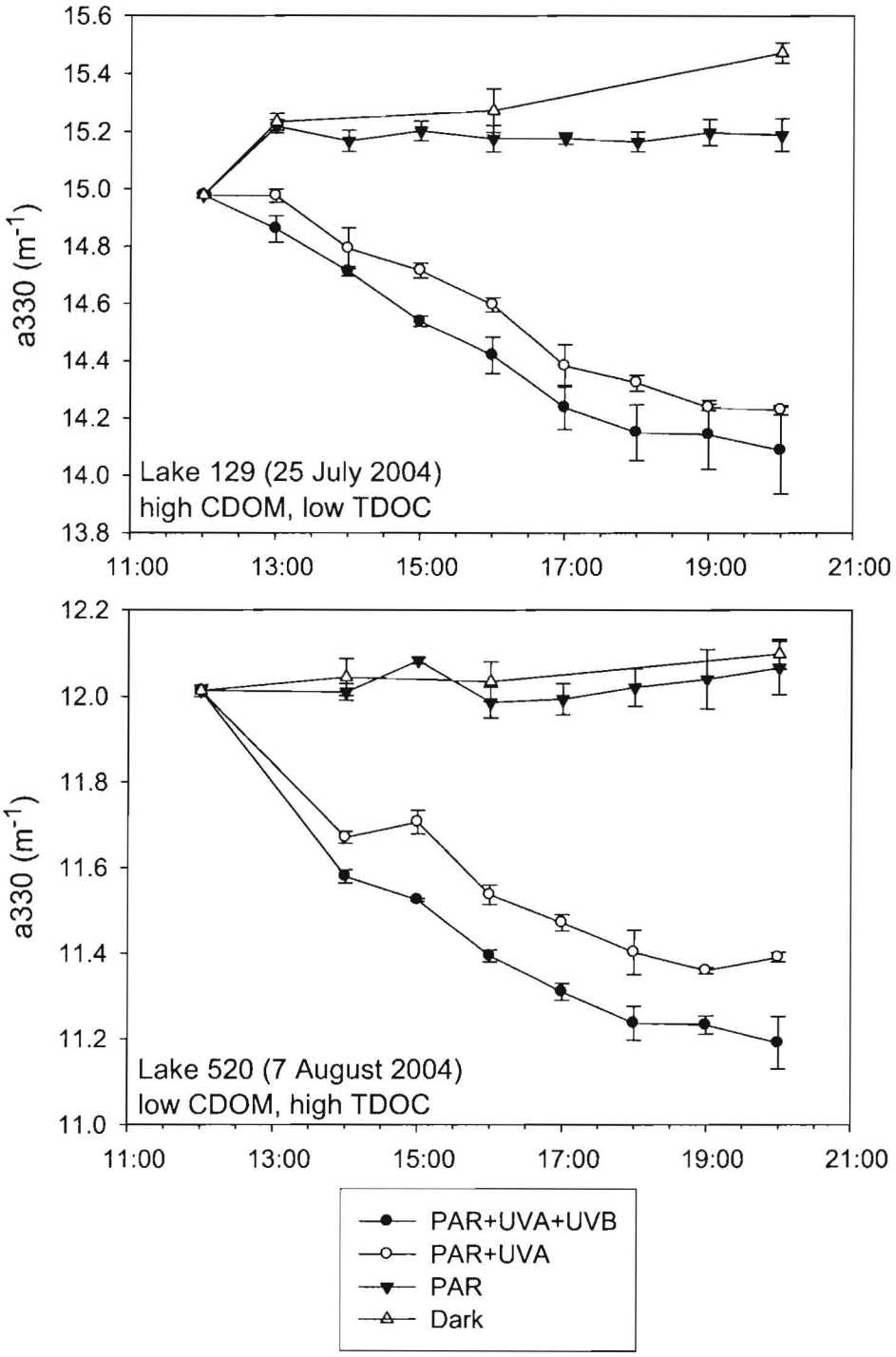

Figure 3.19 Hourly measurements of CDOM absorbency (a330, m^{-1}) during the waveband exclusion outdoor incubator experiments conducted from 12:00PM to 8:00PM on 25 July 2004 (Lake 129) and 7 August 2004 (Lake 520). Error bars represent one standard error of the mean.

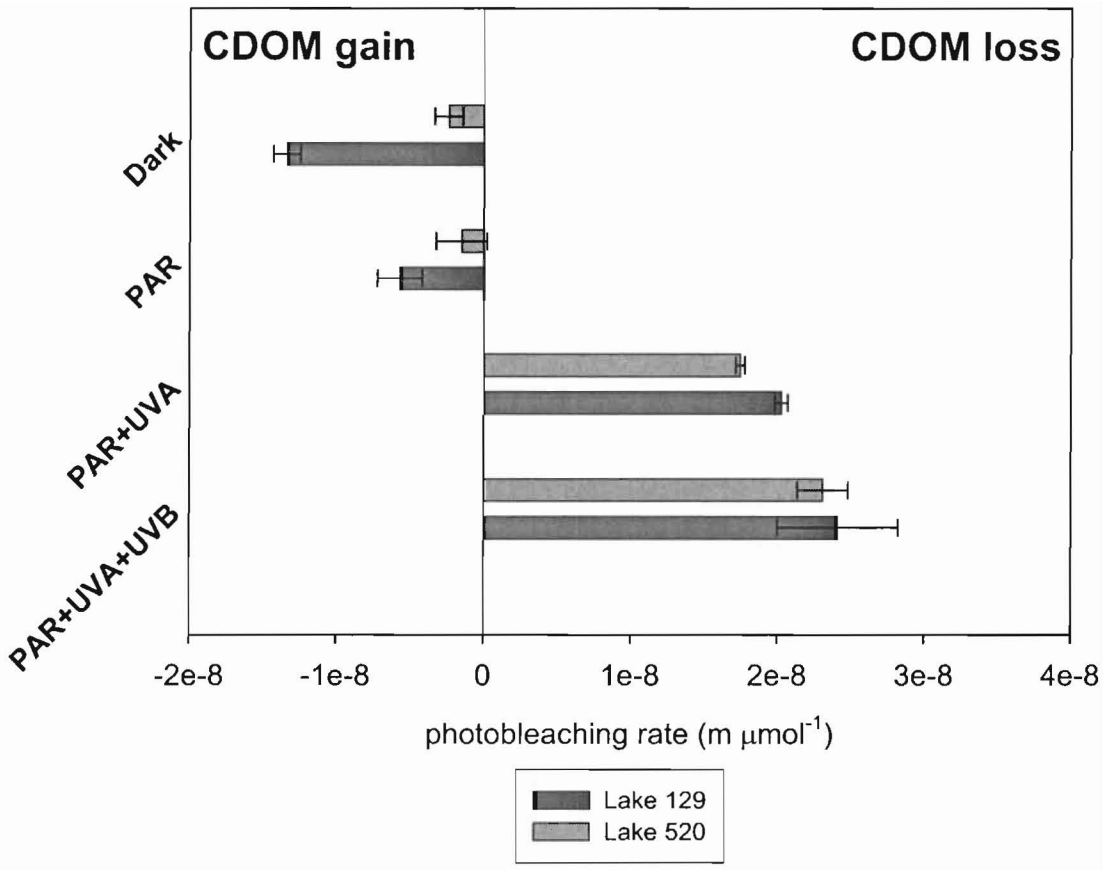

Figure 3.20 Average photobleaching rates (m μmol^{-1}) during the waveband exclusion outdoor incubator experiments conducted from 12:00PM to 8:00PM on 25 July 2004 (Lake 129) and 7 August 2004 (Lake 520). Error bars represent one standard error of the mean.

a)

Source	Nparm	DF	DFDen	F Ratio	p
treatment	3	3	3	25.9849	**0.0120**

b)

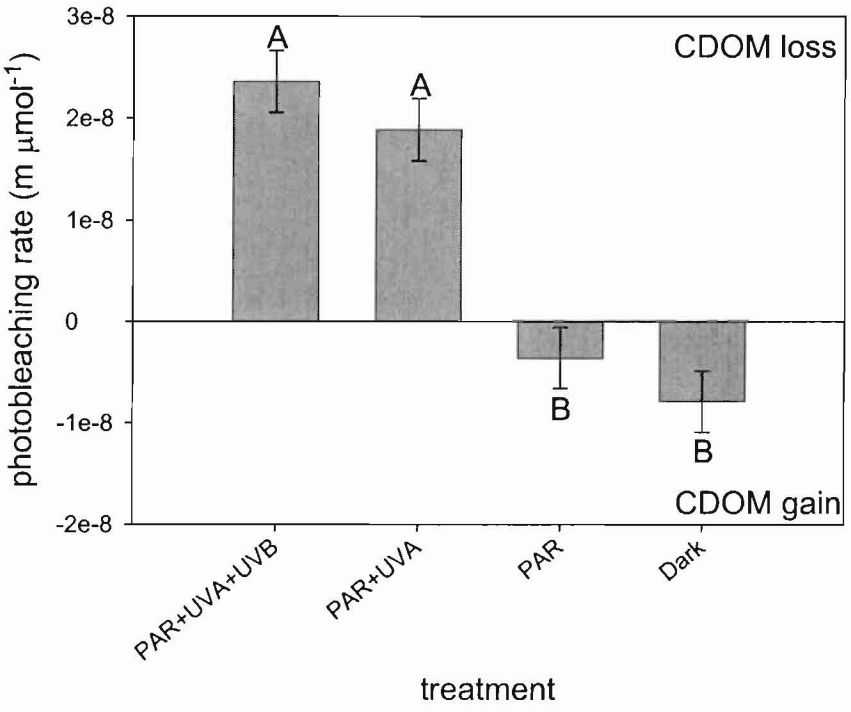

Figure 3.21 a) Preliminary two-way ANOVA analysis (randomized complete block design with lake as a random effect) indicated a significant difference ($p = 0.012$) in photobleaching rates (m μmol^{-1}) between treatments during the waveband exclusion outdoor incubator experiments. b) Photobleaching rates for each treatment, averaged across both lakes. Error bars represent one standard error of the mean. Results accompanied by the same letter are not significantly different at $\alpha = 0.05$ (least squares means differences, Tukey HSD).

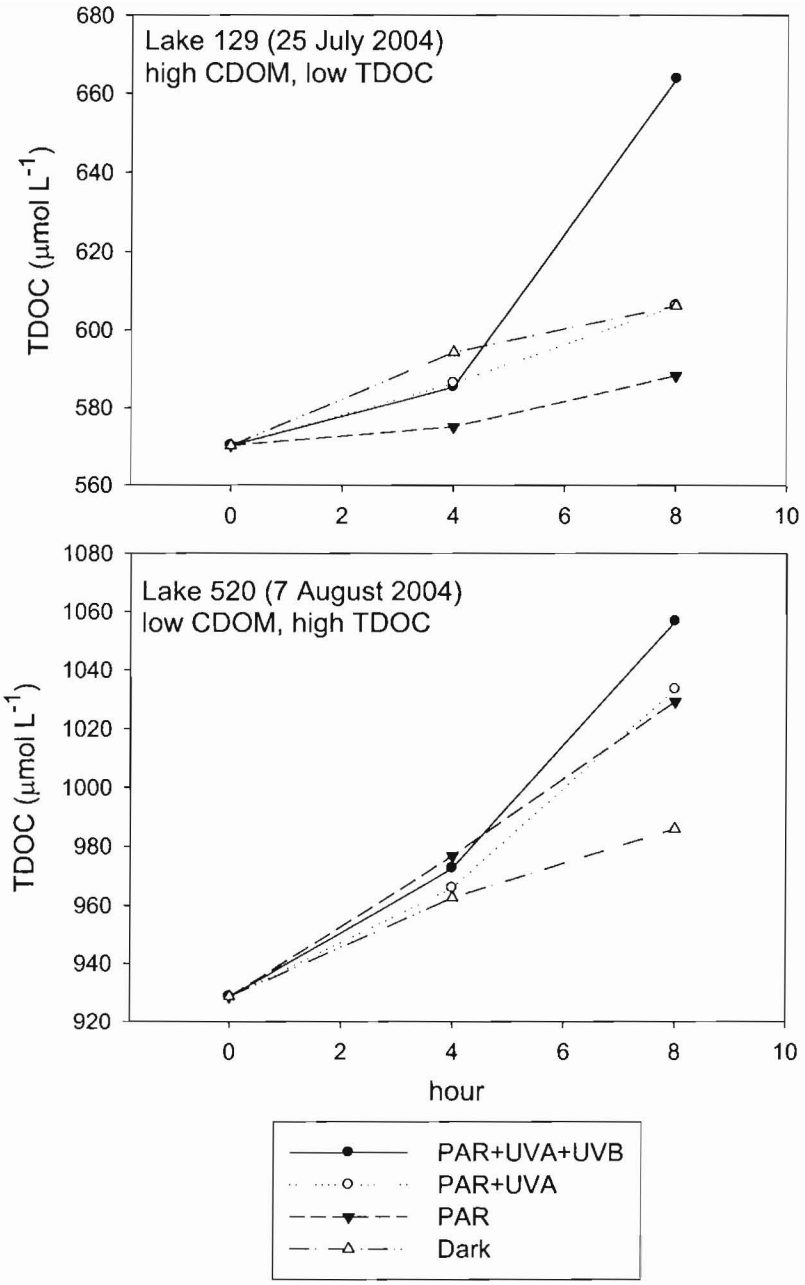

Figure 3.22 TDOC concentrations (µmol L^{-1}) at the beginning (time 0), middle (4 hours) and end (8 hours) of the waveband exclusion outdoor incubator experiments conducted from 12:00PM to 8:00PM on 25 July 2004 (Lake 129) and 7 August 2004 (Lake 520).

APPENDICES

Appendix A: Input Fields for SMARTS2, version 2.9.2

Input fields (cards) for the Simple Model of the Atmospheric Radiative Transfer of Sunshine (SMARTS2) v 2.9.2 (Gueymard, 2002).

The SMARTS2 model requires user input on 19 separate cards that are then used to calculate several characteristics of the irradiance field at the specified site and time. The following is a list of user-defined inputs that were used to calculate global, diffuse and direct surface irradiance over the wavelength range of 280-800 nm (2 nm intervals) for sites in the Mackenzie Delta. All climate and environmental data used in the SMARTS2 model were obtained from Environment Canada's record for weather station Inuvik A (Climate ID 2202570).

Card 1: **Comments**
* Site and Date entered.

Card 2: **Site Pressure**
* Option to enter the surface pressure and altitude selected.
* Altitude used was 68 m (altitude at Inuvik airport).

Card 3: **Atmosphere**
* Reference atmosphere "Arctic Summer" selected.

Card 4: **Water Vapour**
* "Calculate from reference atmosphere and altitude" selected.

Card 5: **Ozone**
* Defaults from reference atmosphere selected.

Card 6: **Gaseous Absorption**
* Defaults from reference atmosphere selected.

Card 7: **Carbon Dioxide**
* Default value of 370 ppm selected.

Card 7a: **Extraterrestrial Spectrum**
* "Gueymard 2002 (synthetic)" spectrum selected.

Card 8: **Aerosol Model**
* "Shuttle and Fen rural" model selected.

Card 9: **Turbidity**
* Prevailing airport visibility (km) entered.

Card 10: **Albedo**
* "Water (specular reflectance)" selected.

Card 10b: **Tilt Albedo**
* Opted to bypass tilt calculations.

Card 11: **Spectral Range**
* Entered wavelength range of 280-800 nm.
* Solar Constant and Solar Constant Distance Correction Factor default values selected.

Card 12: **Output**
* Specified data output in both .OUT and .EXT files.
* Data interval set to 2 nm.
* Selected diffuse horizontal irradiance, global horizontal irradiance and direct horizontal irradiance as output data.

Card 13: **Circumsolar**
* Calculations bypassed.

Card 14: **Smoothing Filter**
* Calculations bypassed.

Card 15: **Illuminance**
* Calculations bypassed.

Card 16: **UV Card**
* "Perform special UV calculations" selected.

Card 17: **Solar Geometry**
* Selected option to input year, month, day, hour, latitude, longitude, and time zone.

Appendix B: Climate Data used in SMARTS2, version 2.9.2

Climate data used to calculate irradiance values using the Simple Model of the Atmospheric Radiative Transfer of Sunshine (SMARTS2) v2.9.2 (Gueymard, 2002). All climate and environmental data used in the SMARTS2 model were obtained from Environment Canada's 2004 record for weather station Inuvik A (Climate ID 2202570).

Site	Day	Time (*MST)	**SZA (°)	***RH (%)	+Vis (km)	T (°C)	P (kPa)	++Sky Cond.
L80	Jun-08	4:24:00 PM	50.75	34.5	24.1	18.1	100.55	clear
S9	Jun-15	11:49:00 AM	49.05	34.0	24.1	13.7	101.65	clear
S8	Jun-15	12:47:00 PM	46.32	33.0	24.1	15.3	101.64	clear
S7	Jun-15	1:50:30 PM	45.12	27.0	24.1	16.8	101.62	clear
S6	Jun-15	2:54:30 PM	45.98	22.0	24.1	18.1	101.62	m. clear
S5	Jun-15	4:17:00 PM	49.92	23.0	24.1	18.3	101.58	m. clear
S4	Jun-17	10:28:00 AM	54.79	32.0	24.1	24.3	100.97	cloudy
S3	Jun-17	11:36:00 AM	49.83	33.5	24.1	25.0	100.95	cloudy
S2	Jun-17	1:08:00 PM	45.67	34.0	24.1	25.8	100.94	cloudy
S1	Jun-17	2:10:30 PM	45.12	33.0	24.1	26.9	100.93	m. cloudy
L129	Jun-21	3:40:00 PM	47.53	36.0	24.1	24.8	100.63	m. cloudy
L80	Jun-21	6:49:30 PM	62.01	34.0	24.1	26.3	100.46	m. cloudy
L520	Jun-21	1:52:30 PM	44.88	38.0	24.1	23.1	100.80	rain
S9	Jun-23	12:00:30 PM	48.45	46.0	24.1	23.8	100.51	m. cloudy
S8	Jun-23	12:52:30 PM	46.14	43.0	24.1	24.0	100.53	cloudy
S7	Jun-24	10:02:00 AM	57.10	49.0	24.1	25.0	100.61	clear
S6	Jun-24	10:56:30 AM	52.72	48.0	24.1	26.5	100.62	m. clear
S5	Jun-24	11:52:00 AM	48.95	46.0	24.1	27.8	100.64	m. clear
S4	Jun-24	12:38:00 PM	46.69	45.5	24.1	28.2	100.65	m. clear
S3	Jun-24	1:28:30 PM	45.31	44.5	24.1	29.1	100.67	m. clear
S2	Jun-24	2:19:00 PM	45.20	44.0	24.1	29.6	100.68	m. clear
S1	Jun-24	3:06:30 PM	46.27	40.0	24.1	29.9	100.71	m. clear
L129	Jun-28	12:49:30 PM	46.33	39.0	24.1	21.0	101.61	clear
L80	Jun-28	11:33:30 AM	50.24	51.0	24.1	18.4	101.65	m. clear
L520	Jun-28	5:03:30 PM	53.02	41.0	24.1	22.9	101.51	m. cloudy
S9	Jun-29	10:12:00 AM	56.53	59.0	24.1	15.8	101.80	clear
S8	Jun-29	11:05:30 AM	52.32	41.0	24.1	18.7	101.77	m. clear
S7	Jun-29	11:56:00 AM	48.98	44.0	24.1	18.3	101.76	m. clear
S6	Jun-29	12:55:00 PM	46.33	44.0	24.1	19.8	101.76	m. clear
S5	Jun-29	1:49:30 PM	45.32	44.0	24.1	20.2	101.74	m. clear
S4	Jun-29	2:37:30 PM	45.67	44.0	24.1	20.4	101.75	m. clear
S3	Jun-29	3:41:30 PM	47.90	47.0	24.1	19.3	101.75	m. clear
S3	Jun-30	3:24:00 PM	47.18	48.5	24.1	16.2	101.62	clear
S2	Jun-30	2:30:00 PM	45.62	50.5	24.1	15.1	101.66	clear
S1	Jun-30	1:41:00 PM	45.45	55.5	24.1	14.5	101.67	clear
L129	Jul-07	1:29:30 PM	46.08	64.5	24.1	17.4	100.34	cloudy
L80	Jul-07	3:01:30 PM	46.79	65.0	24.1	17.1	100.39	cloudy
L129	Jul-09	12:36:30 PM	47.88	39.5	24.1	17.1	100.25	m. cloudy
L520 #1	Jul-09	2:15:00 PM	46.14	39.0	24.1	18.1	100.15	m. cloudy
L520 #2	Jul-09	2:56:30 PM	46.88	38.0	24.1	18.9	100.08	m. cloudy
S9	Jul-13	12:55:30 PM	47.87	67.0	24.1	16.0	100.47	m. cloudy
S8	Jul-13	2:05:00 PM	46.78	66.0	24.1	17.1	100.41	m. cloudy

Site	Day	Time (*MST)	**SZA (°)	***RH (%)	+Vis (km)	T (°C)	P (kPa)	++Sky Cond.
S7	Jul-13	3:03:00 PM	47.76	62.0	24.1	18.2	100.38	m. cloudy
S6	Jul-13	4:12:30 PM	50.92	62.0	24.1	17.5	100.37	cloudy
S5	Jul-13	5:18:00 PM	55.52	64.0	24.1	17.1	100.36	cloudy
L129 #1	Jul-18	2:26:00 PM	47.62	57.5	24.1	19.4	100.28	m. cloudy
L129 #2	Jul-18	2:38:00 PM	47.80	57.5	24.1	19.4	100.28	m. cloudy
S5	Jul-20	1:05:30 PM	48.79	57.0	24.1	20.2	100.31	m. cloudy
S4	Jul-20	12:29:00 PM	50.09	57.0	24.1	20.2	100.32	m. cloudy
S3	Jul-20	12:03:30 PM	51.37	57.0	24.1	20.2	100.32	m. cloudy
S2	Jul-20	11:27:30 AM	53.56	59.0	24.1	19.6	100.33	m.cloudy
S1	Jul-20	11:03:30 AM	55.25	61.0	24.1	18.9	100.34	m.cloudy
S9	Jul-21	12:39:30 PM	49.85	90.0	21.7	11.8	100.95	cloudy
S8	Jul-21	1:04:00 PM	49.00	89.0	24.1	11.9	100.97	cloudy
S7	Jul-21	1:29:00 PM	48.45	87.0	24.1	12.1	100.98	cloudy
S6	Jul-21	2:25:00 PM	48.33	84.5	24.1	12.6	101.02	cloudy
S5	Jul-21	2:54:00 PM	48.88	84.0	24.1	12.8	101.04	cloudy
S4	Jul-21	3:21:00 PM	49.75	83.5	24.1	12.9	101.07	cloudy
S3	Jul-21	3:58:00 PM	51.47	83.0	24.1	13.0	101.09	cloudy
S2	Jul-21	4:38:00 PM	53.90	83.5	24.1	13.0	101.10	cloudy
S1	Jul-21	5:08:00 PM	56.04	84.0	24.1	12.9	101.10	cloudy
EC@CS	Jul-21	5:52:00 PM	59.56	81.0	24.1	13.1	101.12	cloudy
L520 #1	Jul-24	3:09:30 PM	49.81	62.0	24.1	19.7	100.63	m. cloudy
L520 #2	Jul-24	3:25:30 PM	50.40	62.5	24.1	20.2	100.62	m. cloudy
L520 #3	Jul-24	3:39:30 PM	51.01	62.5	24.1	20.2	100.62	m. cloudy
S9 #1	Aug-06	12:43:00 PM	53.47	45.0	24.1	16.6	101.34	clear
S9 #2	Aug-06	1:00:00 PM	52.92	45.0	24.1	16.6	101.34	clear
S8 #1	Aug-06	11:34:30 AM	56.94	51.5	24.1	15.1	101.36	clear
S8 #2	Aug-06	11:59:30 AM	55.48	48.0	24.1	15.6	101.35	clear
S7	Aug-06	10:48:00 AM	60.14	55.0	24.1	14.5	101.36	clear
S6	Aug-06	10:02:00 AM	63.83	63.0	24.1	12.5	101.38	clear
S5	Aug-06	9:40:00 AM	65.73	63.0	24.1	12.5	101.38	clear
S4	Aug-06	9:10:00 AM	68.40	68.0	24.1	9.9	101.40	clear
S3	Aug-06	8:40:30 AM	71.13	68.0	24.1	9.9	101.40	clear
S2	Aug-06	8:16:30 AM	73.33	73.0	24.1	8.1	101.40	clear
S1	Aug-06	7:52:00 AM	75.52	73.0	24.1	8.1	101.40	clear
L129 #1	Aug-08	12:41:00 PM	53.97	42.0	24.1	24.7	100.70	m. cloudy
L129 #2	Aug-08	12:50:00 PM	53.65	42.0	24.1	24.7	100.70	m. cloudy
L129 #3	Aug-08	12:58:00 PM	53.40	42.0	24.1	24.7	100.70	m. cloudy
L129 #4	Aug-08	1:07:00 PM	53.15	42.0	24.1	24.7	100.70	m. cloudy
L520 #1	Aug-08	2:52:00 PM	53.12	37.0	24.1	26.3	100.72	m. cloudy
L520 #2	Aug-08	2:58:00 PM	53.28	37.0	24.1	26.3	100.72	m. cloudy
L520 #3	Aug-08	3:04:00 PM	53.45	37.0	24.1	26.3	100.72	m.cloudy

*MST = mountain standard time (MST = MDT – 1 hour)
**SZA = solar zenith angle
***RH = relative humidity
+ Vis = visibility
++ sky cond. = sky conditions at the time of OL 754 underwater irradiance scans

Appendix C: Time Course of CDOM Absorbency in the East Channel of the Mackenzie Delta

Channel water CDOM absorbencies were tracked in the East Channel of the Mackenzie Delta throughout the open water season of 2004. Samples were taken from the channel immediately adjacent to the chain set connection point.

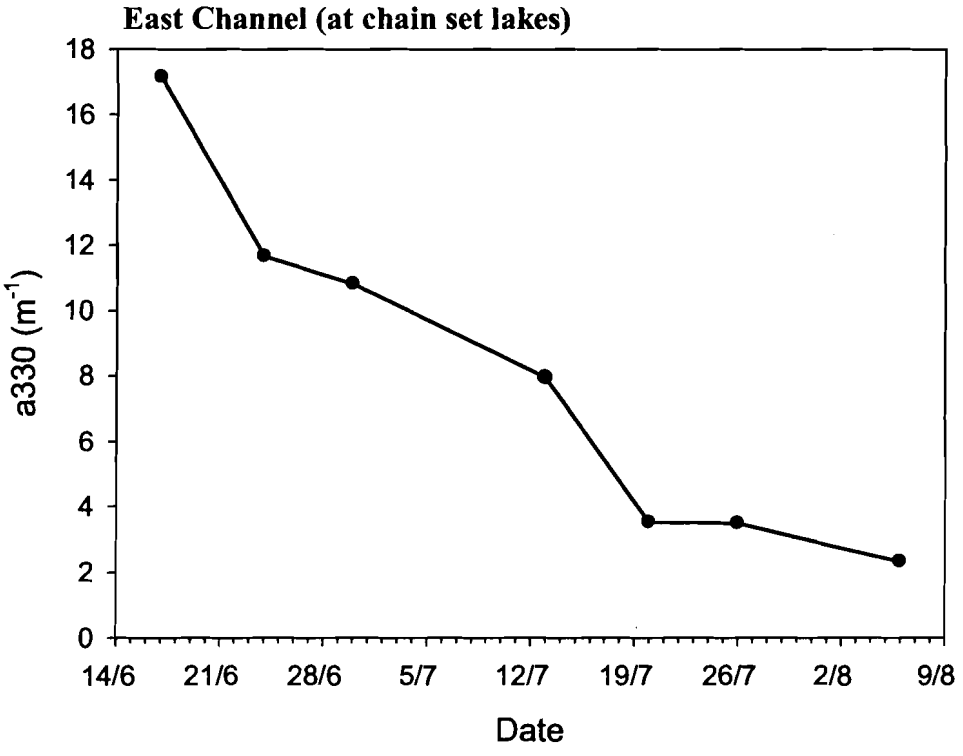

Appendix D: Pairwise Correlation Tables

Pairwise correlations (r^2) resulting from simple linear regressions between all possible pairs of variables measured in the chain and sill set lakes during the open water season of 2004. Sites are considered individually. All linear regressions were performed using JMP 6.0.0 statistical software (SAS Institute, Cary, NC). A single asterix (*) beside a p-value indicates a significant correlation between variables ($p \leq 0.05$), while a double asterix (**) beside a p-value indicates a near significant correlation between variables ($0.06 \geq p > 0.05$).

Chain Set Lakes

S1

Variable	by Variable	r^2	Count	Prob. (p)
KdUVA	KdUVB	0.9366	6	*0.0015
KdPAR	KdUVB	0.8129	6	*0.0141
KdPAR	KdUVA	0.8802	6	*0.0056
TDOC	KdUVB	0.8436	6	*0.0097
TDOC	KdUVA	0.7885	6	*0.0181
TDOC	KdPAR	0.4903	6	0.1213
a330	KdUVB	0.9565	6	*0.0007
a330	KdUVA	0.8686	6	*0.0068
a330	KdPAR	0.7609	6	*0.0234
a330	TDOC	0.7822	6	*0.0193
TSS	KdUVB	0.8538	6	*0.0085
TSS	KdUVA	0.9318	6	*0.0018
TSS	KdPAR	0.9547	6	*0.0008
TSS	TDOC	0.5628	6	0.0858
TSS	a330	0.8205	6	*0.0129
Chl a	KdUVB	0.1242	6	0.4933
Chl a	KdUVA	0.1129	6	0.5150
Chl a	KdPAR	0.3582	6	0.2095
Chl a	TDOC	0.0001	6	0.9875
Chl a	a330	0.0790	6	0.5894
Chl a	TSS	0.2364	6	0.3282

S2

Variable	by Variable	r^2	Count	Prob. (p)
KdUVA	KdUVB	0.9432	6	*0.0012
KdPAR	KdUVB	0.3835	6	0.1898
KdPAR	KdUVA	0.5309	6	0.1005
TDOC	KdUVB	0.8433	6	*0.0097
TDOC	KdUVA	0.6909	6	*0.0404
TDOC	KdPAR	0.0873	6	0.5698
a330	KdUVB	0.9561	6	*0.0007
a330	KdUVA	0.8936	6	*0.0044
a330	KdPAR	0.2372	6	0.3273
a330	TDOC	0.8998	6	*0.0039
TSS	KdUVB	0.0050	6	0.8941
TSS	KdUVA	0.0511	6	0.6668
TSS	KdPAR	0.4736	6	0.1307
TSS	TDOC	0.1056	6	0.5297
TSS	a330	0.0010	6	0.9522
Chl a	KdUVB	0.7843	6	*0.0189
Chl a	KdUVA	0.5872	6	0.0756
Chl a	KdPAR	0.1172	6	0.5064
Chl a	TDOC	0.9090	6	*0.0032
Chl a	a330	0.7456	6	*0.0267
Chl a	TSS	0.1060	6	0.5290

S3

Variable	by Variable	r^2	Count	Prob. (p)
KdUVA	KdUVB	0.7893	7	*0.0075
KdPAR	KdUVB	0.1163	7	0.4542
KdPAR	KdUVA	0.4787	7	0.0850
TDOC	KdUVB	0.7505	7	*0.0117
TDOC	KdUVA	0.6957	7	*0.0197
TDOC	KdPAR	0.0679	7	0.5725
a330	KdUVB	0.6854	7	*0.0215
a330	KdUVA	0.6153	7	*0.0368
a330	KdPAR	0.0731	7	0.5578
a330	TDOC	0.9021	7	*0.0011
TSS	KdUVB	0.1430	7	0.4029
TSS	KdUVA	0.0000	7	0.9984
TSS	KdPAR	0.4812	7	0.0839
TSS	TDOC	0.1995	7	0.3149
TSS	a330	0.1232	7	0.4401
Chl a	KdUVB	0.1138	7	0.4592
Chl a	KdUVA	0.4090	7	0.1220
Chl a	KdPAR	0.5951	7	*0.0422
Chl a	TDOC	0.0748	7	0.5529
Chl a	a330	0.0069	7	0.8597
Chl a	TSS	0.1530	7	0.3856

S4

Variable	by Variable	r^2	Count	Prob. (p)
KdUVA	KdUVB	0.9220	5	*0.0095
KdPAR	KdUVB	0.2473	5	0.3940
KdPAR	KdUVA	0.3884	6	0.1862
TDOC	KdUVB	0.9065	5	*0.0125
TDOC	KdUVA	0.8523	6	*0.0086
TDOC	KdPAR	0.1048	6	0.5315
a330	KdUVB	0.9425	5	*0.0060
a330	KdUVA	0.9151	6	*0.0028
a330	KdPAR	0.1751	6	0.4089
a330	TDOC	0.9888	6	*<.0001
TSS	KdUVB	0.2132	5	0.4338
TSS	KdUVA	0.1175	6	0.5060
TSS	KdPAR	0.2555	6	0.3063
TSS	TDOC	0.4113	6	0.1700
TSS	a330	0.3183	6	0.2435
Chl a	KdUVB	0.7322	5	0.0644
Chl a	KdUVA	0.4843	6	0.1247
Chl a	KdPAR	0.2034	6	0.3694
Chl a	TDOC	0.3965	6	0.1803
Chl a	a330	0.4434	6	0.1488
Chl a	TSS	0.0867	6	0.5711

S5

Variable	by Variable	r^2	Count	Prob. (p)
KdUVA	KdUVB	0.9843	7	*<.0001
KdPAR	KdUVB	0.7314	7	*0.0141
KdPAR	KdUVA	0.7829	7	*0.0081
TDOC	KdUVB	0.4808	7	0.0841
TDOC	KdUVA	0.4254	7	0.1123
TDOC	KdPAR	0.0737	7	0.5560
a330	KdUVB	0.8250	7	*0.0047
a330	KdUVA	0.8314	7	*0.0042
a330	KdPAR	0.4688	7	0.0896
a330	TDOC	0.6485	7	*0.0289
TSS	KdUVB	0.0475	7	0.6388
TSS	KdUVA	0.0296	7	0.7124
TSS	KdPAR	0.0678	7	0.5729
TSS	TDOC	0.7096	7	*0.0174
TSS	a330	0.2259	7	0.2811
Chl a	KdUVB	0.9465	7	*0.0002
Chl a	KdUVA	0.9031	7	*0.0010
Chl a	KdPAR	0.5666	7	**0.0508
Chl a	TDOC	0.6801	7	*0.0224
Chl a	a330	0.8332	7	*0.0041
Chl a	TSS	0.1571	7	0.3788

S6

Variable	by Variable	r^2	Count	Prob. (p)
KdUVA	KdUVB	0.9508	6	*0.0009
KdPAR	KdUVB	0.5940	6	0.0729
KdPAR	KdUVA	0.7553	6	*0.0246
TDOC	KdUVB	0.4521	6	0.1434
TDOC	KdUVA	0.3434	6	0.2217
TDOC	KdPAR	0.0419	6	0.6974
a330	KdUVB	0.7403	6	*0.0279
a330	KdUVA	0.7086	6	*0.0356
a330	KdPAR	0.2525	6	0.3097
a330	TDOC	0.7273	6	*0.0309
TSS	KdUVB	0.2422	6	0.3215
TSS	KdUVA	0.2316	6	0.3339
TSS	KdPAR	0.4651	6	0.1356
TSS	TDOC	0.0072	6	0.8734
TSS	a330	0.0002	6	0.9805
Chl a	KdUVB	0.0446	6	0.6880
Chl a	KdUVA	0.1075	6	0.5259
Chl a	KdPAR	0.5177	6	0.1070
Chl a	TDOC	0.0523	6	0.6631
Chl a	a330	0.0127	6	0.8314
Chl a	TSS	0.4746	6	0.1301

S7

Variable	by Variable	r^2	Count	Prob. (p)
KdUVA	KdUVB	0.9839	6	*<.0001
KdPAR	KdUVB	0.8017	6	*0.0158
KdPAR	KdUVA	0.8757	6	*0.0060
TDOC	KdUVB	0.0010	6	0.9519
TDOC	KdUVA	0.0011	6	0.9494
TDOC	KdPAR	0.1251	6	0.4916
a330	KdUVB	0.6555	6	**0.0510
a330	KdUVA	0.7016	6	*0.0374
a330	KdPAR	0.5091	6	0.1113
a330	TDOC	0.1094	6	0.5220
TSS	KdUVB	0.0946	6	0.5533
TSS	KdUVA	0.1363	6	0.4713
TSS	KdPAR	0.2313	6	0.3343
TSS	TDOC	0.0077	6	0.8689
TSS	a330	0.2501	6	0.3123
Chl a	KdUVB	0.4582	6	0.1397
Chl a	KdUVA	0.4036	6	0.1752
Chl a	KdPAR	0.2207	6	0.3471
Chl a	TDOC	0.2405	6	0.3234
Chl a	a330	0.4556	6	0.1413
Chl a	TSS	0.2378	6	0.3265

S8

Variable	by Variable	r^2	Count	Prob. (p)
KdUVA	KdUVB	0.9565	6	*0.0007
KdPAR	KdUVB	0.8830	6	*0.0053
KdPAR	KdUVA	0.8077	6	*0.0149
TDOC	KdUVB	0.5204	6	0.1056
TDOC	KdUVA	0.5526	6	0.0903
TDOC	KdPAR	0.5788	6	0.0790
a330	KdUVB	0.6892	6	*0.0408
a330	KdUVA	0.7567	6	*0.0243
a330	KdPAR	0.3901	6	0.1849
a330	TDOC	0.1651	6	0.4241
TSS	KdUVB	0.2549	6	0.3070
TSS	KdUVA	0.3229	6	0.2394
TSS	KdPAR	0.0603	6	0.6391
TSS	TDOC	0.0024	6	0.9265
TSS	a330	0.7735	6	*0.0209
Chl a	KdUVB	0.0986	6	0.5445
Chl a	KdUVA	0.0590	6	0.6426
Chl a	KdPAR	0.0101	6	0.8496
Chl a	TDOC	0.1023	6	0.5366
Chl a	a330	0.2269	6	0.3396
Chl a	TSS	0.4163	6	0.1664

S9

Variable	by Variable	r^2	Count	Prob. (p)
KdUVA	KdUVB	0.9579	6	*0.0007
KdPAR	KdUVB	0.9289	6	*0.0019
KdPAR	KdUVA	0.9401	6	*0.0014
TDOC	KdUVB	0.4078	6	0.1723
TDOC	KdUVA	0.4136	6	0.1683
TDOC	KdPAR	0.2039	6	0.3687
a330	KdUVB	0.6856	6	*0.0418
a330	KdUVA	0.7574	6	*0.0241
a330	KdPAR	0.6263	6	0.0607
a330	TDOC	0.5402	6	0.0960
TSS	KdUVB	0.0050	6	0.8936
TSS	KdUVA	0.0101	6	0.8496
TSS	KdPAR	0.0001	6	0.9817
TSS	TDOC	0.0133	6	0.8276
TSS	a330	0.0025	6	0.9257
Chl a	KdUVB	0.9916	6	*<.0001
Chl a	KdUVA	0.9775	6	*0.0002
Chl a	KdPAR	0.9399	6	*0.0014
Chl a	TDOC	0.4159	6	0.1667
Chl a	a330	0.7031	6	*0.0370
Chl a	TSS	0.0008	6	0.9571

Sill Set Lakes

Lake 129

Variable	by Variable	r^2	Count	Prob. (p)
KdUVA	KdUVB	0.9712	5	*0.0021
KdPAR	KdUVB	0.5311	5	0.1624
KdPAR	KdUVA	0.6150	5	0.1164
TDOC	KdUVB	0.4899	5	0.1882
TDOC	KdUVA	0.5404	5	0.1570
TDOC	KdPAR	0.0360	6	0.7187
a330	KdUVB	0.7641	5	**0.0526
a330	KdUVA	0.8466	5	*0.0268
a330	KdPAR	0.2912	6	0.2692
a330	TDOC	0.8413	6	*0.0100
TSS	KdUVB	0.2680	5	0.3716
TSS	KdUVA	0.1617	5	0.5022
TSS	KdPAR	0.0477	6	0.6775
TSS	TDOC	0.0002	6	0.9770
TSS	a330	0.0352	6	0.7221
Chl a	KdUVB	0.7793	5	*0.0473
Chl a	KdUVA	0.8499	5	*0.0259
Chl a	KdPAR	0.5799	6	0.0786
Chl a	TDOC	0.3814	6	0.1914
Chl a	a330	0.7607	6	*0.0235
Chl a	TSS	0.1957	6	0.3797

Lake 80

Variable	by Variable	r^2	Count	Prob. (p)
KdUVA	KdUVB	0.9964	3	*0.0378
KdPAR	KdUVB	0.9916	3	**0.0586
KdPAR	KdUVA	0.9791	4	*0.0105
TDOC	KdUVB	0.7331	3	0.3456
TDOC	KdUVA	0.7449	4	0.1369
TDOC	KdPAR	0.8105	4	0.0997
a330	KdUVB	0.9948	3	*0.0461
a330	KdUVA	0.9698	4	*0.0152
a330	KdPAR	0.9052	4	*0.0486
a330	TDOC	0.5961	4	0.2279
TSS	KdUVB	0.9944	3	*0.0477
TSS	KdUVA	0.9308	4	*0.0352
TSS	KdPAR	0.9673	4	*0.0165
TSS	TDOC	0.6879	4	0.1706
TSS	a330	0.8653	4	0.0698
Chl a	KdUVB	0.5379	3	0.4759
Chl a	KdUVA	0.2902	4	0.4613
Chl a	KdPAR	0.3993	4	0.3681
Chl a	TDOC	0.7676	4	0.1239
Chl a	a330	0.1502	4	0.6124
Chl a	TSS	0.3264	4	0.4287

Lake 520

Variable	by Variable	r^2	Count	Prob. (p)
KdUVA	KdUVB	0.9750	5	*0.0017
KdPAR	KdUVB	0.0015	5	0.9512
KdPAR	KdUVA	0.0007	5	0.9661
TDOC	KdUVB	0.6480	5	0.1003
TDOC	KdUVA	0.5206	5	0.1689
TDOC	KdPAR	0.0482	5	0.7226
a330	KdUVB	0.9136	5	*0.0111
a330	KdUVA	0.8703	5	*0.0207
a330	KdPAR	0.0393	5	0.7492
a330	TDOC	0.8216	5	*0.0339
TSS	KdUVB	0.3247	5	0.3159
TSS	KdUVA	0.1908	5	0.4621
TSS	KdPAR	0.0156	5	0.8412
TSS	TDOC	0.7644	5	**0.0525
TSS	a330	0.4115	5	0.2434
Chl a	KdUVB	0.0155	5	0.8419
Chl a	KdUVA	0.0733	5	0.6595
Chl a	KdPAR	0.0000	5	0.9976
Chl a	TDOC	0.0737	5	0.6587
Chl a	a330	0.0083	5	0.8841
Chl a	TSS	0.4878	5	0.1895

Appendix E: Open Water Climate Record, Inuvik NT

Open water climate record for Inuvik, Northwest Territories, during both 2004 and 2005. Temperature (T) and precipitation data from Environment Canada weather station Inuvik A (Climate ID 2202570). Dashed lines indicate the date of annual peak flood.

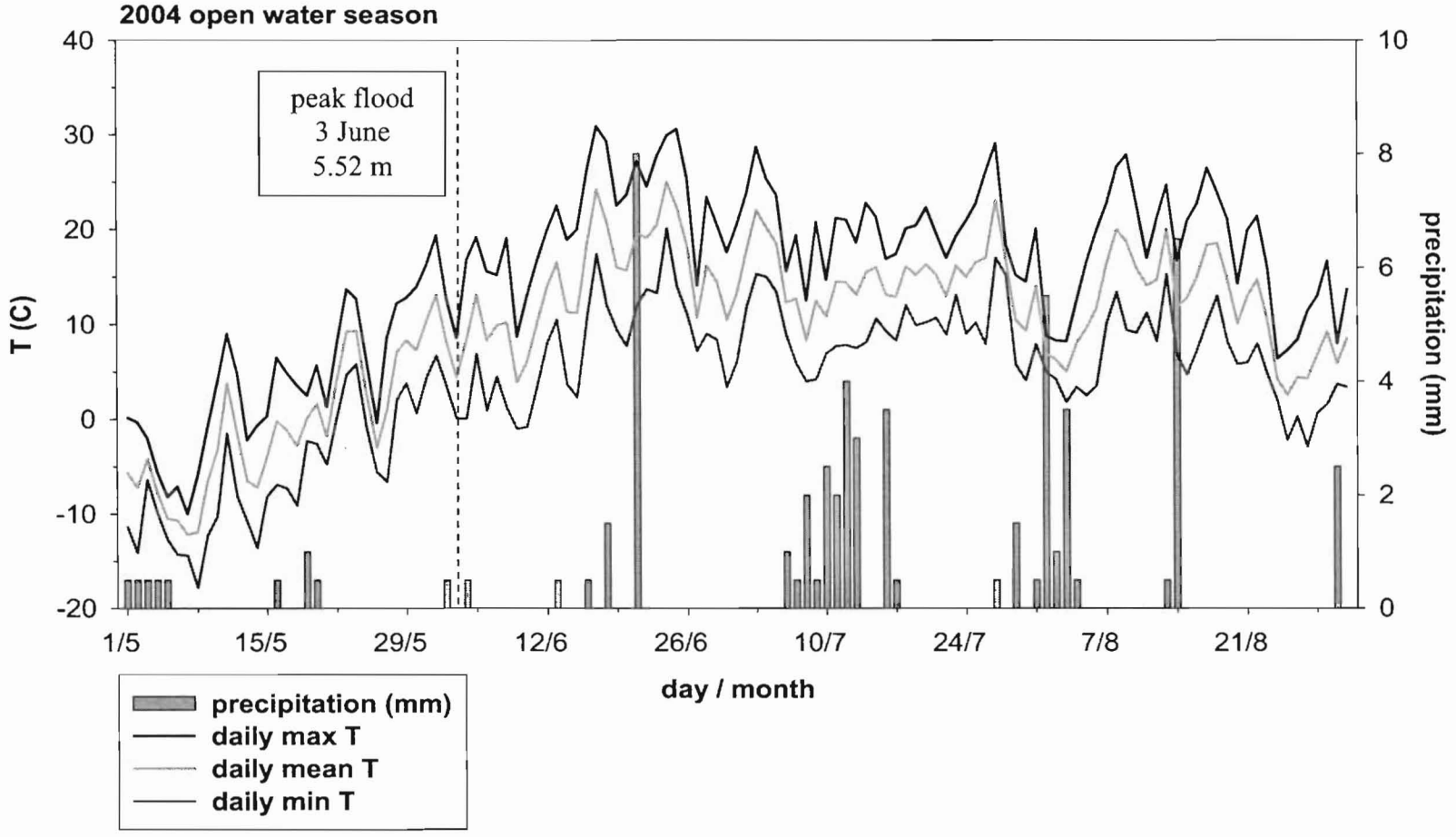

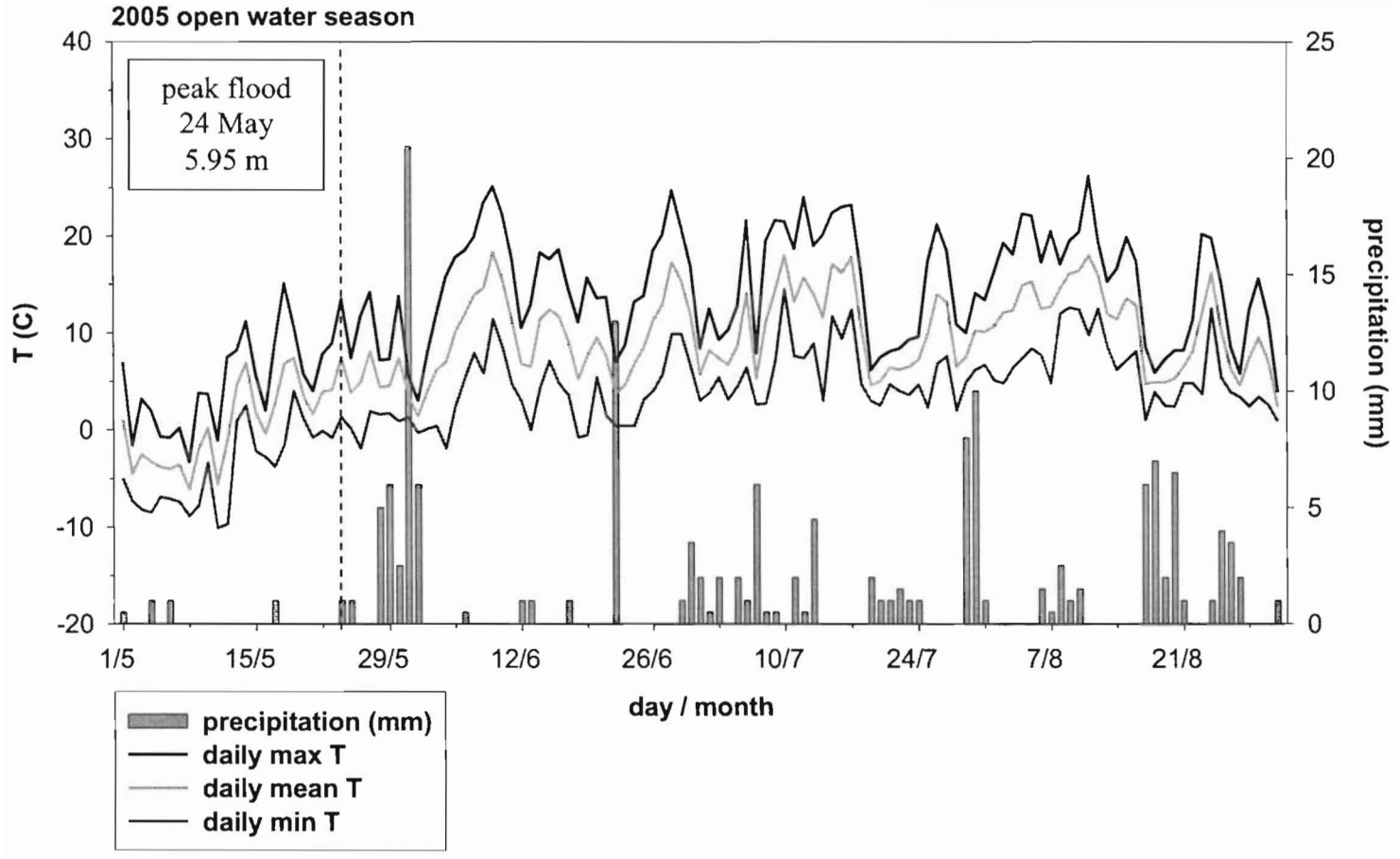
2005 open water season
peak flood
24 May
5.95 m
T (C)
precipitation (mm)
day / month
1/5
15/5
29/5
12/6
26/6
10/7
24/7
7/8
21/8
40
30
20
10
0
-10
-20
25
20
15
10
5
0
precipitation (mm)
daily max T
daily mean T
daily min T